1991

Neutron energy determination utilizing a high-purity germanium detector

E. A. (Eugen A.) Beck
San Jose State University

Order Number 1345789

Neutron energy determination utilizing a high-purity germanium detector

Beck, Eugene Arnold, M.S.

San Jose State University, 1991

U·M·I
300 N. Zeeb Rd.
Ann Arbor, MI 48106

NEUTRON ENERGY DETERMINATION UTILIZING A HIGH-PURITY GERMANIUM DETECTOR

A Thesis

Presented to

The Faculty of the Nuclear Science Program

Radiation Health Physics

San Jose State University

In Partial Fulfillment

of the Requirements for the Degree

Master of Science

By

Eugene A. Beck

August, 1991

APPROVED FOR THE DEPARTMENT OF RADIATION HEALTH PHYSICS
NUCLEAR SCIENCE PROGRAM

Dr. Peter Englert

Dr. Allen Tucker

Dr. Carlos Castaneda

APPROVED FOR THE UNIVERSITY

ABSTRACT

NEUTRON ENERGY DETERMINATION UTILIZING A HIGH-PURITY GERMANIUM DETECTOR

by Eugene A. Beck

This thesis evaluates the use of germanium gamma-ray detectors to determine the energy of incident neutrons in the range of 10-70 MeV. Methods were developed to separate the nuclear recoil spectra the gamma ray spectra produced in neutron inelastic scattering. The germanium 596, 690 and 835 kev (n,n'γ) peaks were evaluated for full width maximum values, and the slopes were determined for the leading edge and for the primary downslope.

Findings indicate that the full width maximum values were not useful indicators of neutron energies. This may be due to the "bleeding" of activity ie. background, from one recoil peak into the next recoil peak. Evaluation of the upslope and downslope measurements showed a relationship between the neutron energy and the values of these slopes for all three recoil peaks. A series of equations were developed to describe these relationships empirically. The germanium detector can now be used by Health Physicists to measure gamma ray spectra as well as to evaluate neutron sources for energy and exposure.

ACKNOWLEDGEMENT

I would like to thank Dr. Peter Englert for the guidance and inspiration for this thesis. My thanks also go to Drs. Allen Tucker and Carlos Castaneda for taking the time to review this thesis for the faculty. I would also like to acknowledge the staff at the Crocker Nuclear Laboratory for there efforts in my data acquisition and to Steve Shimose for the computer program he wrote for this thesis. Finally I would like to thank Barbara, the one person who has pushed and pulled and generally made this all possible for me. This has taken a long time and I appreciate every minute you have given to this effort.

TABLE OF CONTENTS

List of Tables

Table

List of Figures

Figure

List of Figures Cont.

Chapter 1: Introduction

Neutron interactions with germanium detectors were first described by Chasman, Jones, Ristinen and Sample, (1965a) at the Brookhaven National Laboratory. They studied the effect of 1.2, 2.2, 4.7, and 16.3 MeV neutrons incident on a planar lithium-drifted germanium detector. The detector had a surface area of 6 cm^2 and a sensitive depth of 5 mm. At each of the neutron energies utilized they observed the five primary recoil broadened $(n, n'\gamma)$ peaks identified in Table 1. They also observed that as the energy of the neutrons increased the width of the peaks increased. The work reported in this thesis is an analysis of the relation between neutron energy and the shape of the $(n, n'\gamma)$ photopeaks.

Neutron dosimetry, particularly when applied to fast neutrons, depends strongly on the energy of the neutrons (NCRP, 1971; Attix, 1986). The current methods used for measuring exposure from neutrons are valid up to approximately 15 MeV. Present methods include the use of Hurst counters, rem meters, and albedo neutron dosimeters (Cember, 1983). The principal problem that these instruments have at higher energy levels is their non-linear response to the neutron energy. There are many instances where the exposure from neutrons having higher energies must be determined. Some of these applications include working near spontaneous fission neutron sources, linear accelerators or cyclotrons, and in space flight.

The purpose of this thesis is to explore the possibilities of using high-purity germanium detectors as instruments for measuring the maximum neutron energy incident on the detectors. This work will demonstrate that coaxial or planar high-purity germanium detectors have the potential for being used in neutron dosimetry. An additional application of the technique developed in this study would include calibration of neutron energies from high-energy neutron sources.

Germanium has five stable isotopes with an atomic number (Z) of 32 and isotopic mass numbers (A) of 70, 72, 73, 74, 76. The relative abundances of these isotopes are 20.5, 27.4, 7.8, 36.5, and 7.8%, respectively (Lederer and Shirley, 1978). Table 1 shows the first and second excitation states of the germanium isotopes. The states denoted by * are of importance in the spectra from neutron inelastic scattering. The other states listed are likely present but not easily detected due to low abundance of the isotope or low cross section values for the interaction.

Table 1

Stable Germanium Isotope Abundance and Excitation States

Isotopic Mass A	Abundance %	Energy of Excitation State(MeV)	Spin/ Parity
70	20.5	First 1.041 *	2+
		Second 1.215	0+
72	27.4	First 0.690 *	0+
		Second 0.835 *	2+
73	7.8	First 0.013	9/2+
		Second 0.067	5/2+
74	36.5	First 0.596 *	2+
		Second 1.205 *	2+
76	7.8	First 0.563 *	2+
		Second 1.130	2+

Additional gamma rays in the energy range listed above have been reported for germanium. These gamma rays result from the transition of higher level excitation states to lower levels. These include: 1) 609 keV in the transition of the ^{74} Ge from 1205 to 596 keV, 2) 630 keV in the transition of ^{72}Ge from 1565 to 835 keV, 3) 669 keV in the transition of ^{70}Ge from 1790 to 1041 keV, 4) 868 keV in the transition of ^{74}Ge from 1464 to 596 keV, 5) 888 keV in the transition of ^{74}Ge from 1484 to 596 keV and 6) 895 keV in the transition of ^{72}Ge from 1730 to 835 keV (K. Chung, Mittler, Brandenberger and McEllistrem, 1970).

Germanium is a Group IV tetravalent element and forms a crystal by covalent bonding of its four valence electrons. These electrons can be maintained in two different states within the crystal. The first state is called the valence band and involves the bonding between atoms of the matrix. The second state called the conduction band represents the electrons that are free to migrate throughout the crystal. The difference in energy needed to move an electron between these two states is referred to as the band gap. For a germanium crystal the band gap is 2.96 eV. Any process that is capable of exciting an electron with this amount of energy will cause it to move from the valence band to the conduction band. This will also result in the formation of a hole in the valence band at the site formerly occupied by the electron. The electrons and holes are collected with the application of an electrical field across the detector. The size of the collected electrical signal produced by the electrons and holes is proportional to the amount of energy deposited in the detector. The energy needed to elevate the electrons may come from ionizing events or thermal excitation.

High-purity germanium semi-conductor detectors are characterized by having excellent energy resolution and a tolerance of high counting rates. The energy resolution is often 1-2 keV at 1.33 MeV gamma ray energy. This results from requiring only 2.96 eV to produce an electron-hole pair. The high speed counting is the result of a very low resolving time of the detector in collecting the electrons and holes produced in the detector.

The incident of a neutron beam upon a germanium detector produces atypical pulse height peaks whose shape changes with changes in the neutron energy. These peaks are asymmetrically broadened, with a sharp leading edge and a long high-energy tail. This broadening effect can be explained in the following manner. In inelastic scattering, a portion of the incident neutron's energy is lost to excitation of the nucleus. This energy is released by the nucleus in the form of either a gamma ray or a conversion electron. The scattered neutron n' is scattered from the nucleus isotropically. The angle of scatter will determine the amount of energy that is transferred to the germanium nucleus in the form of recoil energy. The recoil nucleus will generally receive sufficient energy to overcome the binding energy. The recoil nucleus will disassociate from the crystal and move through the surrounding matrix of the detector causing electron-hole pair formations. The recoil nucleus' electron-hole pair formation occurs simultaneously with the absorption of the gamma ray or conversion electron and the two events will appear as a single pulse in the spectra. The recoil energy transferred to the nucleus is dependent on the angle of the scattered neutron. The amount of energy transferred to the electron-hole pair formations is variable based on the recoil energy of the germanium atom. The combination of these effects produces the broadening of the peak with the narrow gamma ray or conversion electron peak superimposed on the wide recoil germanium energy distribution forming a single compound peak.

Chapter 2: Review of Literature

The amount of nuclear recoil energy transferred to the electron-hole pairs has been investigated by a number of different groups. Lindhard, Nielsen, Scharff, and Thomsen (1963) generated a group of equations that accounted for the amount of energy needed for a heavy ion to create a single electron-hole pair in a germanium detector. They proposed that heavy ions required more energy than photoelectrons, compton electrons or pair production electrons from primary gamma ray interactions, to raise the electrons from the valence band to the conduction band to form an electron-hole pair. This prediction was verified by Chasman, Jones and Ristinen (1965b, 1967) for germanium recoil energies up to 100 keV and extended by Bockisch, Braun and Neuwirth (1982) to recoil energies of 800 keV. As the maximum recoil energy increased it would appear from their data that the fractional amount of energy transferred to electron-hole pairs also increased.

Since these earlier works, very little reference has been made of these peaks except to note their presence (Bunting and Krushaar; 1974, and Brüchner, Wänke and Reedy, 1987) and/or interference (Youngblood, Bearse, Williams and Blaugrund, 1966; Lieb, Kent and Moore, 1968) during collection of data from in-beam counting systems. Lack of interest in these (n, n'γ) peaks has left a void in the literature as to whether there is information that can be obtained from them.

Recently C. Chung and Chen (1991) evaluated the gamma ray and the conversion electron portions of these curves. They converted the count rate determinations into a measure of the dose rate equivalent in μSv. Their work showed that the 596 keV peak could be used to estimate the dose rate from thermal and epithermal neutrons (E_n > 0.02 MeV) with an accuracy of 17.4% in the dose range of 0.08-120 μSv/h. The 690 keV conversion electron peak was used to estimate the dose rate from fast and relativistic neutrons (E_n < 0.7 MeV) with an accuracy of 32.3% in the dose range of 0.8-75 μSv/h. Their approach was to evaluate the gamma ray and electron conversion data portion of the spectra. One difficulty that appears to be present in their method was the handling of the recoil portion of the curve. Examination of their data indicates that the gamma rays were not separated from the recoil energies. The count rate determination was based on a combination of both the gamma rays and the recoil energies. Lindhard's analysis showed that the germanium recoil nucleus contributed a larger percentage of its energy to the detector as the recoil energy increased. The maximum recoil energy also increased as the neutron energy increased. Kinematics shows that at a neutron energy of 4.8 MeV the 596 keV peak recoil energy will extend into the 690 keV peak and some of the data from the 596 keV peak will be lost. The same results will also occur with the 690 keV peak data crossing into the 835 keV peak at a neutron energy of 6.6 MeV. The amount of data lost increased as the neutron energy increased above these levels. A determination of the neutron energy would allow for a closer estimation of the dose received through the use of different quality factors for varying neutron energies.

Chapter 3: Experimental Setup and Data Acquisition

The 79 inch cyclotron at the Crocker Nuclear Laboratory on the campus of the University of California, Davis, was utilized to generate beams of energetic neutrons. Protons accelerated to energies of 20.5, 40.0 and 67.5 MeV were directed onto a 93 mil thick ^{7}Li target, with the $^{7}Li(p,n)^{8}Be$ reaction producing neutron beams with maximum energies of 18.8, 38.4 and 65.5 MeV. An Ortec GMX Series, Gamma-X HPGE, 5.0 cm diameter by 6.0 cm long, closed-end high purity germanium detector was placed in the neutron beam for the 18.8 and 38.4 MeV runs. An Ortec GEM series HPGe, 5.1 cm diameter by 5.4 cm long coaxial high purity germanium detector was used for the 65.5 MeV run. Energy calibrations were performed with the 662 keV gamma rays of ^{137}Cs and the 1.17 and 1.32 MeV gamma rays of ^{60}Co. The 1.32 MeV gamma ray line was also utilized to check the energy resolution of the detector during the data acquisition. Germanium detectors are subject to damage from neutrons (Stelson, Dickens, Raman and Trammell 1972); however, minimal changes in the energy resolution, measured before and after data acquisition, were observed in either detector.

Neutron doses to the detectors were estimated by the method described by Stelson et al. (1972) to be 4.15 x 10^{5} neutrons/cm^{2} at 18.8 MeV, 1.38 x 10^{6} neutrons/cm^{2} at 38.4 MeV and 6.68 x 10^{5} neutrons/cm^{2} at 65.5 MeV.

Off-beam spectra were acquired during the 65.5 MeV neutron run to estimate the scattered neutron contribution to the spectra. This contribution to the spectra was estimated to be less than 5% of the total data.

The spectra were acquired onto a personal computer utilizing the Nuclear Data Accuspeck acquisition and processing program. The data was stored to disc in the spectral and ASCII format. Figures 1-3 are the obtained spectra displayed with the Canberra System 100 spectral display system. The lower curve was the entire 4096 channel spectrum with the upper curve showing the areas of the spectrum with the recoil-broadened peaks. The 563, 596, 690, 835 keV lines were present at all three neutron energies. The 1035 keV line was seen in the spectra from the 18.8 and 38.4 MeV neutrons. The difficulty in defining the 1035 line from the 65.5 MeV neutrons was attributed to the low count rate obtained during this run. The 563 and 1035 keV lines were not considered for processing due to the low counting statistics.

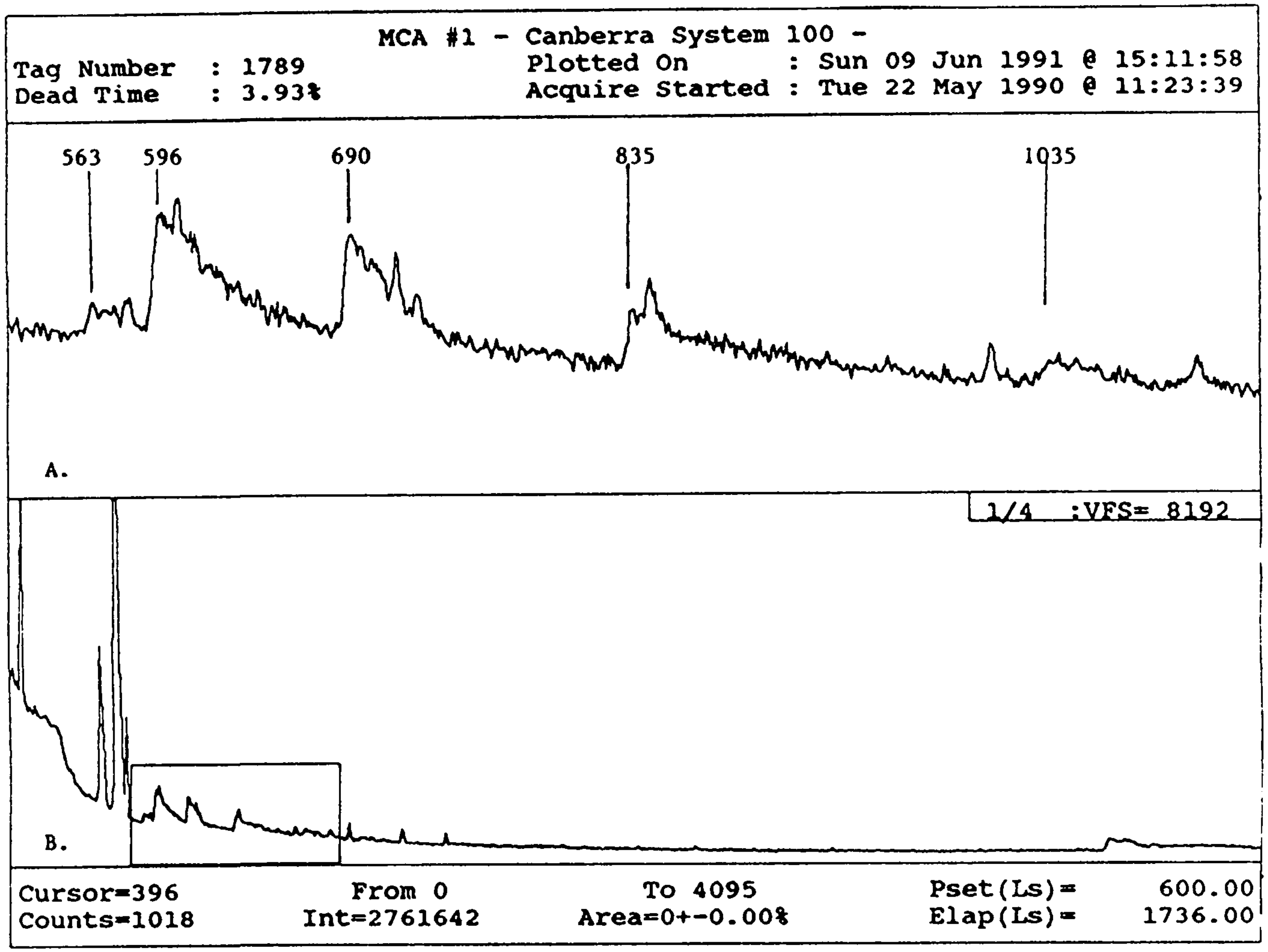

Fig. 1 Acquired Spectrum for 18.8 MeV Neutrons A. Region of Recoil Curves
B. Full 4096 Channel Spectrum.

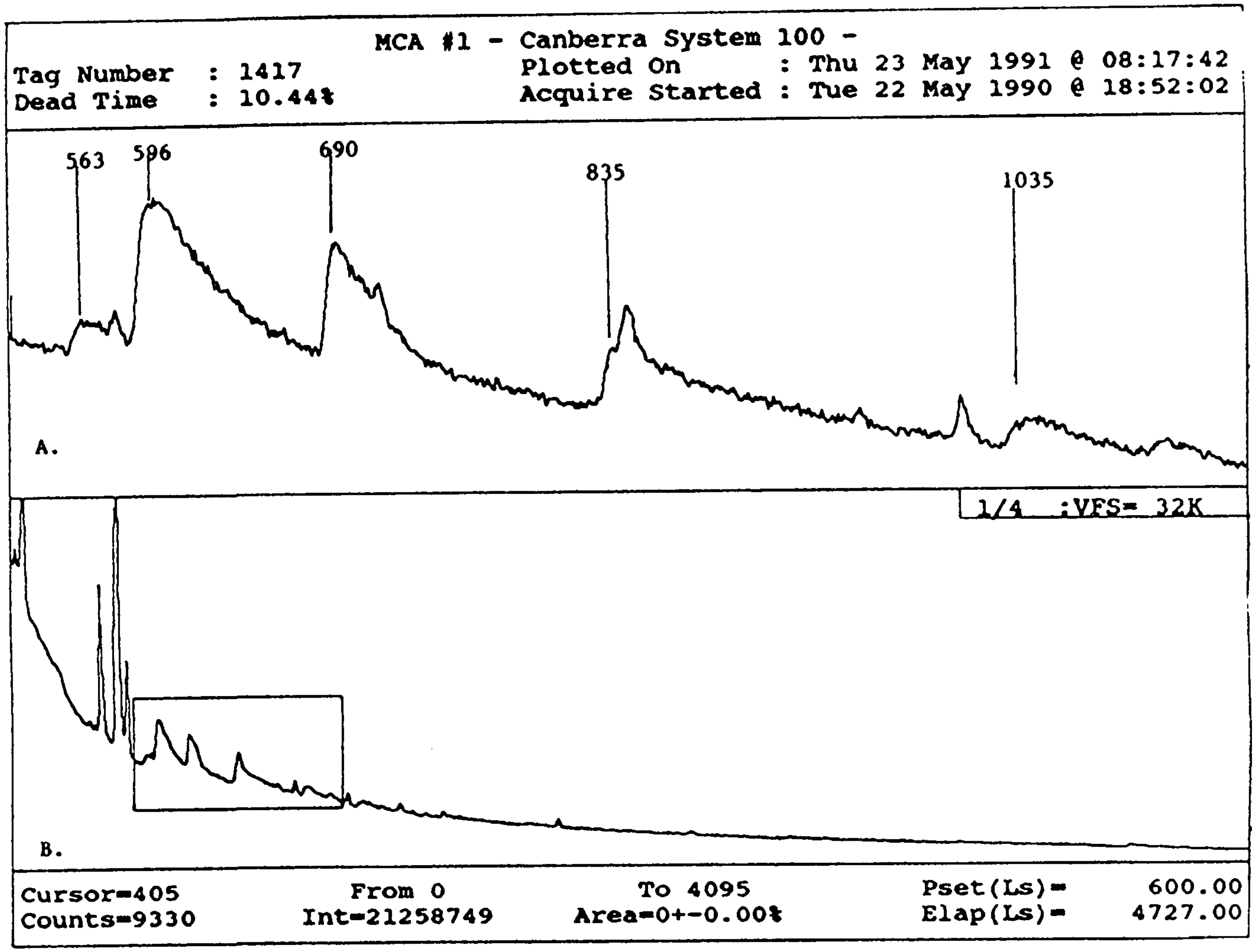

Fig. 2 Acquired Spectrum for 38.4 MeV Neutrons A. Region of Recoil Curves
B. Full 4096 Channel Spectrum

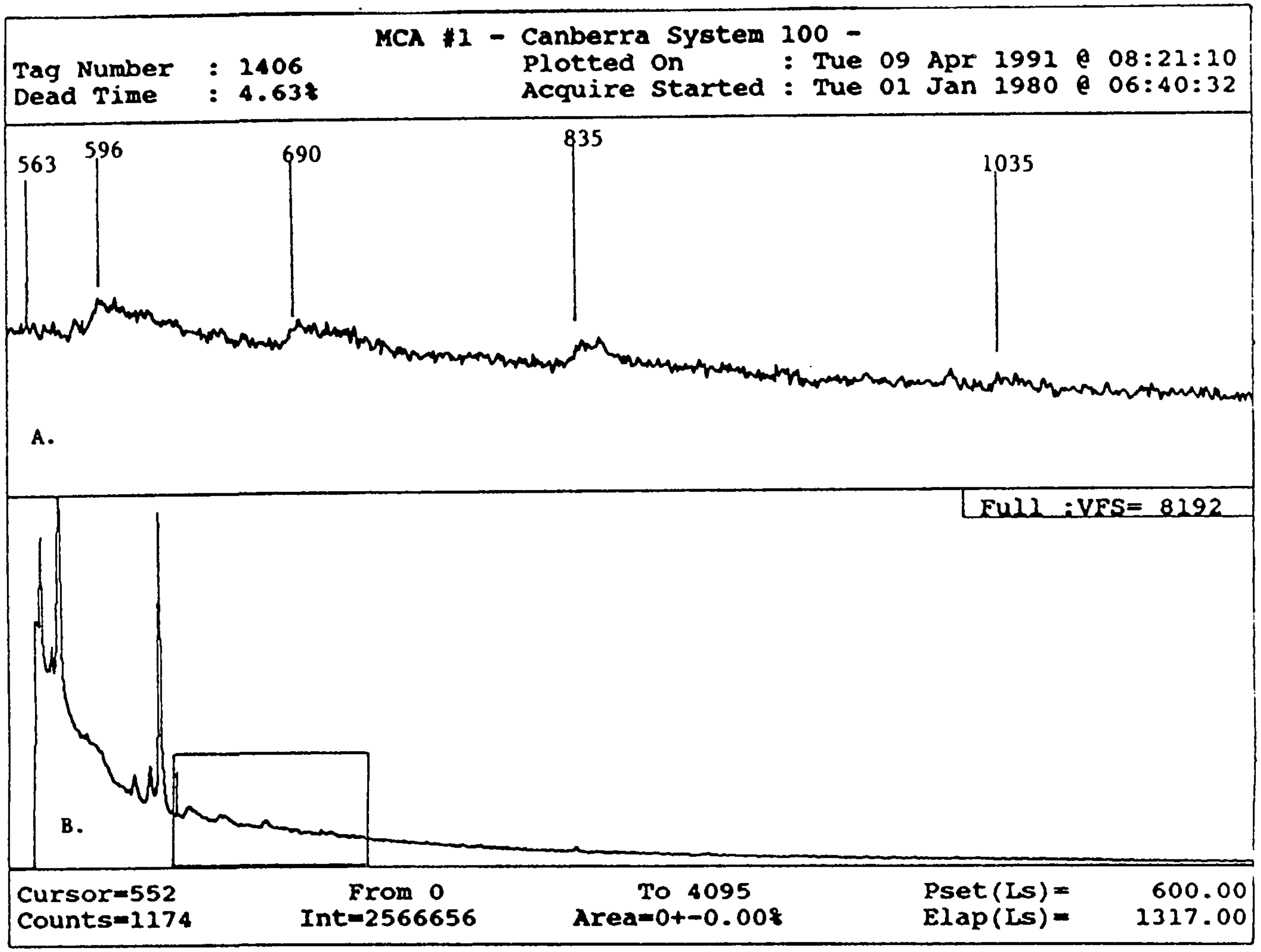

Fig. 3 Acquired Spectrum for 65.5 MeV Neutrons A. Region of Recoil Curves B. Full 4096 Channel Spectrum.

Chapter 4: Data Analysis

The ASCII coded data for all three neutron energies were transferred to the spectra analyzing program Ganymed (Kruse 1979). This program uses a modified Gauss-Newton algorithm to fit the peaks with a polynomial background of order 1-6. A region of interest was selected with a maximum of 150 channels. For the processing of the spectra used in this study, the area of interest was set to two channels prior to the upslope of the peak and extended to the first point of the upslope for the next peak. This end point was valid for the 596 and 690 keV peaks. For the 835 keV peak the full 150 channel limit was used to define the region of interest with the starting point the same as described above.

Three variables were entered affecting the fitting of the gamma ray peak and the shape of the background curve. The first value P sets the degree of polynomial for the background curve fit. Values between one and six were allowable for this parameter. A higher value for the background polynomial allowed for a better fit to backgrounds of the type of curve expected from the recoil germanium atoms. A value of 5 or 6 was used for P throughout all data processing. The second variable sets the value of a residuum. The residuum was defined as the difference between each data point in the region of interest and the fitted value for that data point, divided by the standard deviation of the data point. The residuum acts as a sensitivity threshold for determining peaks; higher values reject more spurious peaks. For this work the highest residuum was used that allowed for the fitting of the primary gamma ray or electron conversion peaks for each selected peak. The third variable was the percent error rejection or confidence limit of the peak area. This value allows for the removal of peaks from the selection process if the confidence limit for the peak area exceeds this value. The higher this value was set the more likely a peak would be kept whether it was a spurious peak or a real peak. The default value of 30% was used for the processing of most peak selections. A 50% value was used for the 690 keV peak from the 65.5 MeV neutron run. This peak was difficult to fit due to low counting statistics and the 50% error provided for the selection and fitting of the 690 keV gamma ray peak.

After processing, the program presented a display of the raw data curve, the fitted curve and the background curve for the entered parameters. Figures 4-6 represent the fittings for the 596, 690, and 835 keV peak from the 18.8 MeV neutrons, respectively. Figures 7-9 represent the 38.4 MeV neutrons and Figures 10-12 represent the 65.5 MeV neutrons. The numerical values for all nine curves were plotted to a file for later evaluation. The printouts for these files are found in Appendix A.

Additional gamma ray photopeaks were present within the regions of interest used for the recoil peaks. These included the 609 keV peak which results from the transition of the 1205 keV excitation state of ^{74}Ge to 596 keV, and is also a gamma ray produced in the neutron capture and decay of ^{73}Ge. Also identified was the 846 keV peak resulting from the $^{27}Al(n,p)^{27}Mg$ reaction.

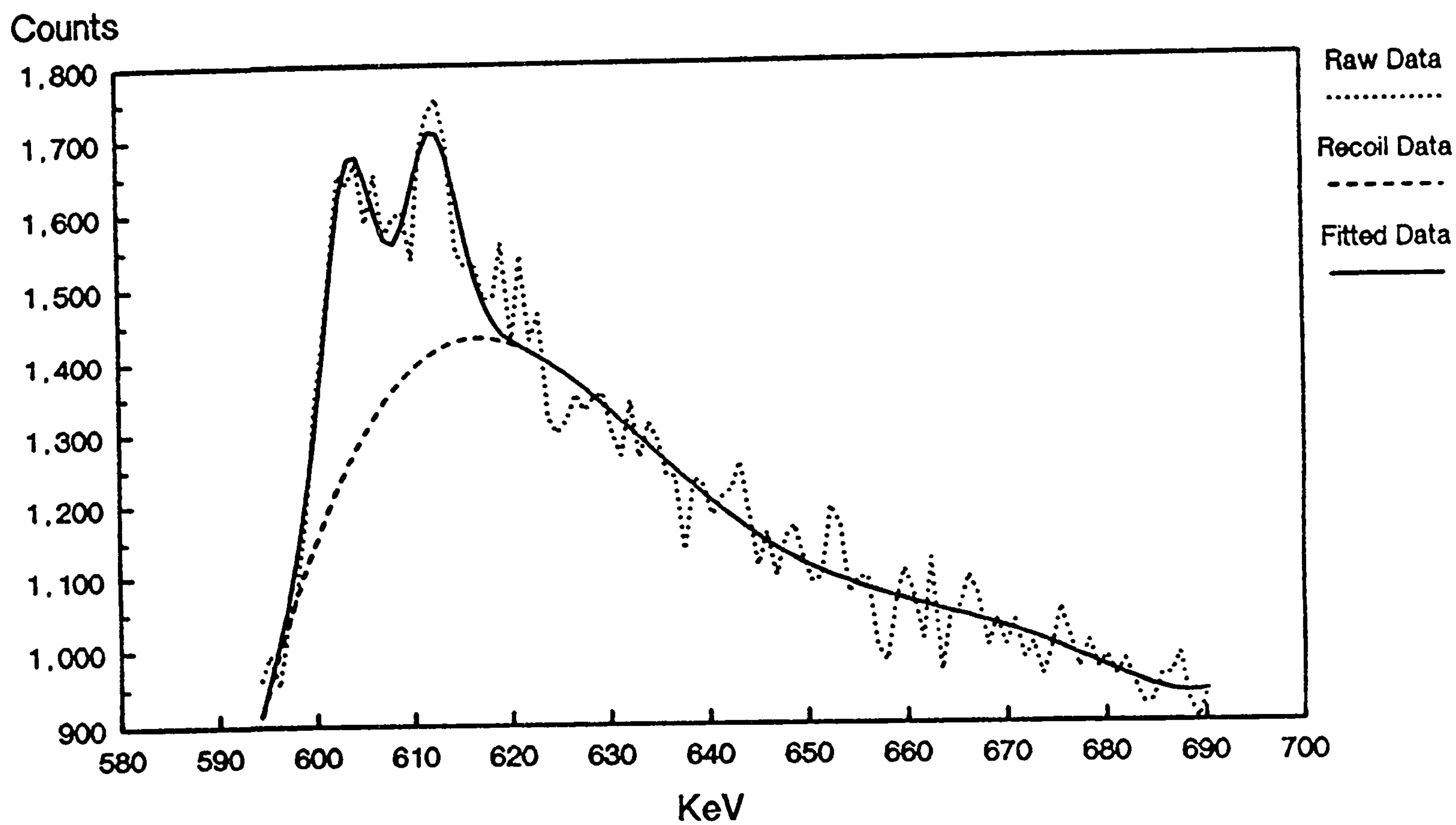

Fig. 4 Ganymed Fitting of 596 keV Peak from
18.8 Mev Neutrons

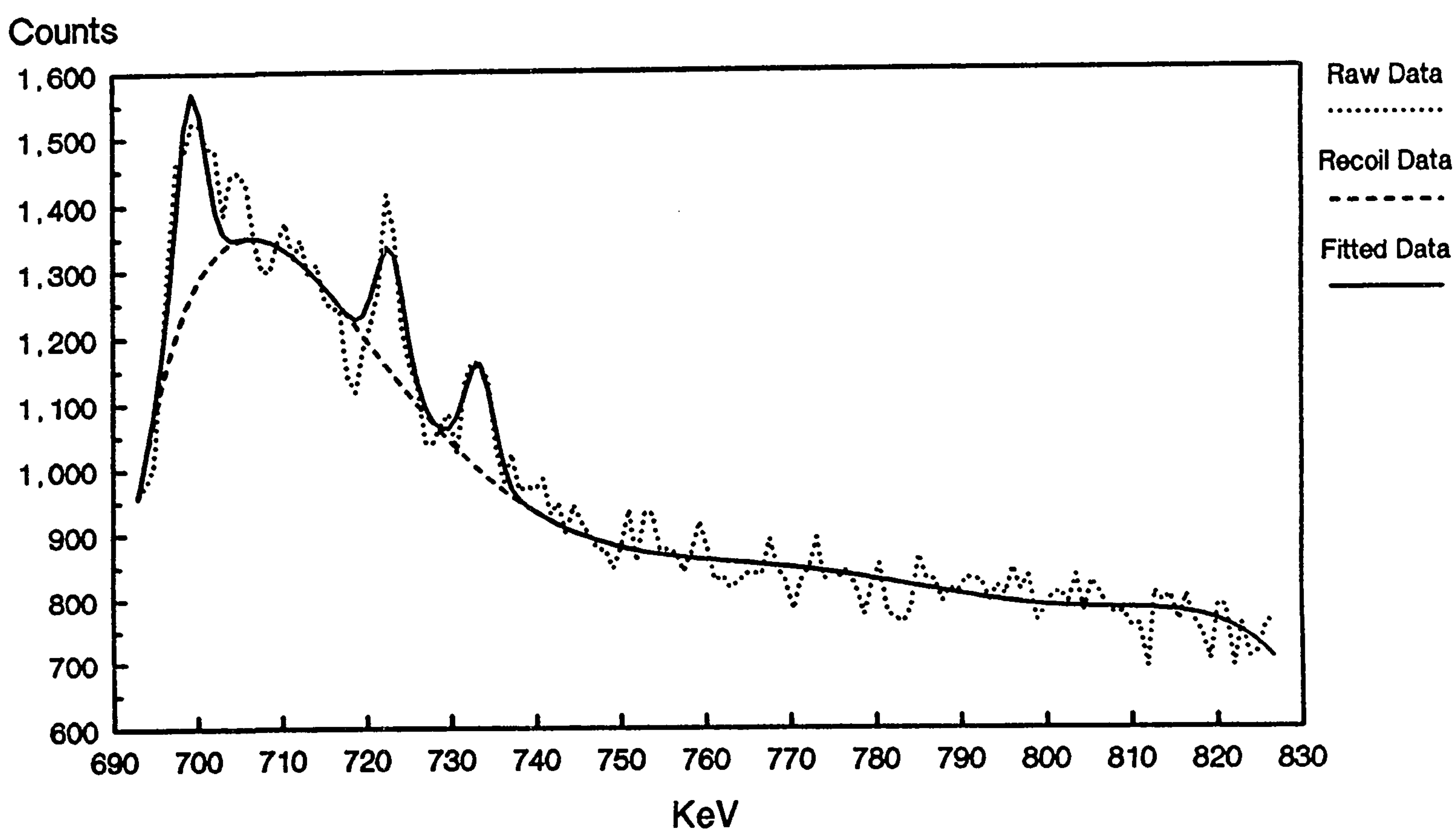

Fig. 5 Ganymed Fitting of 690 keV peak from
18.8 MeV Neutrons

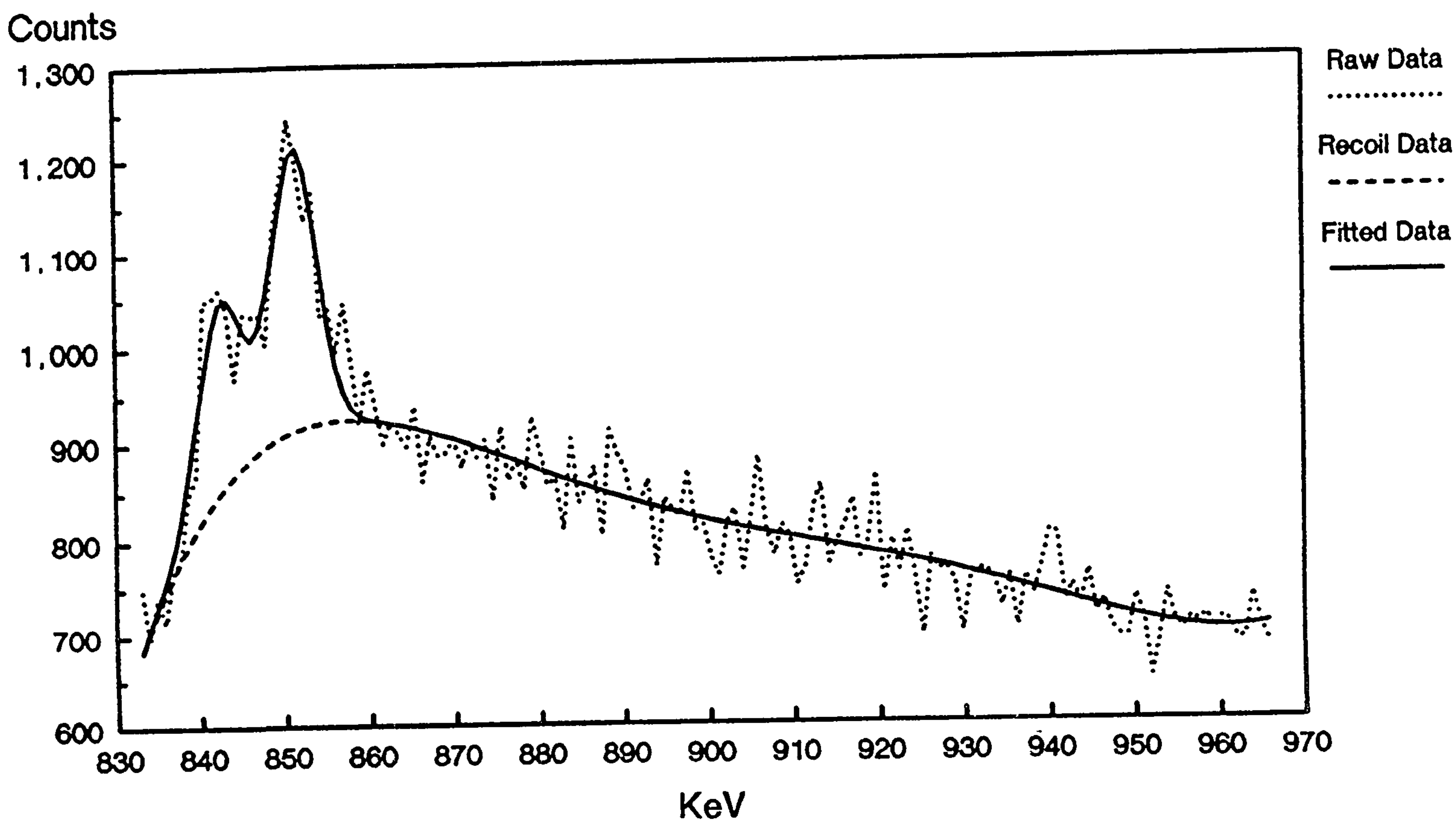

Fig. 6 Ganymed Fitting of 835 keV from
18.8 MeV Neutrons

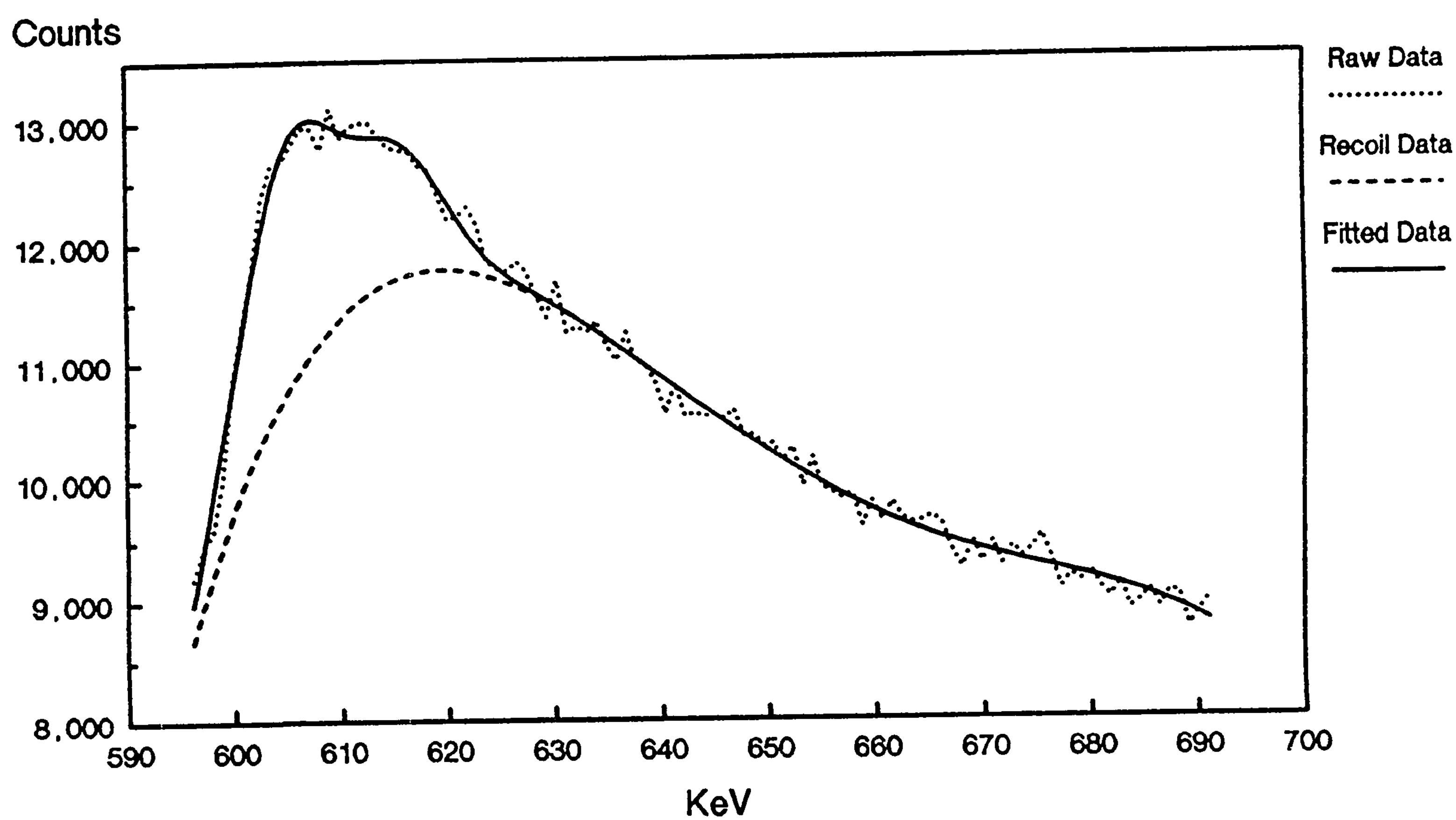

Fig. 7 Ganymed Fitting of 596 keV from
38.4 MeV Neutrons

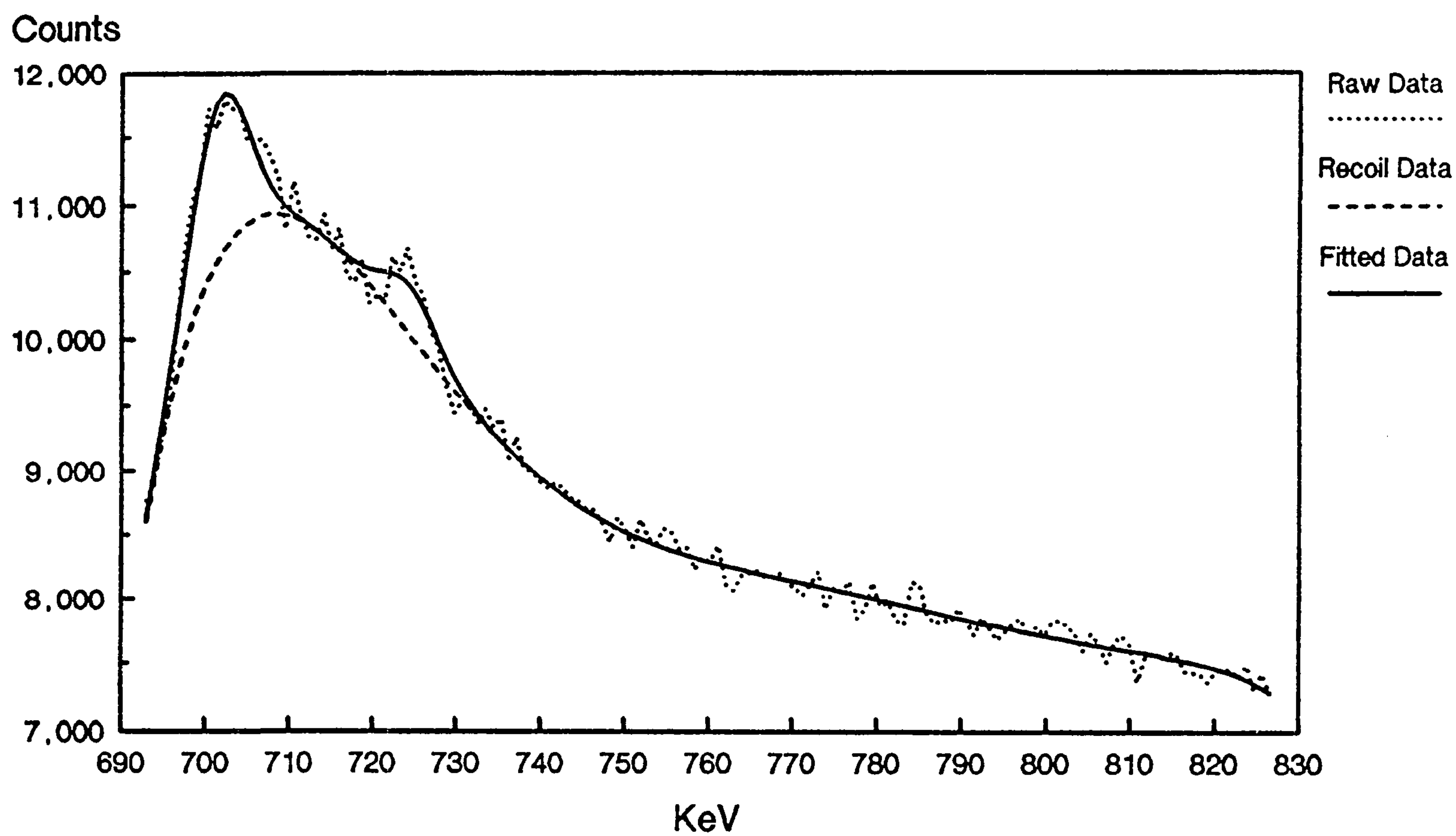

Fig. 8 Ganymed Fitting of 690 keV from
38.4 MeV Neutrons

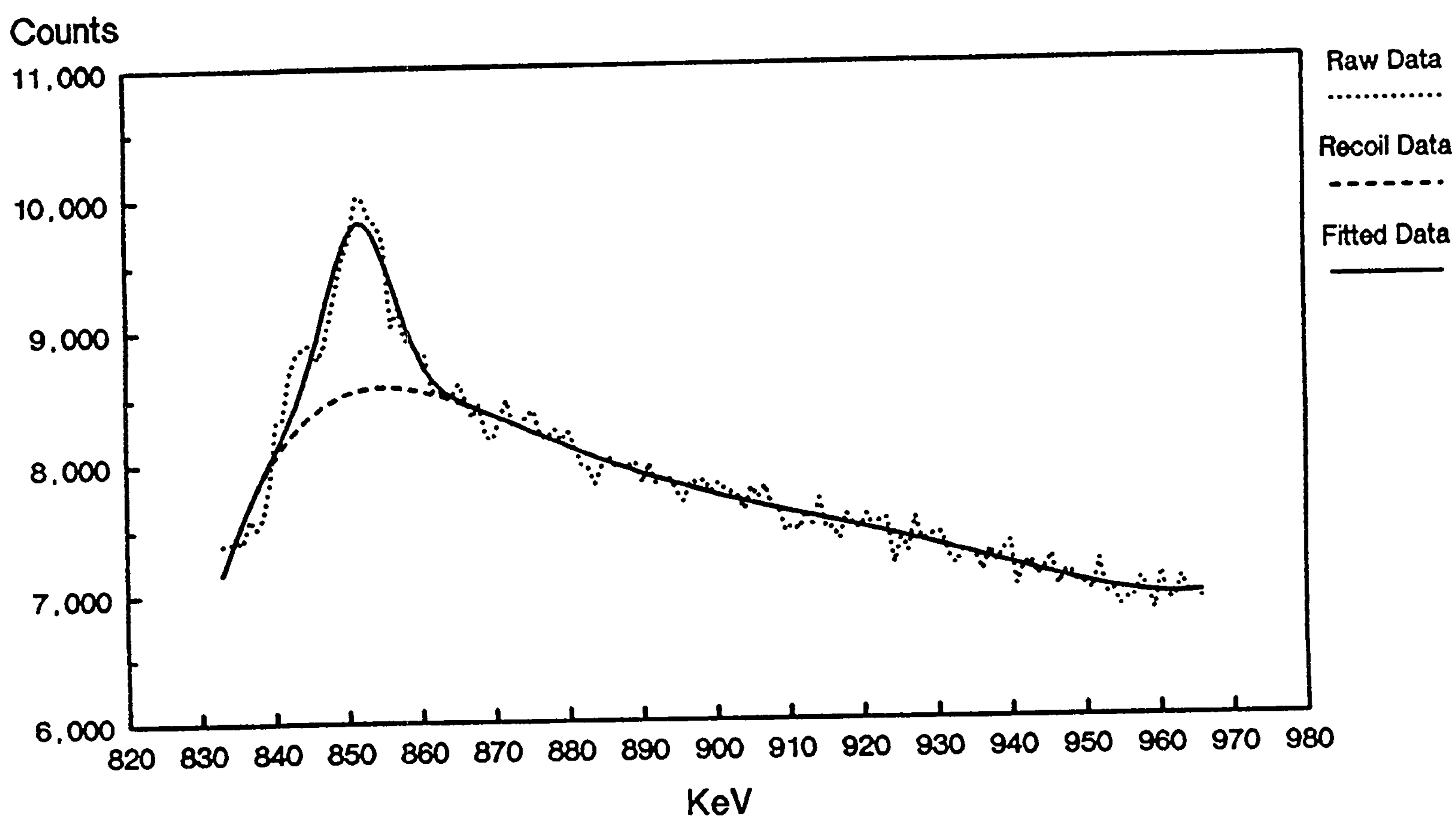

Fig. 9 Ganymed Fitting of 835 keV Peak For
38.4 Mev Neutrons

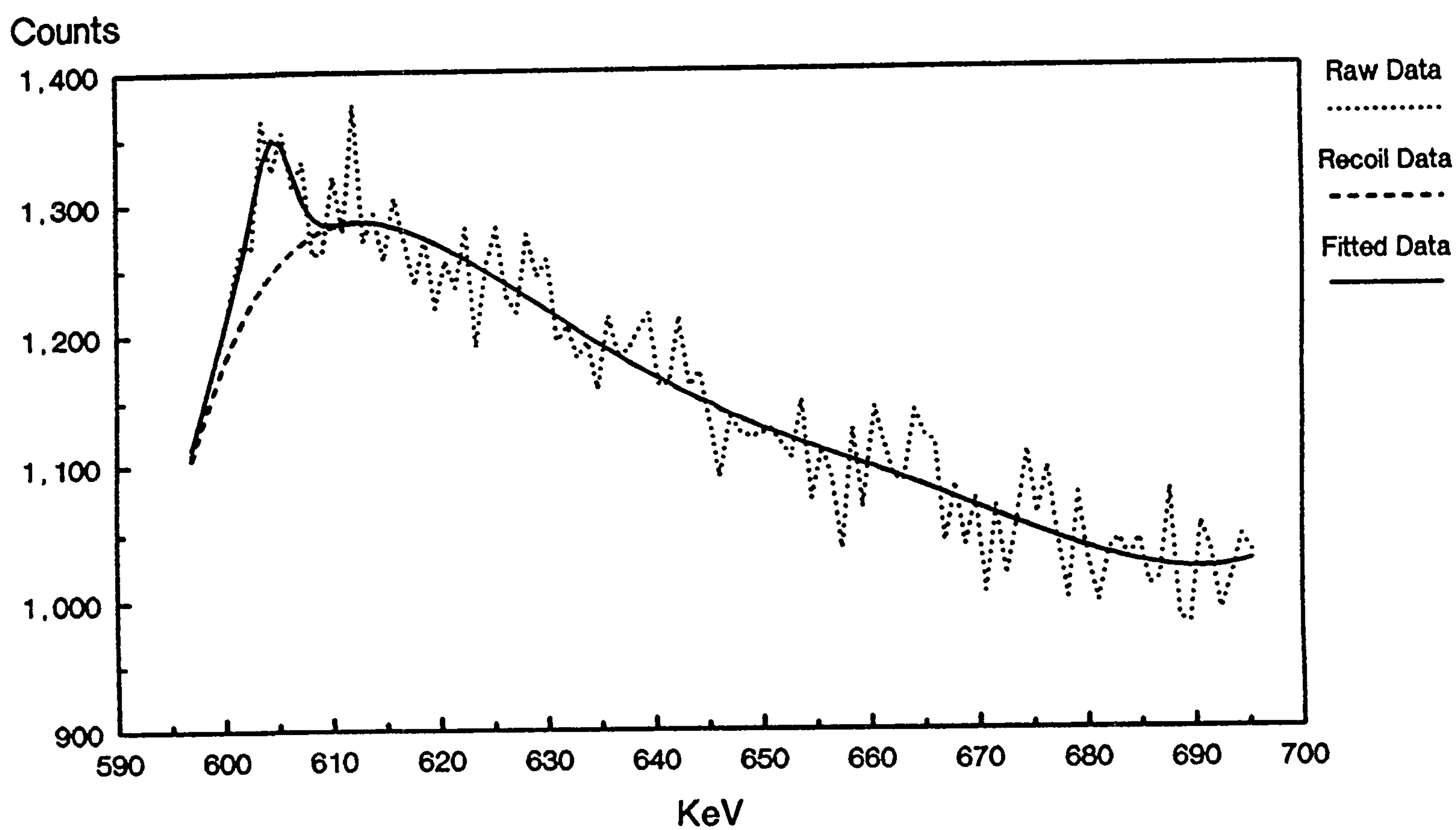

Fig. 10 Ganymed Fitting of 596 keV Peak from
65.5 MeV Neutrons

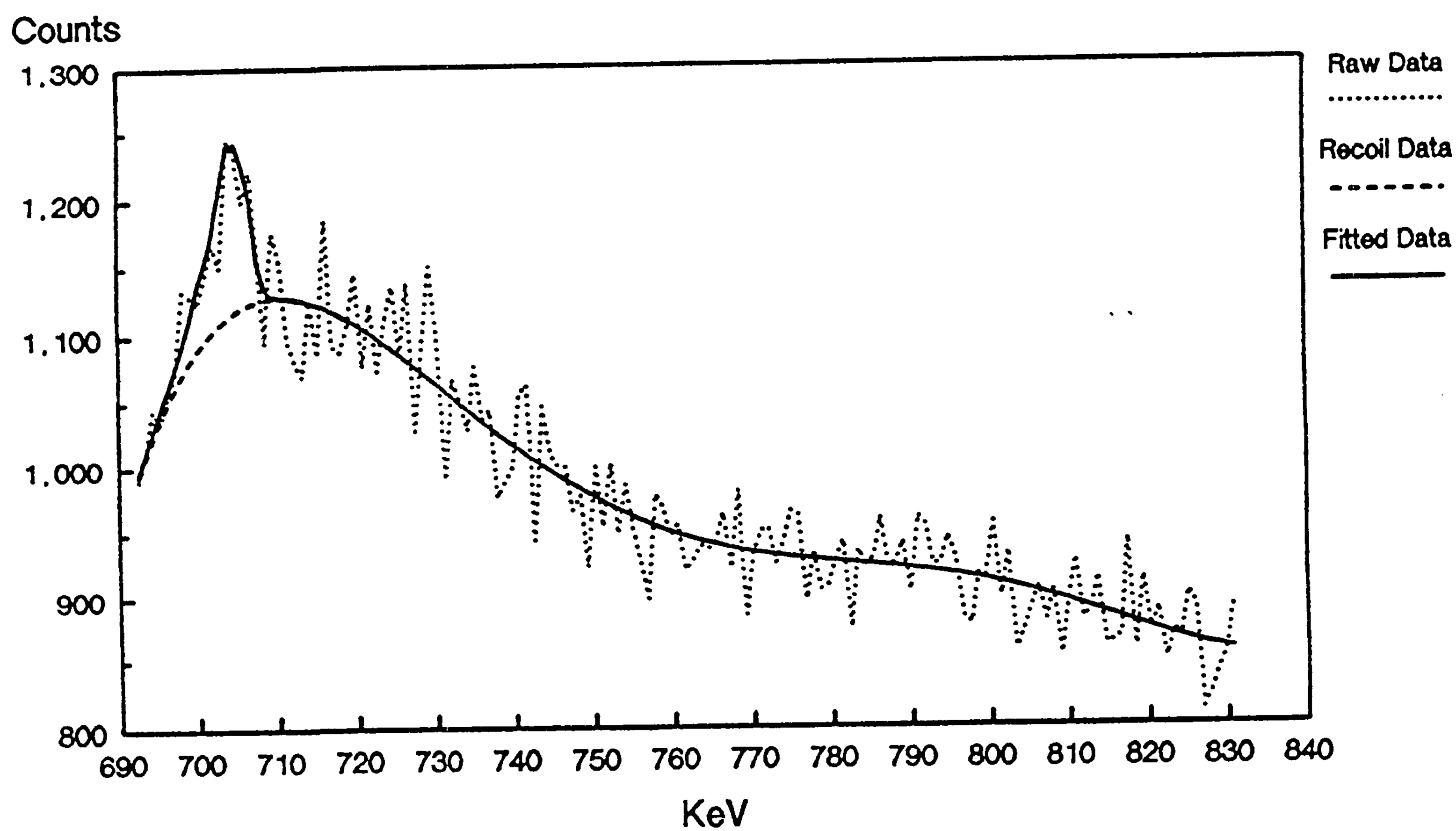

Fig. 11 Ganymed Fitting of 690 keV Peak of
65.5 MeV Neutrons

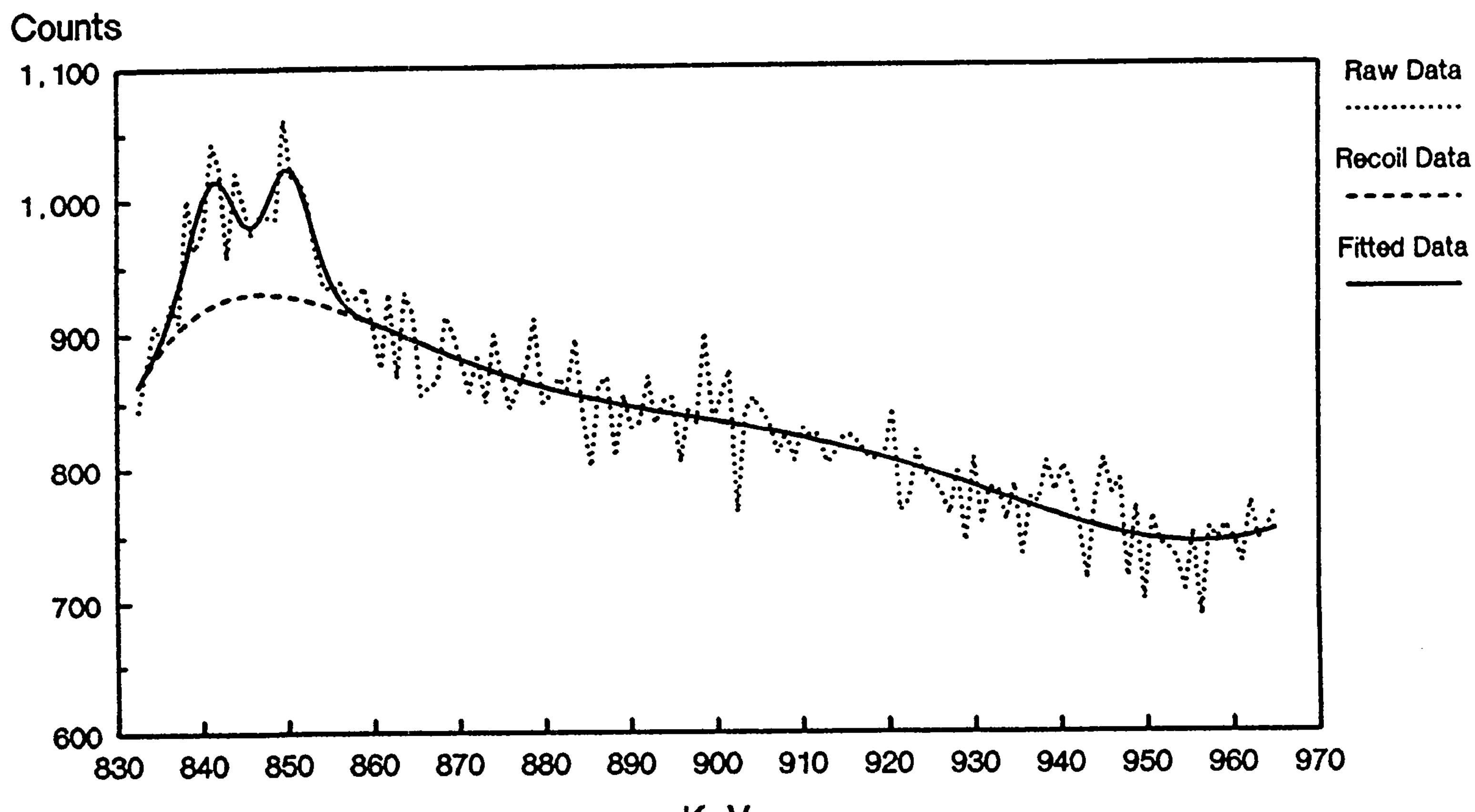

Fig. 12 Ganymed Fitting of 835 keV Peak from
65.5 MeV Neutrons

Three characteristics of the germanium recoil background curve were evaluated: 1) the full width at half, third, fourth, fifth, tenth and twentieth maximums; 2) the slope of different segments of the low energy upslope leg of the curve; and 3) the slope of the first leg of the high energy downslope segment of the curve.

The background germanium recoil portion of the printout was imported into the Lotus 123 program for evaluation of the full width measurements. Utilizing a macro previously written for the Lotus program with modifications made to incorporate a larger number of data points, full widths at half, third, fourth, fifth, tenth and twentieth maximum were calculated for each of the nine recoil curves. (See Appendix B for Lotus 123 macro.) The results from this analysis are presented in Table 2.

The next step was to evaluate the slopes of the recoil germanium spectra. The data was entered into another Lotus program called Graphwriter. This program has the capabilities of performing a group of regression fitting calculations for the entered data. The results are presented with a slope and intercept for the fit and a regression coefficient (R^2). An R^2 value of 1 indicates a perfect fit to the data. The slope measurements for these curves are the change in counts divided by the change in keV. The neutron energy curves all had approximately the same change in keV channel; however, the relative change in counts was vastly different. To overcome this relative difference in counts, all curves were normalized to a maximum count of 10000 for evaluation.

The upslope was evaluated with a linear fit over the first three, five and ten keVs of the curve. The slopes and the regression coefficients were recorded (see Table 3).

The first leg of the downslope was also evaluated with a linear fit. Four methods were used for selecting the area to be fitted. The first method was to select visually the most linear segments of the downslope leg. The other methods were based on determining the point on the downslope leg of the curve where the second derivative was equal to zero (zero point). This point was used as the center point for the area to be fitted. The second and third method utilized the zero point and one and five points on either side of it, respectively. The fourth method utilized the maximum equal number of points on either side of the zero point that maintained a regression coefficient greater than 0.999. The absolute value of the slope was used to facilitate the use of the computer programs. Values are recorded in Table 4.

Table 2

Width Measurements (keV) for the Recoil Germanium Curves

	Curves (keV)								
	596			690			835		
	Neutron Energy (MeV)								
Peak Width	18.8	38.4	65.5	18.8	38.4	65.5	18.8	38.4	65.5
Half	42.5	48.0	33.4	26.3	30.9	33.9	69.1	53.1	29.2
Third	56.3	60.8	41.1	31.7	37.6	39.4	93.3	37.6	34.9
Fourth	67.7	69.8	45.5	34.5	41.4	42.9	102.7	81.3	36.9
Fifth	75.3	76.9	48.2	36.3	43.4	44.0	108.0	87.4	38.7
Tenth	85.8	89.9	54.1	40.3	51.3	48.6	119.7	98.4	42.5
20th	93.3	94.1	57.3	42.1	53.3	50.8	124.2	103.4	44.5

Table 3

Upslope Fittings and Regression Coefficient Values

Curve Peak keV	Neutron Energy MeV	3 keV	R^2	5 keV	R^2	10 keV	R^2
596							
	18.8	313.2	0.9999	302.9	0.9993	270.6	0.9962
	38.4	255.0	0.9998	240.2	0.9987	203.7	0.9922
	65.5	203.1	0.9988	183.0	0.9953	138.6	0.9759
690							
	18.8	474.2	0.9991	423.1	0.9950	310.3	0.9691
	38.4	310.1	0.9993	280.7	0.9962	213.9	0.9734
	65.5	145.0	0.9995	133.1	0.9973	106.9	0.9853
835							
	18.8	256.3	0.9997	239.5	0.9983	200.8	0.9911
	38.4	178.3	0.9995	165.4	0.9988	135.9	0.9889
	65.5	109.8	0.9991	98.3	0.9954	73.0	0.9723

Table 4

Absolute Value of Downslope Fittings and Regression Coefficient Values

Curve Peak (kev) / Neutron Energy (MeV)	Visual	R^2	3 Point*	11 Point	R^2	Maximum Points	R^2
596							
18.8	85.8	0.9998	88.9	87.5	0.99995	83.4	0.9992
38.4	53.6	0.9996	56.0	55.5	0.99998	52.6	0.9992
65.5	40.0	0.9991	42.3	41.8	0.99997	39.9	0.9991
690							
18.8	117.9	0.9994	123.1	120.8	0.99993	117.0	0.9992
38.4	69.8	0.9993	72.8	72.3	0.99996	68.8	0.9992
65.5	41.8	0.9994	43.6	43.4	0.99993	41.8	0.9991
835							
18.8	33.2	0.9992	35.3	34.6	0.99993	32.6	0.9990
38.4	27.3	0.9995	28.6	28.3	0.99999	26.9	0.9991
65.5	26.9	0.9992	28.4	28.1	0.99996	27.1	0.9993

* All R^2 are greater than 0.9999999

Figures 13-21 are graphic representations of the upslope fitting utilizing the first five keV and the downslope fitting utilizing the second derivative zero point and ± 5 keV technique for point selection.

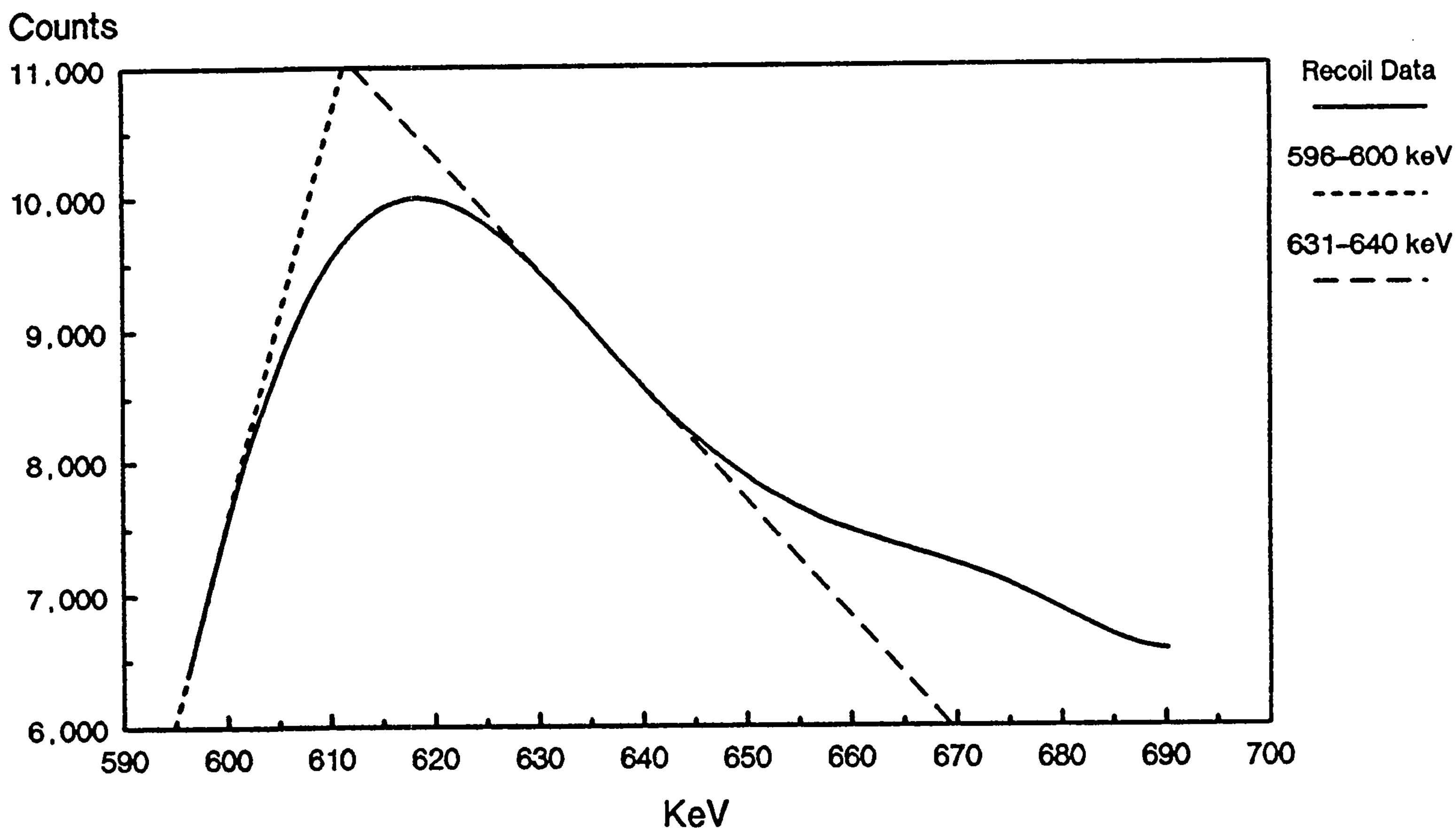

Fig. 13 Slope Fittings for 596 keV Recoil
Data from 18.8 MeV Neutrons

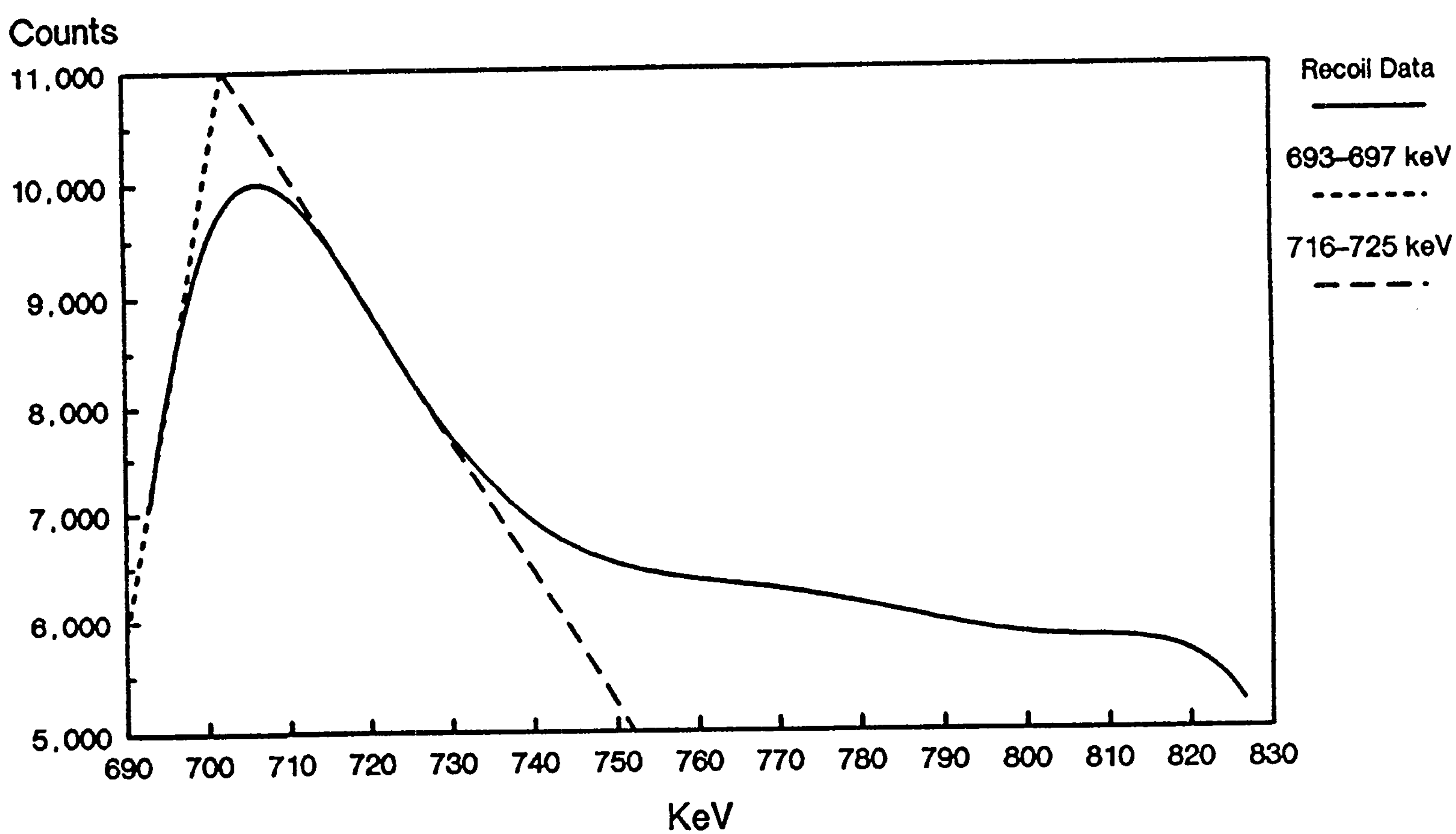

Fig. 14 Slope Fitting for 690 keV Recoil
Data from 18.8 MeV Neutrons

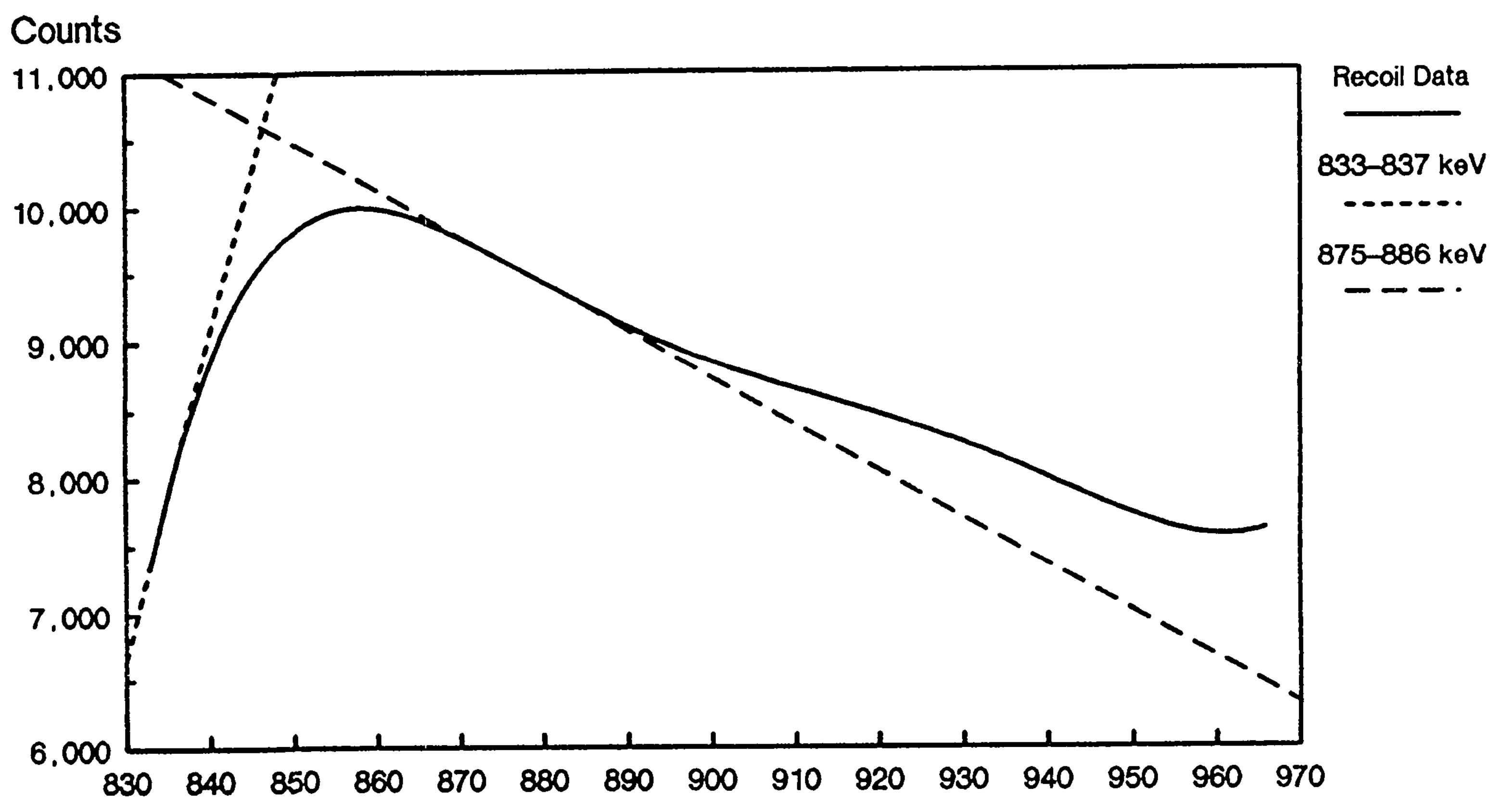

Fig. 15 Slope Fittings for 835 keV Recoil
Data from 18.8 MeV Neutrons

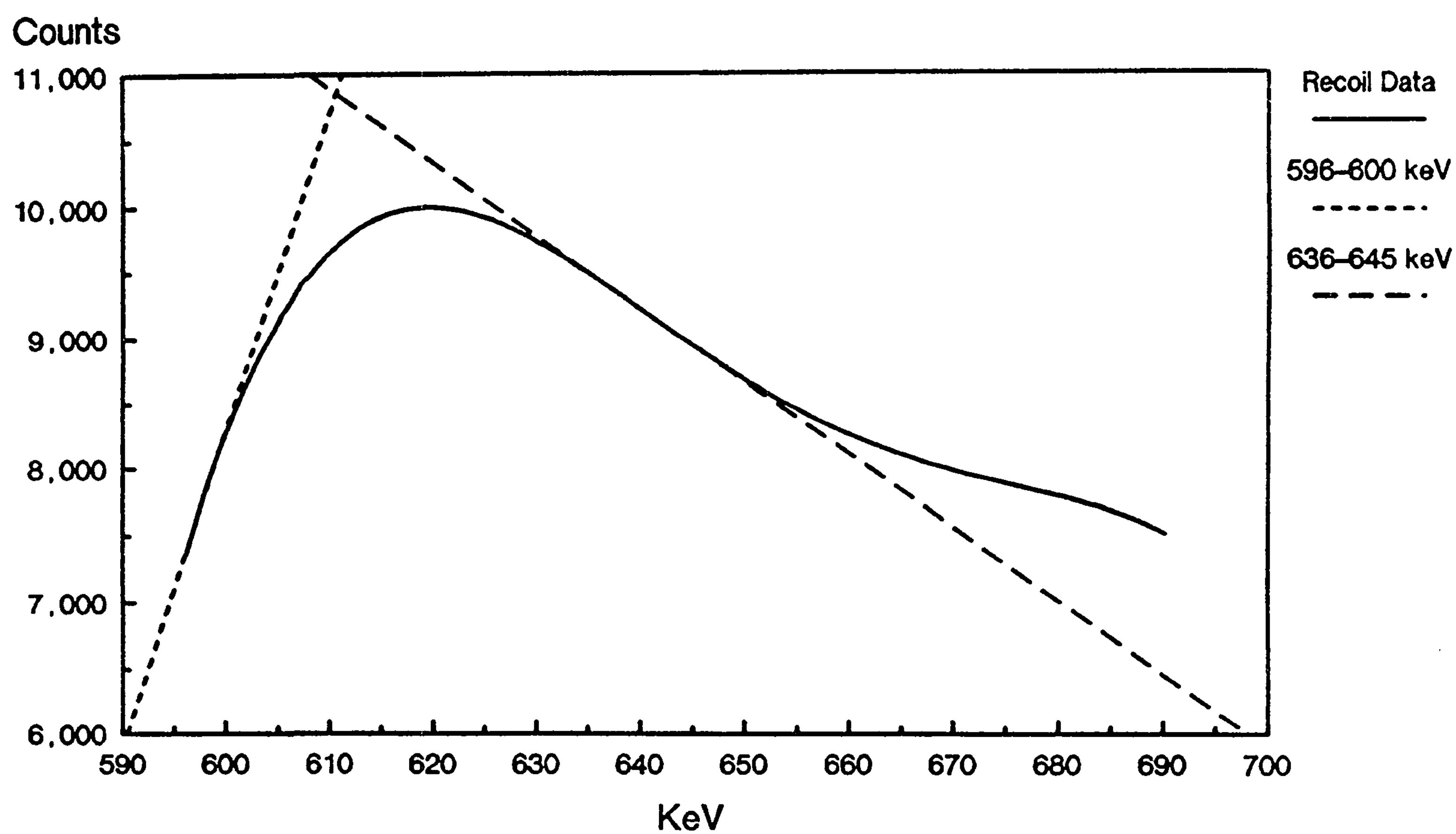

Fig. 16 Slope Fitting for 596 keV Recoil
Data from 38.4 MeV Neutrons

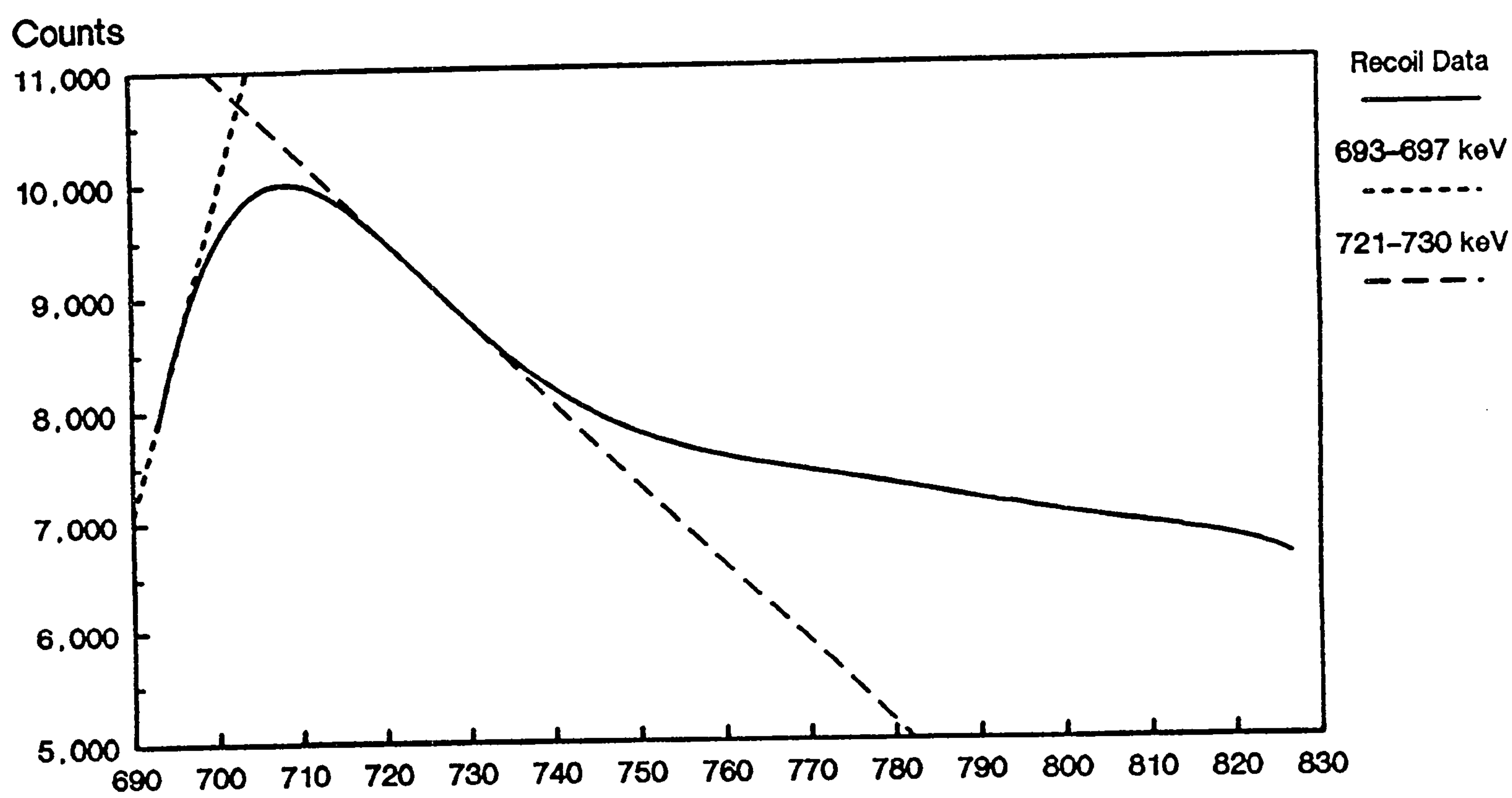

Fig. 17 Slope fittings for 690 keV Recoil
Data from 38.4 MeV Neutrons

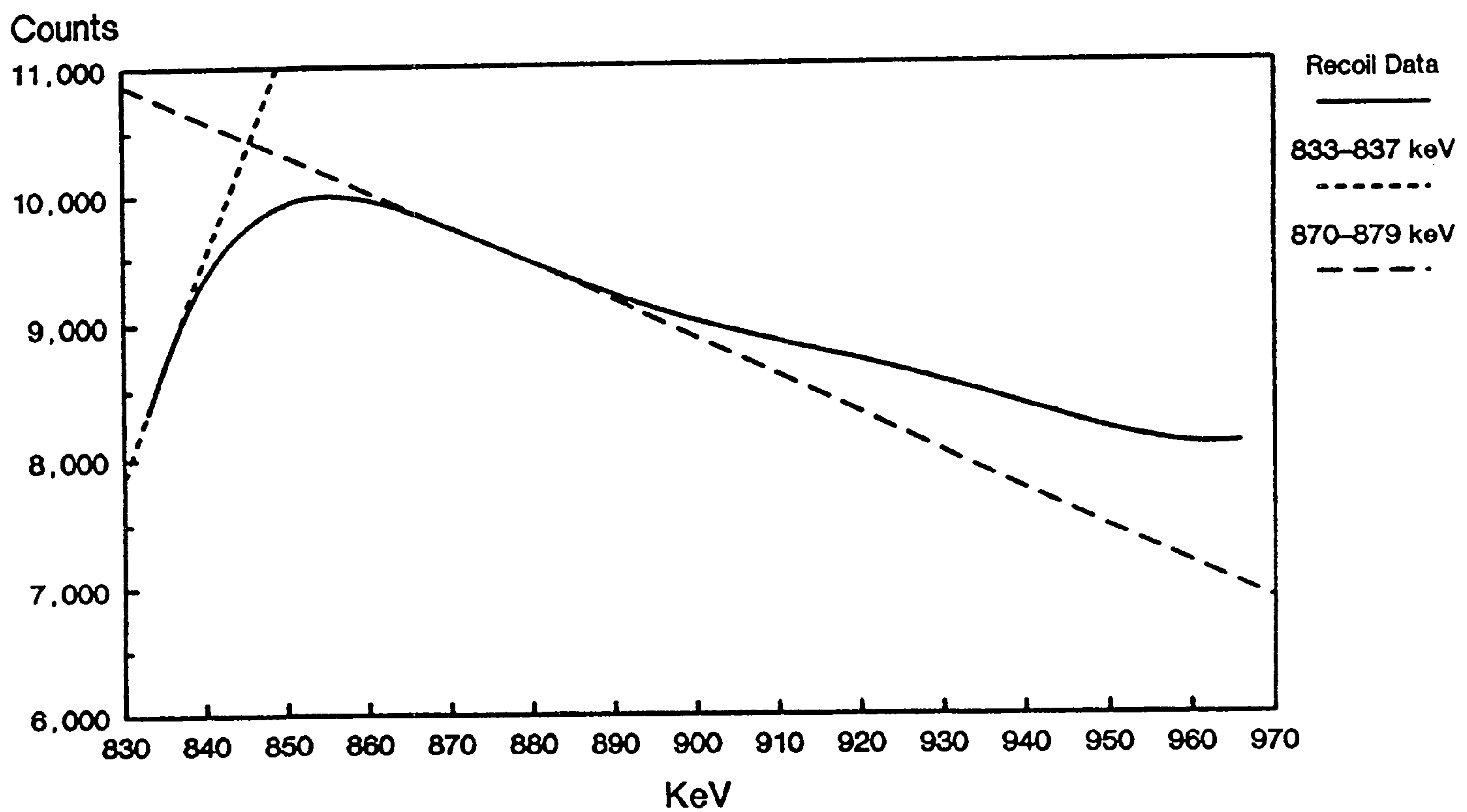

Fig. 18 Slope Fittings for 835 keV Recoil
Data from 38.4 MeV Neutrons

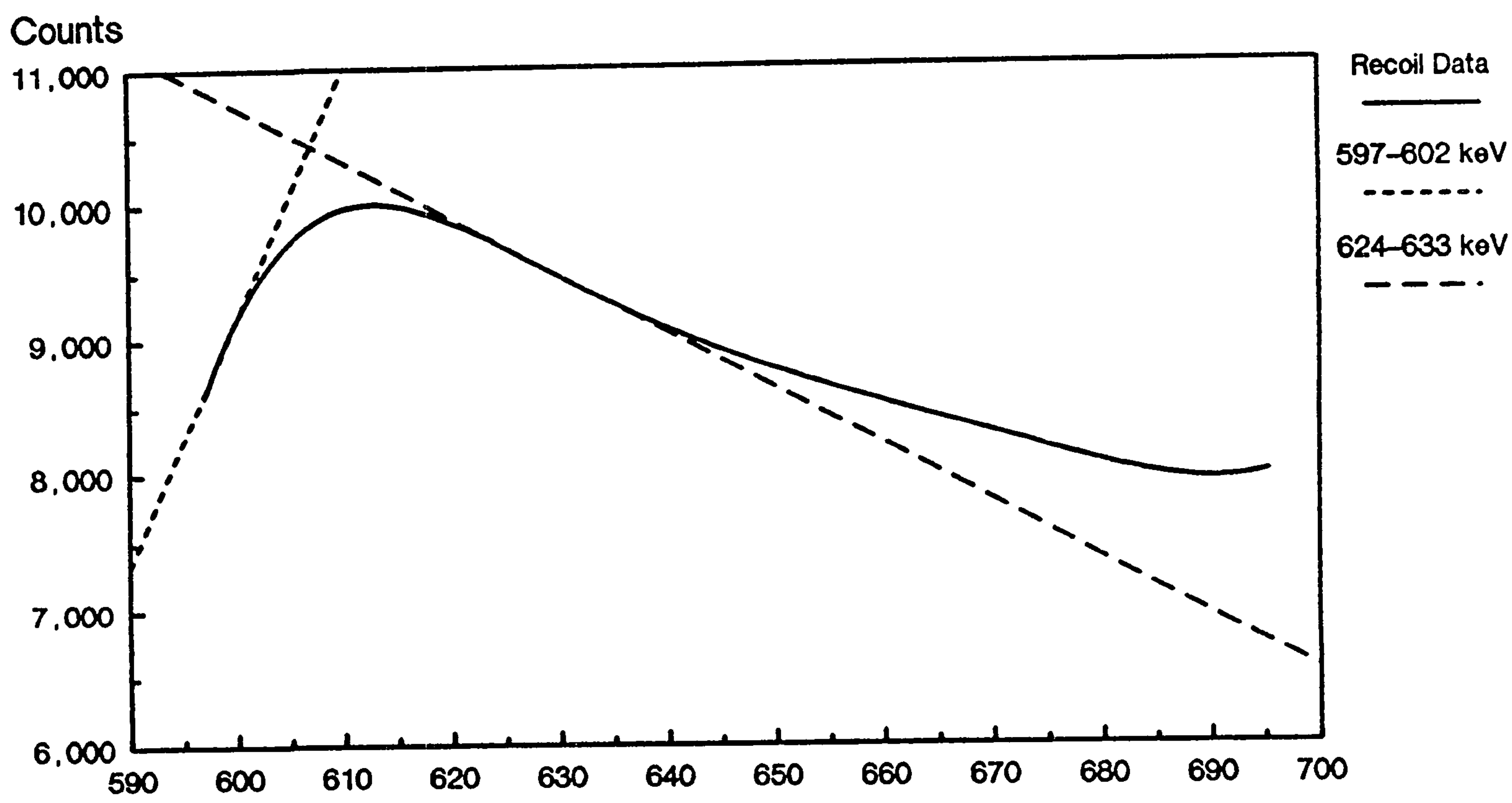

Fig. 19 Slope Fittings for 596 keV Recoil
Data from 65.5 MeV Neutrons

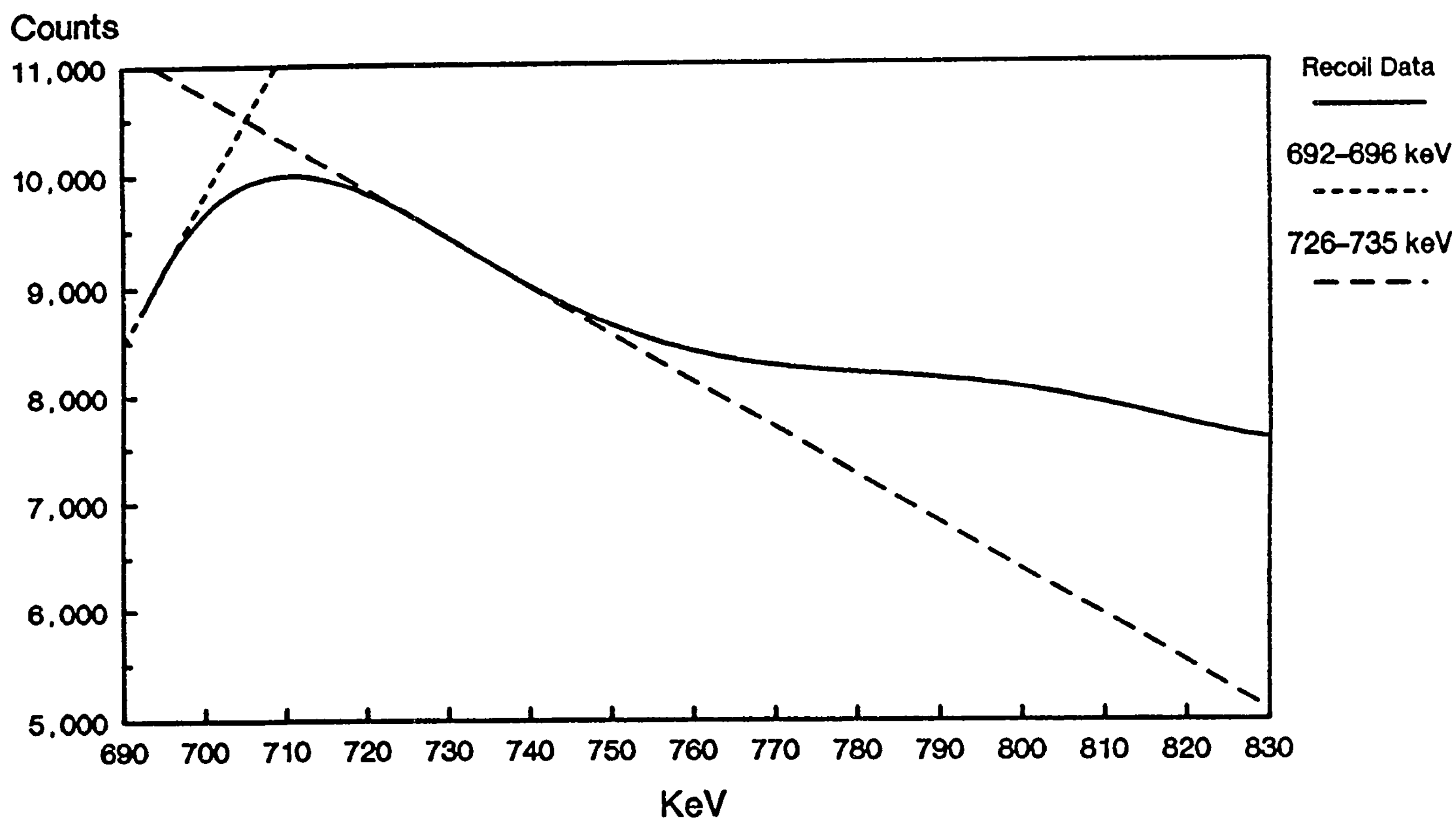

Fig. 20 Slope Fittings for 690 keV recoil
Data from 65.5 MeV Neutrons

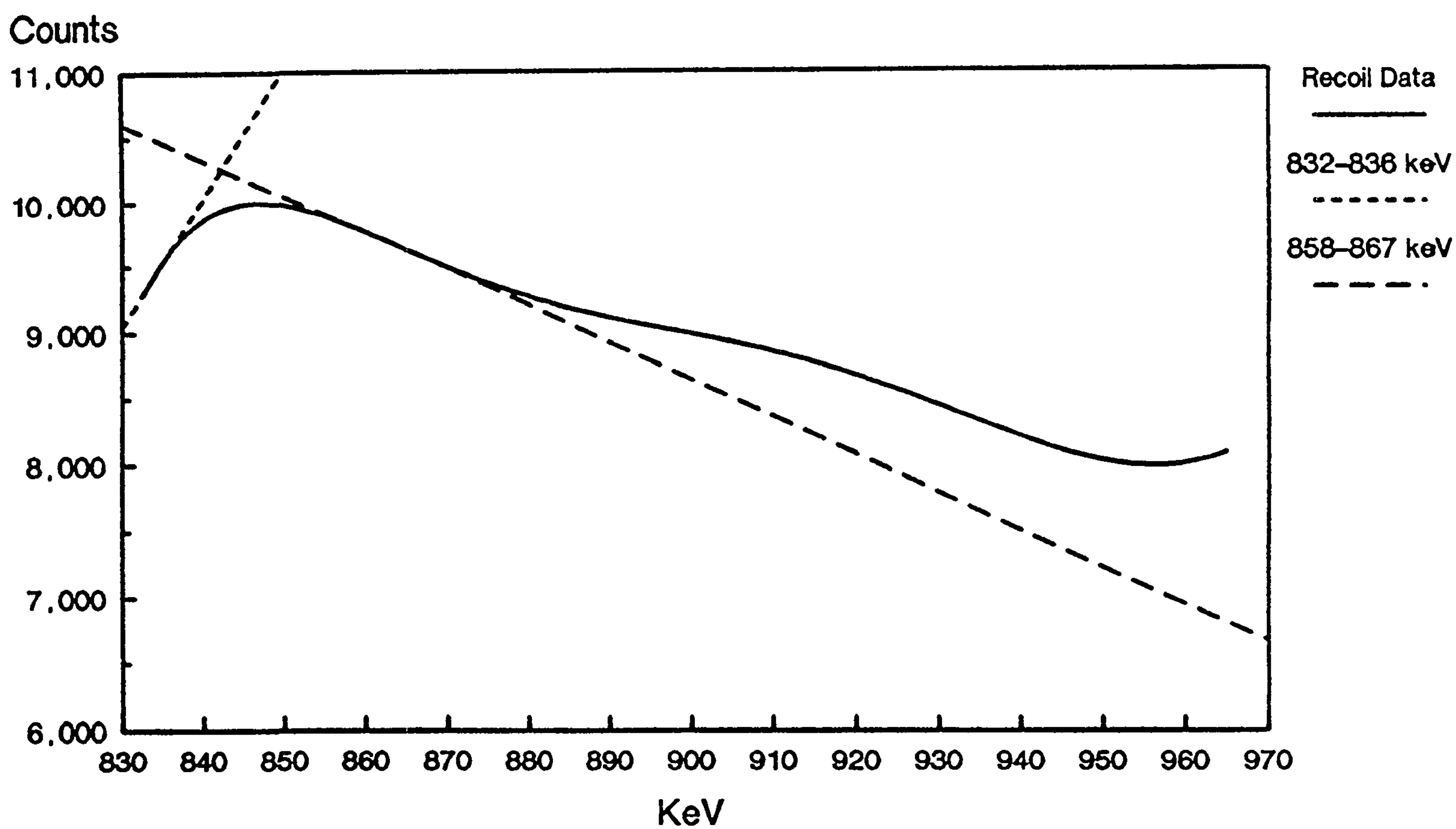

Fig. 21 Slope Fitting For 835 keV Recoil
Data from 65.5 MeV Neutrons

Chapter 5: Discussion

The three different peaks (595, 690, 835 keV) that were evaluated were created in the same manner, i.e. the combination of gamma ray or electron conversion energy and the recoil germanium nucleus energy. The primary difference between the peaks should be the amount of energy the germanium nucleus transferred to the electron-hole pairs. It would therefore be reasonable to conclude that the three parameters evaluated would respond in a similar manner for all three recoil curves. However, when the full width measurements in Table 2 were graphed (Figures 22-24), the curves demonstrated that each of the peaks responded in a different manner as the energy of the neutrons increased.

It was shown by Chasman et al. (1965a) and Smith (1972) that the curves were visually wider with increasing neutron energy. However, the calculations for the 596 keV peak decreased between neutron energies of 38.4 and 65.5 MeV and the 835 keV peak decreased over all three neutron energies. The 690 keV peak increased between each of the neutron energies, however, the amount it increased between 38.4 and 65.5 MeV was minimal. Overlaying the normalized data that was used for slope measurements (Figures 25-27), demonstrated that the amount of activity for the leading minimum point of each curve is greater at higher neutron energies.

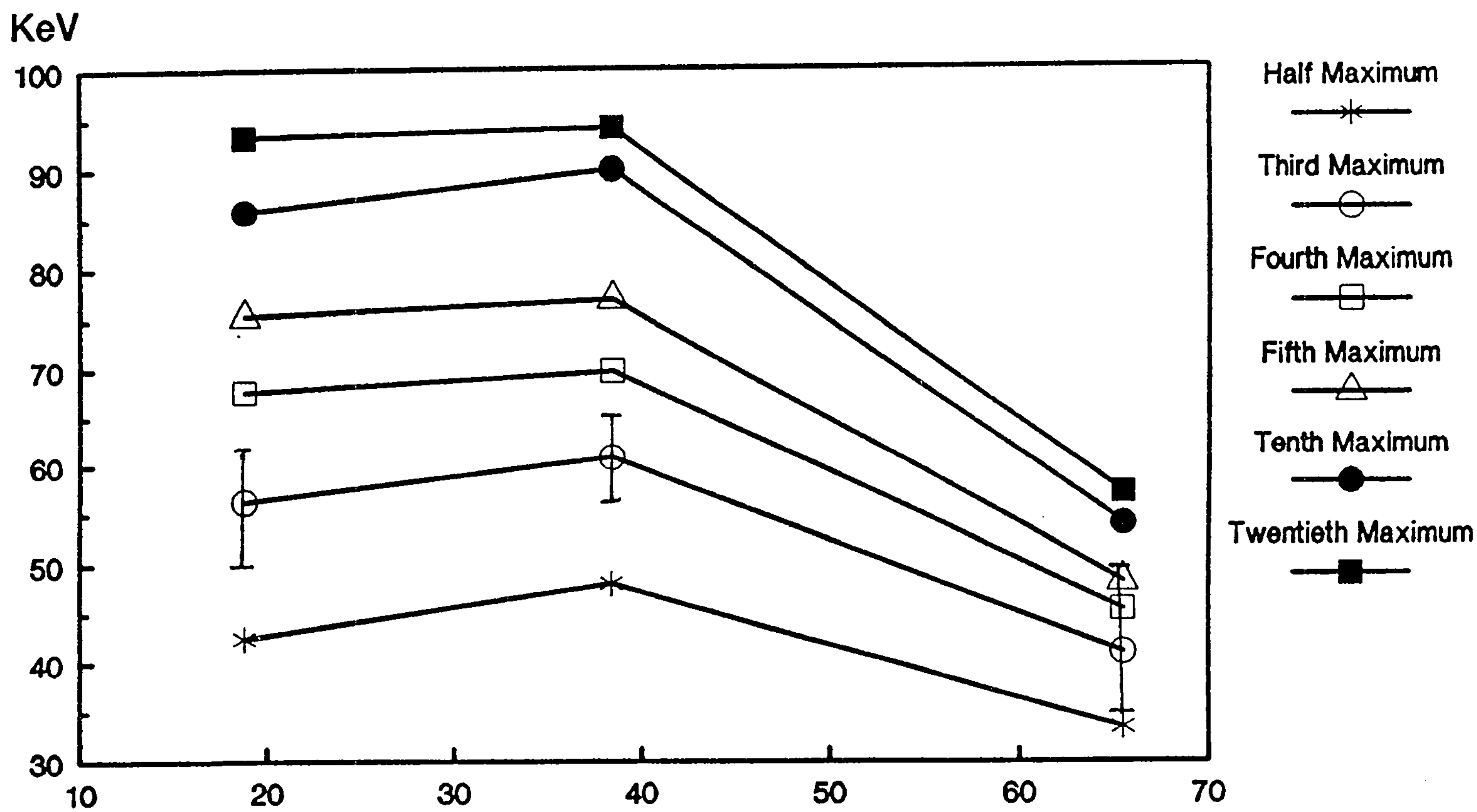

Fig. 22 Curve Width Comparisons for 596 keV Recoil Data

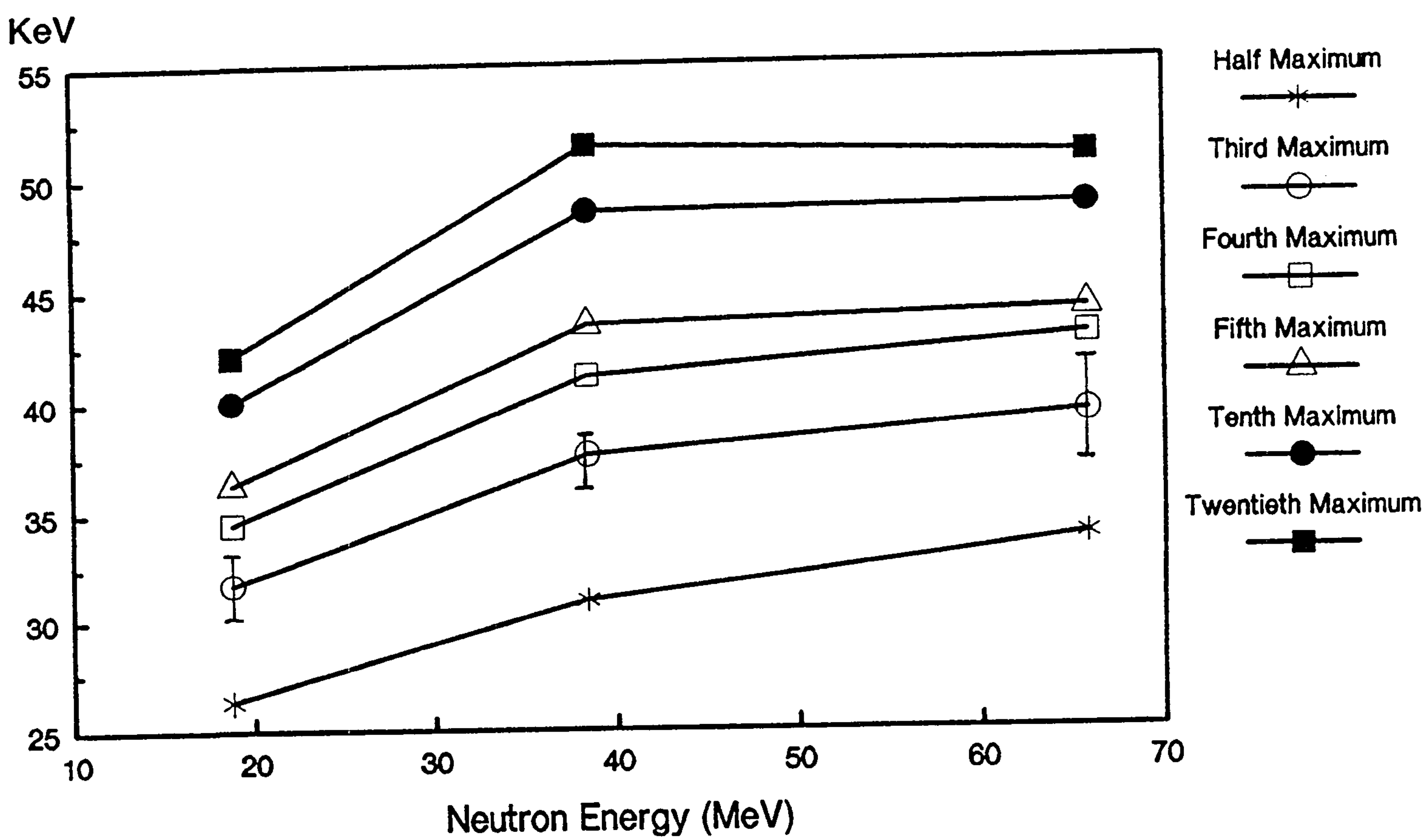

Fig. 23 Curve Width comparisons for 690 keV
Recoil Data

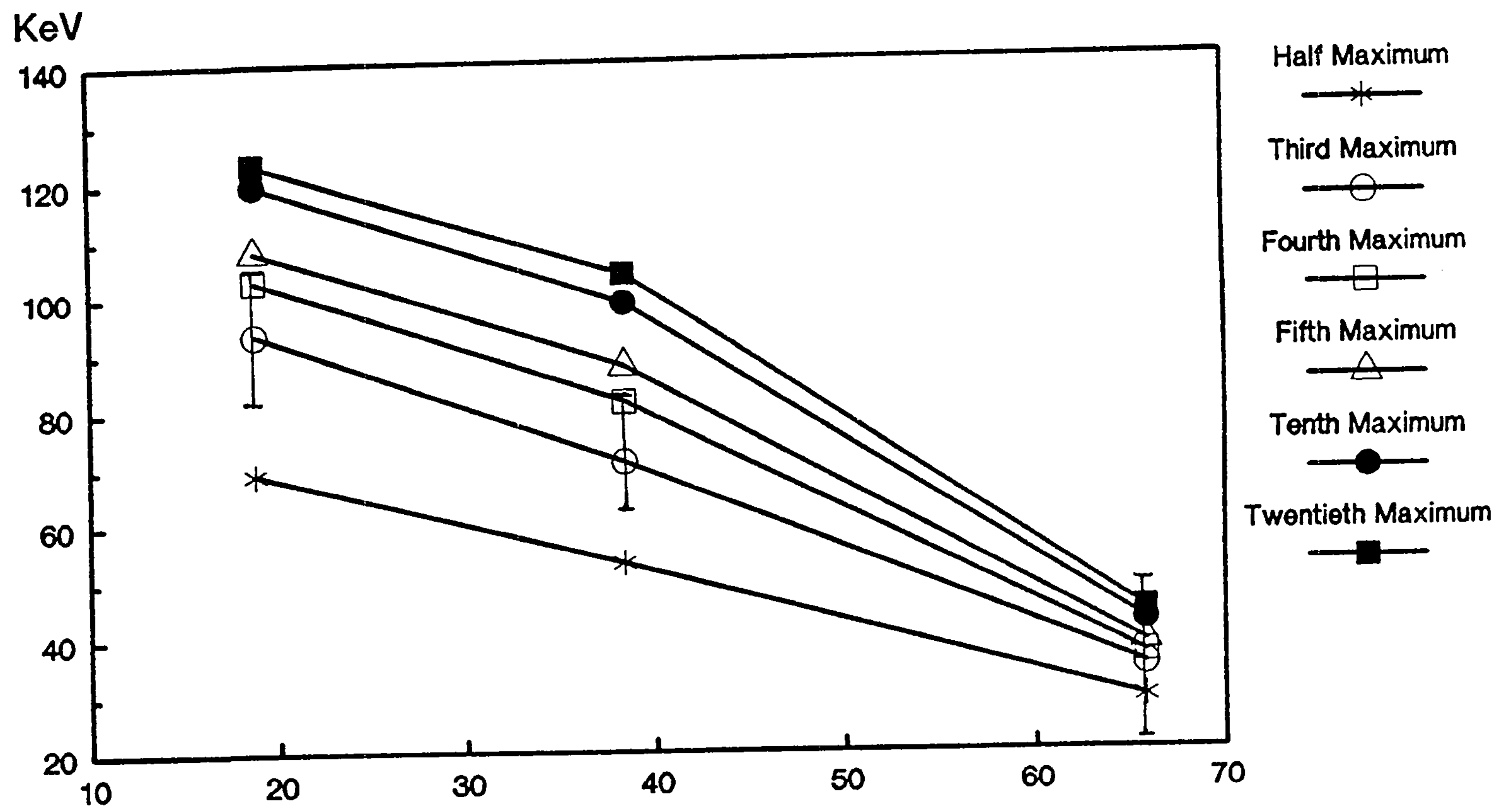

Fig. 24 Curve Width Comparison for 835 keV
Recoil Data

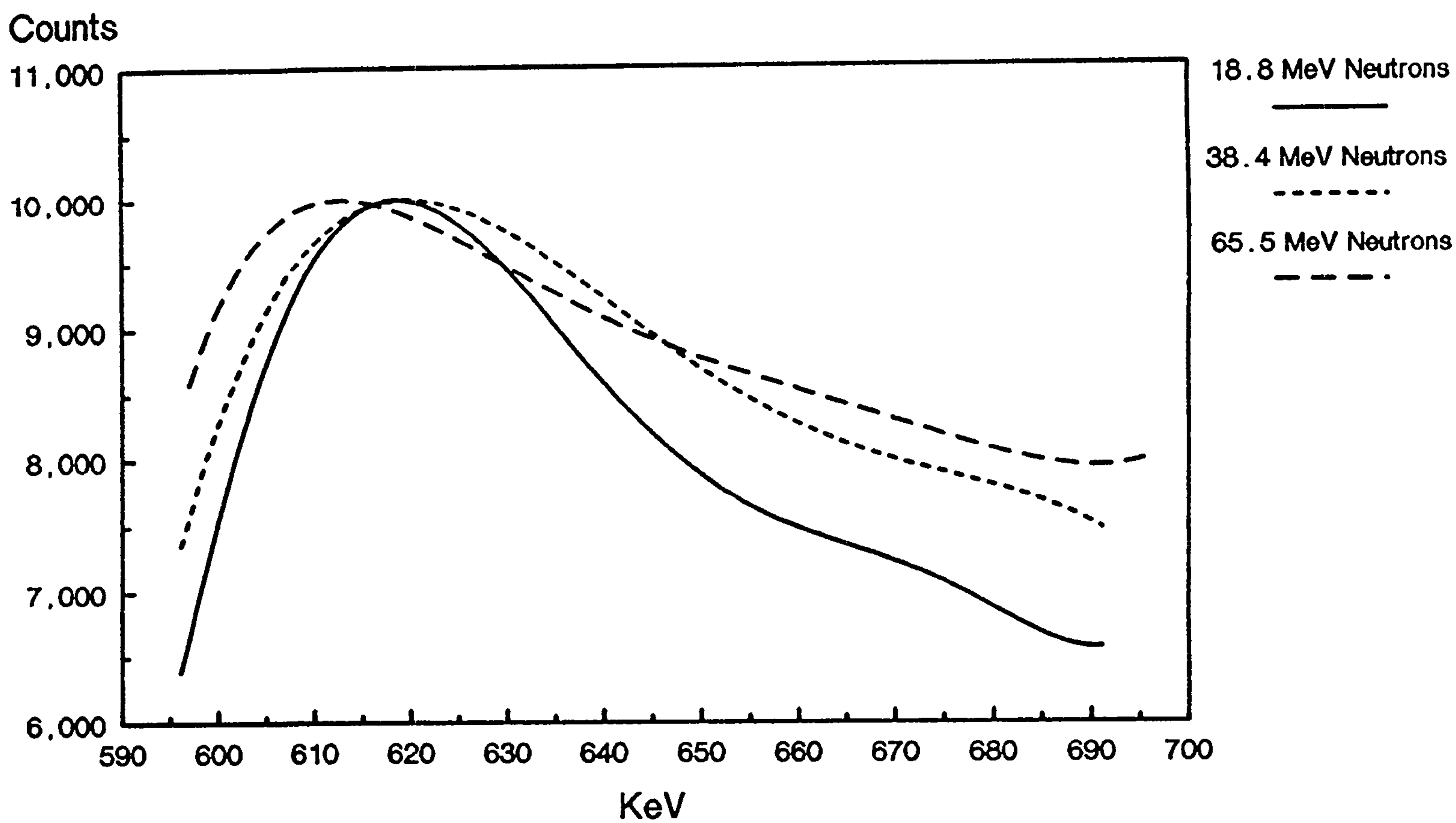

Fig. 25 Normalized Overlay of 596 keV
Recoil Data

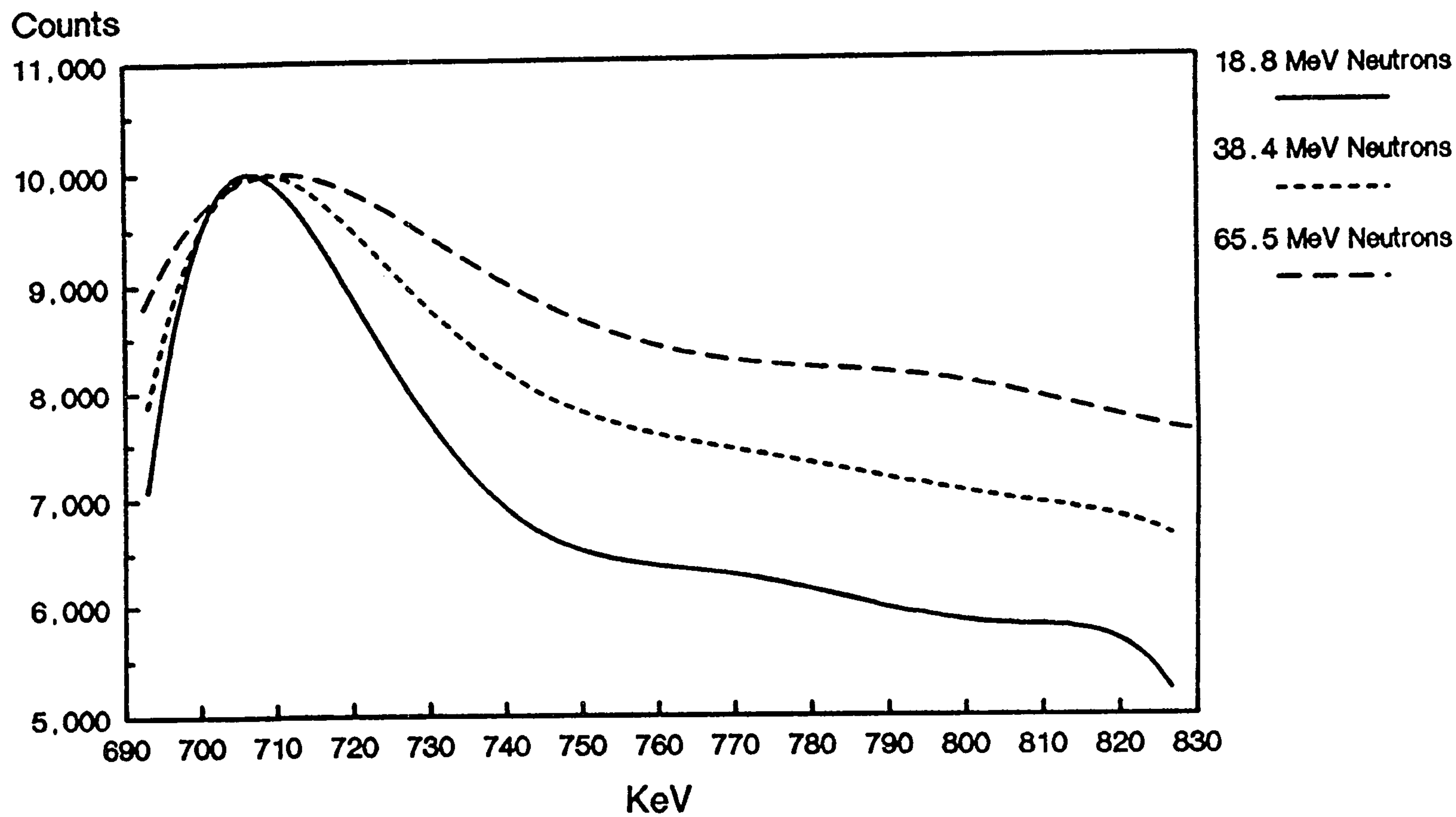

Fig. 26 Normalized Overlay of 690 keV
Recoil Data

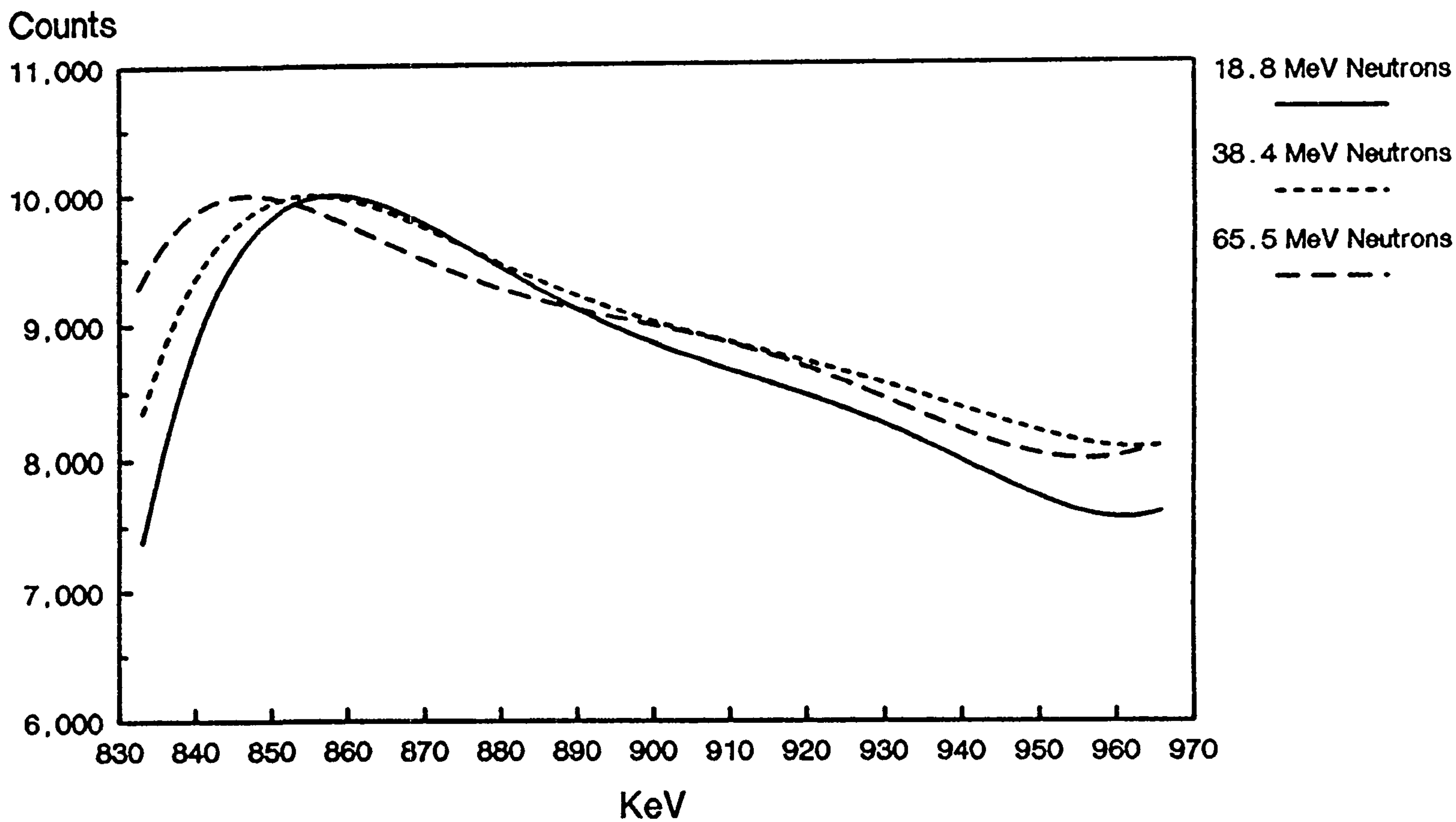

Fig. 27 Normalized Overlay for 835 keV
Recoil Data

The increase in the leading minimum point was caused by a "bleeding" of activity from the lower energy recoil curve into the curve of interest. The increase in the leading point value resulted in a higher calculated value of the width line and thus a smaller width measurement. Using the kinematics of neutron scattering one can explain the "bleeding" of activity from one curve into another.

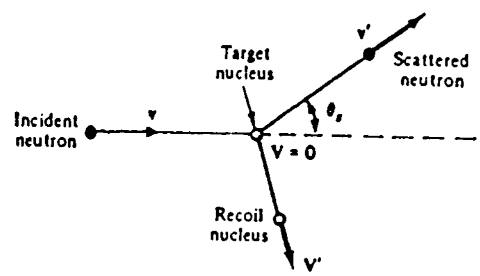

Figure 28 Laboratory system for the kinematics of neutron scattering (Chilton, Shultis and Faw, 1984).

In the laboratory system (see Figure 28) conservation of energy and momentum require:

$$\tfrac{1}{2}mv^2 = \tfrac{1}{2}mv'^2 + \tfrac{1}{2}MV'^2 - Q \qquad 5.1$$

$$mv = mv' + MV' \qquad 5.2$$

where v, v' and V' are the velocities of the neutron before and after the scattering event and the velocity of the recoil nucleus respectively. The magnitude of Q is the excitation energy that the recoil nucleus radiates.

The law of cosines can be written with $\Omega = \cos\theta$:

$$|v' - v|^2 = v^2 + v'^2 - 2vv'\Omega \qquad 5.3$$

After squaring equation 5.2 and rearranging the terms the equation becomes:

$$V'^2 = (m/M)^2 (v^2 + v'^2 - 2vv'\Omega) \quad 5.4$$

Substitution of V'^2 of equation 5.4 into equation 5.2 yields:

$$mv^2 (m - M) + mv'^2 (m + M) - 2m^2 vv'\Omega = 2MQ \quad 5.5$$

Expressing the speeds v and v' in terms of the initial and final neutron energies E and E' and rearranging the equation yields:

$$\Omega(E,E') = \tfrac{1}{2}[(A + 1)\sqrt{(E'/E)} - (A - 1)\sqrt{(E'/E)} - QA/\sqrt{(EE')}] \quad 5.6$$

where A = M/m. This equation presents the relationship between the neutron energies before and after scattering and the cosine of the scattering angle in the laboratory system. Equation 5.6 is a quadratic equation in $\sqrt{E}'$ whose solution is:

$$E'(\Omega,E) = [1/(A + 1)^2][\Omega\sqrt{E} \pm \sqrt{\{E(\Omega^2 + A^2 - 1) + A(A + 1)Q\}}]^2 \quad 5.7$$

(Chilton, Shultis and Faw, 1984).

Equation 5.7 was used to calculate the energy of the expelled neutron n' based on the angle of scattering and the initial energy of the neutron. Substituting these values back into equation 5.1 the energy of the recoil germanium nucleus was calculated. A computer program was written that evaluated this equation with variable inputs for neutron energy, A and Q over scattering angles of 0 to 180°. The program along with the results for the neutron energies used and Q values observed in the scattering of neutron with germanium nuclei are found in Appendix C. The maximum recoil energies were 984, 2024 and 3504 keV for the 18.8, 38.4 and 65.5 MeV neutrons respectively at a Q value of -0.596 MeV. For a Q value of -0.690 MeV the maximum recoil energies were 1010, 2080 and 3580 keV.

The energy transferred to the electron-hole pairs from the recoil germanium nuclei, as calculated with Lindhard's equations (1963) is shown in Figures 29 and 30. There is a 33 keV difference between the 563 and 596 keV recoil energy levels. The difference between 596 and 690 keV is 94 keV and between 690 and 835 keV is 140 keV. The results shown in Figures 29 and 30 indicate that much of the recoil energy from the lower excitation state was recorded in the higher excitation levels. As the neutron energy increased, the maximum amount of energy that was transferred to the electron-hole pairs also increased and more of this activity appeared in the next higher excitation state. Figure 31 schematically demonstrates this relationship between the two excitation states. The solid line is the shape from a lower neutron energy and the broken line from a higher neutron energy. The difficulty in removing the "bleeding" of activity from a lower state into a higher state resulted from the uncertainty as to the level of the background continuum in this area of the curve as seen in Figures 1-3.

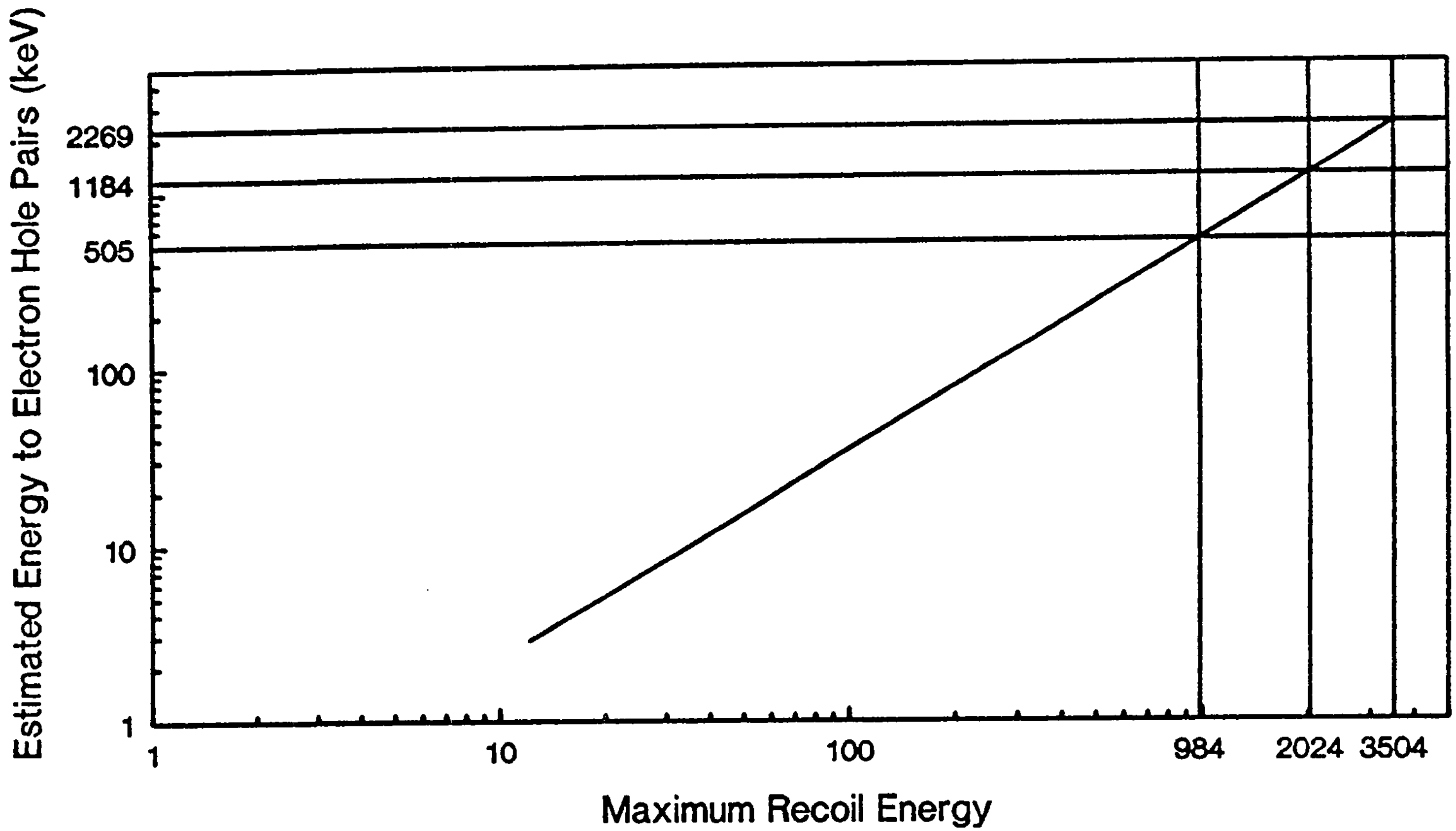

Fig. 29 Relationship between Recoil Energy and Energy Transfered to Electron Hole Pairs for 596 keV Recoil Data

Adapted From Lindhard et al.

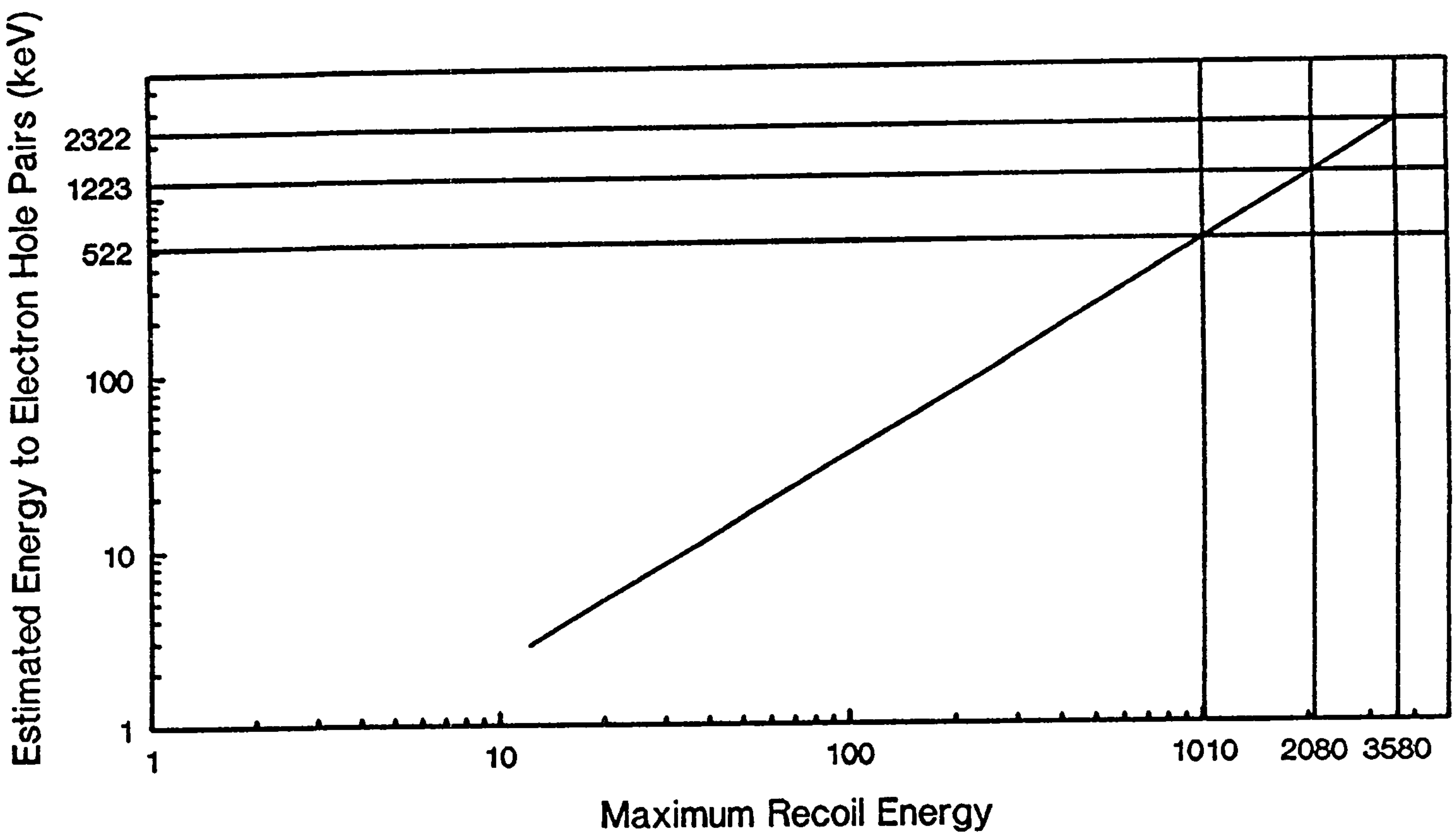

Fig. 30 Relationship between Recoil Energy and Energy Transfered to Electron Hole Pairs for 690 keV Recoil Data

Adapted From Lindhard et al.

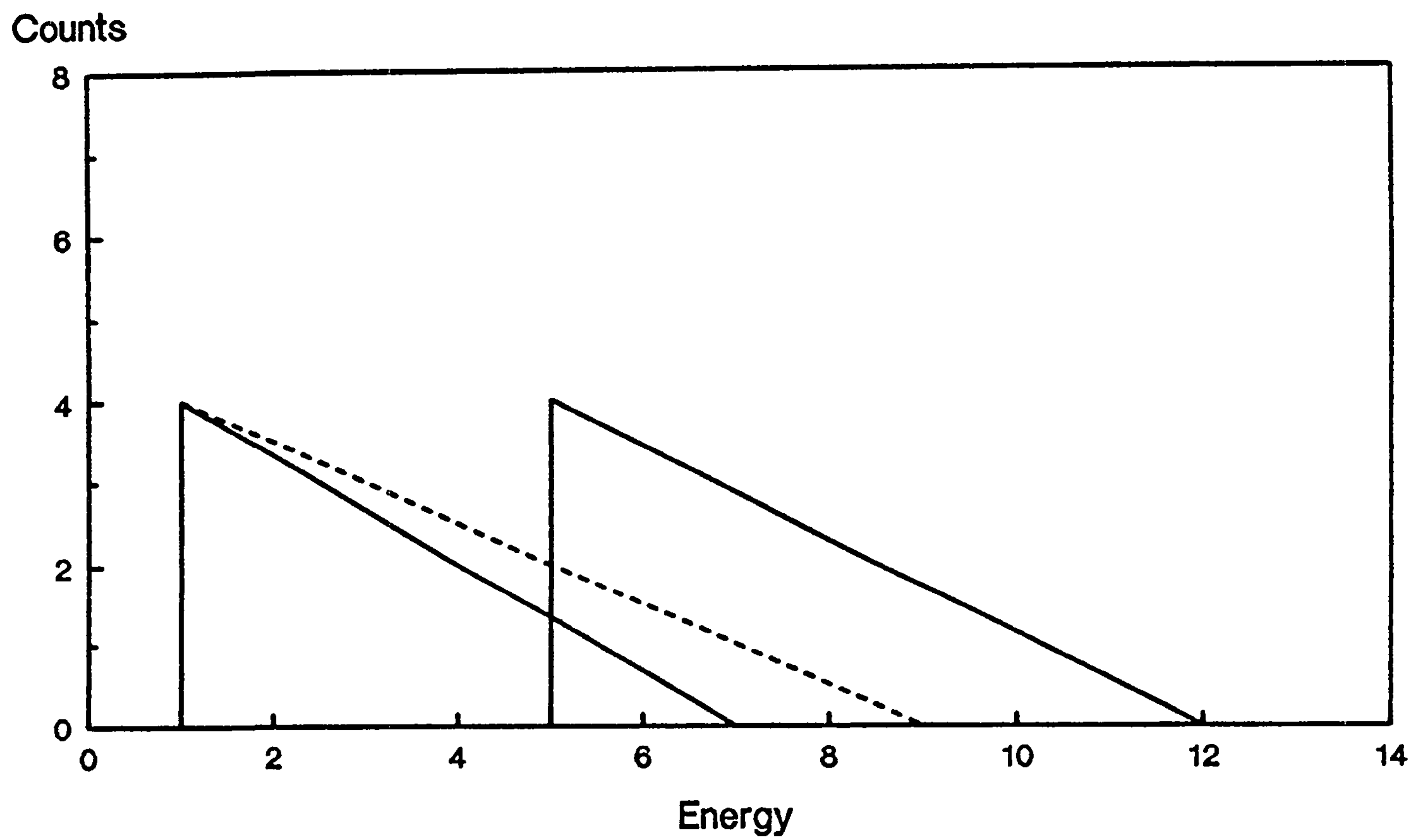

Fig. 31 Schematic Representation of the Bleeding of Recoil Energy from one Excitation State to the Next High Excitation State

It was seen from the data shown in Table 3 the upslopes measured at 3, 5 or 10 keV all followed a similar pattern. When this data was graphed, with the neutron energy on the x-axis and the slope plotted on a logarithmic scale, all three recoil peaks plotted a straight line. The graphs for the 5 keV slope fittings are shown in Figure 32.

A logarithmic fit was performed on each of these lines to determine an equation to describe the lines in the form:

$$Y = a(e^{(bX)}) \qquad 5.8$$

where a is the intercept and b is the slope of the line. All three recoil peaks presented the same pattern (Figure 33). In following the argument that an increase in neutron energy will result in a larger "bleeding" from a lower to a higher peak, it was noted that the curves from the 65.5 Mev neutrons demonstrated a spread of only 13 keV from the initial point of the curve to the maximum point. Consequently, if this determination were to extend beyond the neutron energies studied, the 10 keV slope determination would begin to involve portions of the peak and downslope and no longer be a true measure of the upslope. Tables 5 and 6 present values for a, b and the R^2 regression coefficient for the 3 and 5 keV fits respectively.

Table 5 Line Function Parameters for the 3 keV Upslope Fit

Peak Curve	b	a	R^2
596	-0.009220	369.10142	0.9960160
690	-0.025537	788.05459	0.9951706
835	-0.018135	359.44913	0.9999077

Table 6 Line Function Parameters for the 5 keV Upslope Fit

Peak Curve	b	a	R^2
596	-0.010744	367.80462	0.9978301
690	-0.024935	695.88448	0.9945830
835	-0.019077	343.28974	0.9999789

Solving equation 5.8 for X, the neutron energy and using a factor to account for the normalization of the recoil curves to a maximum count of 10000 we have:

$$X = (\ln (S * (10000/M))/a)/b \qquad 5.9$$

where X = Neutron energy
S = Slope of first 3 or 5 keV of upslope for the recoil curve
M = Maximum count in recoil curve
a and b are values for the respective curves found in Tables 5 and 6.

A check of these values was performed by evaluating the original slope calculations with the above formulas. All recalculations showed a reasonable estimation of the original neutron energy as seen in Table 7.

Table 7 Evaluation of Measured Slopes Utilizing 3 and 5 keV Upslope Formulas

Original Neutron Energy (MeV)	3 keV Calculation			5 keV Calculation		
	Recoil Curves			Recoil Curves		
	596	690	835	596	690	835
18.8	17.8	19.9	18.6	18.0	19.9	18.9
38.4	40.1	36.5	38.7	39.7	36.4	38.3
65.5	64.8	66.3	65.4	65.0	66.3	65.6

Both equations provided acceptable estimations of the neutron energy with all three recoil curves. The best results were obtained with the 835 keV recoil curve. If the values obtained from the 596 and 690 keV recoil curves were averaged, the estimation of the neutron energy was equal to that of the 835 keV curve. The results for the 10 keV slope determination were similar to the results shown above.

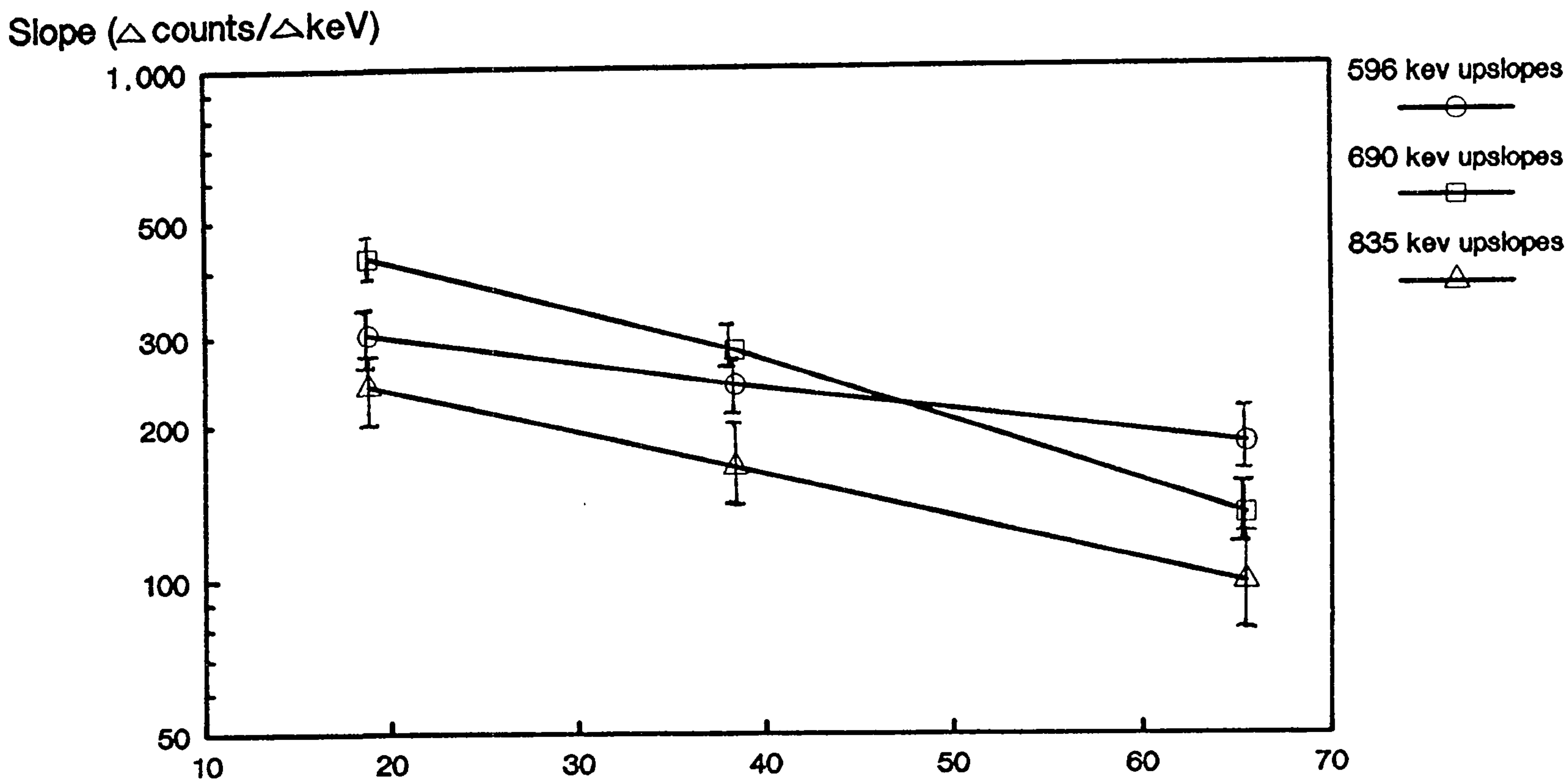

Fig. 32 Linear Slope Fittings for the Upslope Leg Determined from 5 keV Segments

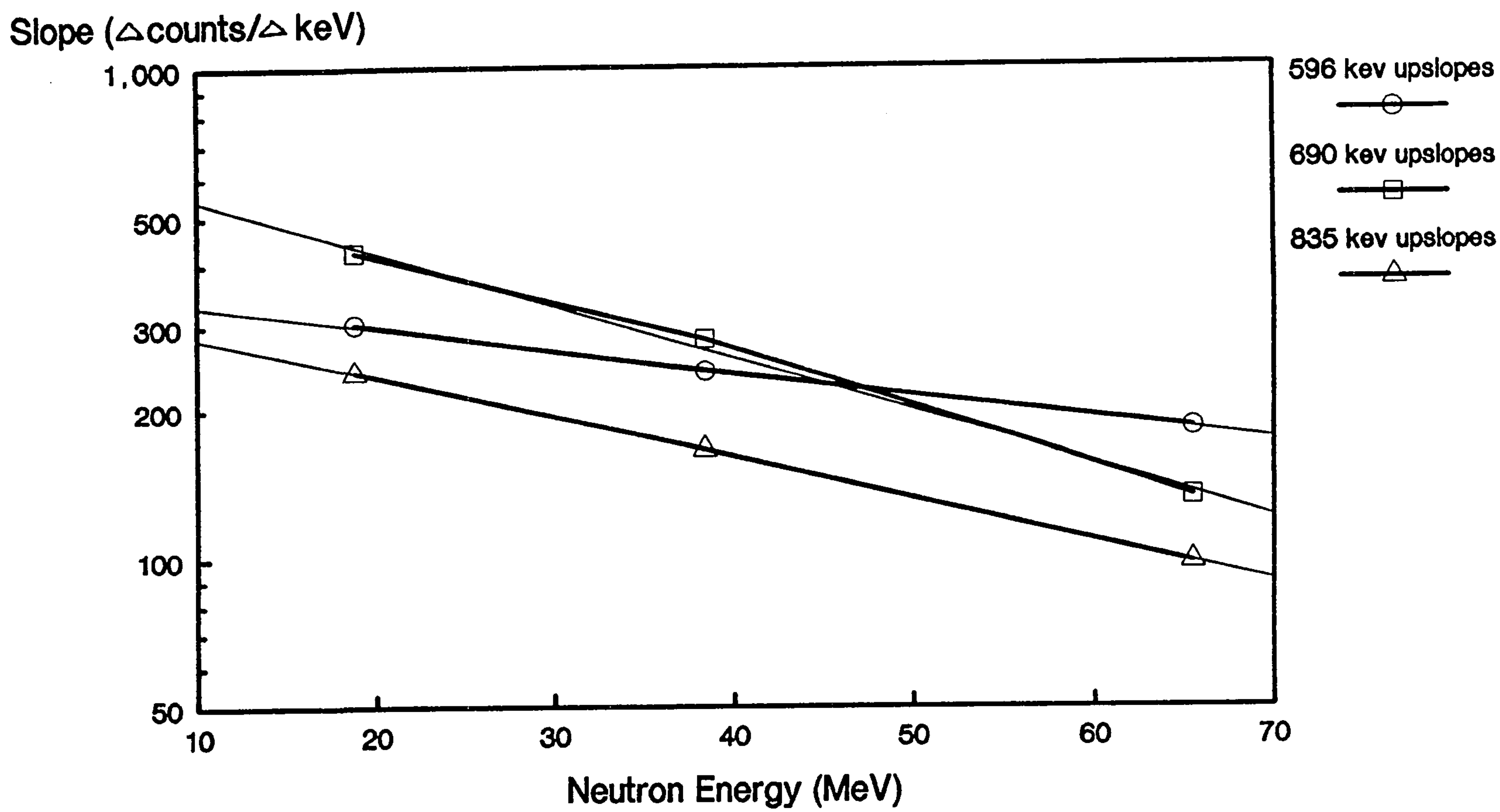

Fig. 33 Logarithmic Fitting of the Linear Upslope Values

The downslope values from Table 4 were plotted on a log-log scale (see Figure 34 for the 11 keV values). These values when plotted demonstrated a straight line. However, a mild variation was observed for the 835 keV recoil curve. There was excellent agreement amoung the four methods used for determining the slope of the curves.

The 835 keV curve probably had reached a point where a large change in neutron energy was needed to show a small change in the downslope of the recoil curve. An evaluation of this curve should be performed at energies between 18.8 and 38.4 MeV to determine where this transition occurred.

The 596 and 690 keV recoil curves were fitted with a power function:

$$Y = aX^b \quad 5.10$$

a and b again represent the intercept and slope of these fitted lines, respectively (Figure 35). Both the visual and maximum ($R^2 > 0.999$) determinations required multiple guesses as to the end points of the fitted areas. This would result in an excessive amount of time for the users of this type of evaluation. Although the results from the visual and maximum types of selections were very similar to the results obtained for the 3 and 11 keV lines the latter two will be discussed here. Tables 8 and 9 present the values for a, b and R^2 for these fittings.

Table 8 Line Function Parameters for the
3 keV Downslope Fit

Recoil Curve	b	a	R^2
596	-0.597885	508.3128	0.9967462
690	-0.826296	1417.5361	0.9942136

Table 9 Line Function Parameters for the
11 keV Downslope Fit

Recoil Curve	b	a	R^2
596	-0.594343	495.7806	0.9974738
690	-0.814584	1345.4889	0.9933723

Using the same symbol designation used for the upslope equation and solving equation 5.10 for the neutron energy yields:

$$X = (-S * (10000/M)/a)^{(1/b)} \qquad 5.11$$

The negative sign appears before the slope value S to account for the negative downslope. The downslopes were plotted as an absolute value in order to perform the power fitting on the computer.

This equation was also checked against the values measured for the three neutron energies utilized for this experiment. The results of this check are seen in Table 10.

Table 10 Evaluation of Measured Slopes Utilizing 3 and 11 keV Downslope Formulas

Original Neutron Energy (MeV)	3 keV Calculation		11 keV Calculation	
	Recoil Curves		Recoil Curves	
	596	690	596	690
18.8	18.5	19.2	18.5	19.2
38.4	40.0	36.3	39.8	36.2
65.5	64.0	67.6	64.2	67.7

Both line lengths provided a reasonable estimation of the maximum neutron energy used to produce the slopes. There appeared to be very little difference between the 3 and 11 keV line lengths used for the slope measurements. The maximum spread and visual selections had similar results.

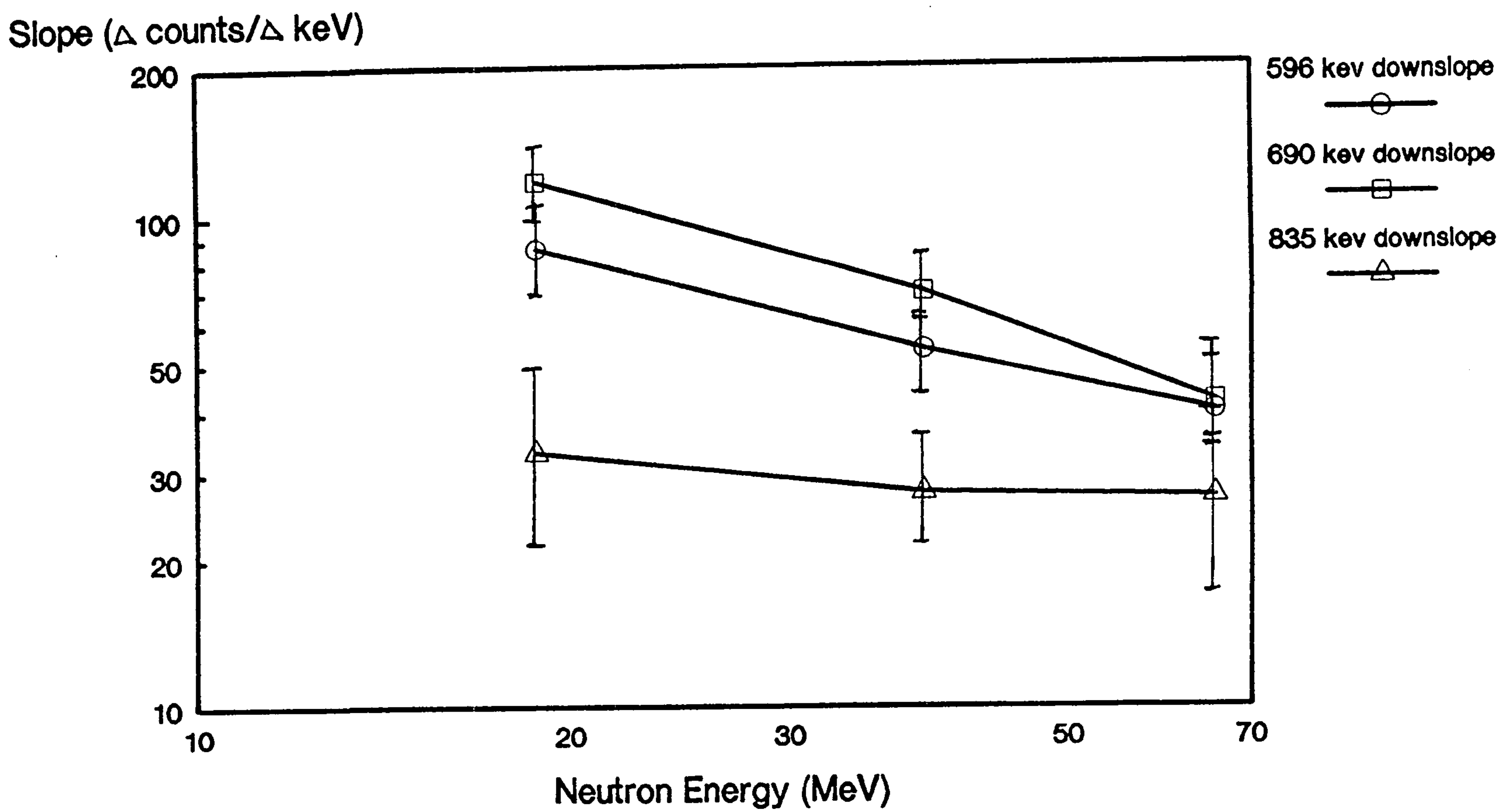

Fig. 34 Linear Slope Fitting for the Downslope Leg Determined From 11 keV Segments

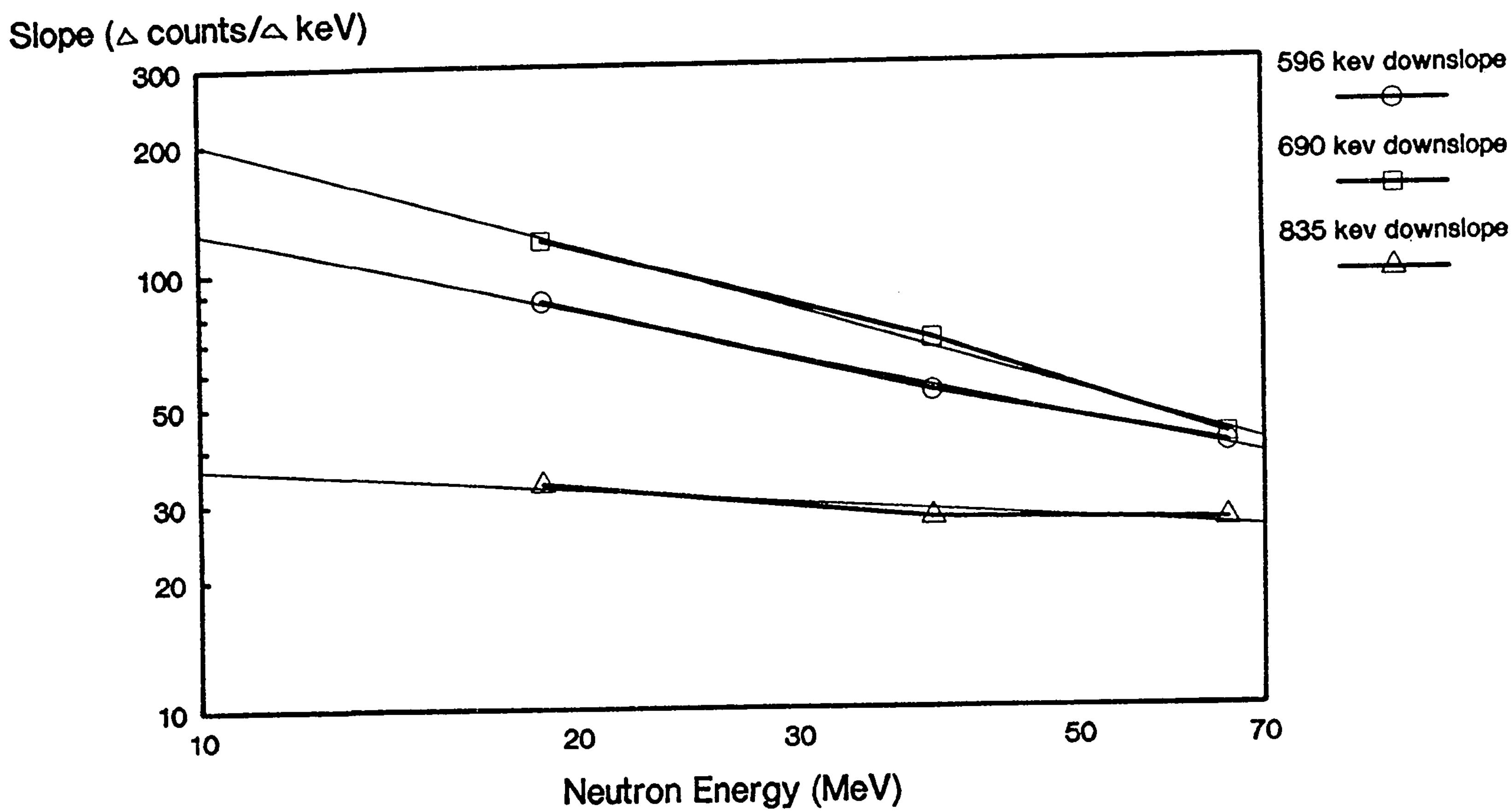

Fig. 35 Power fitting of the Linear Downslope Values

Chapter 6: Conclusion

The recoil germanium portion of a spectrum produced by the (n, n'γ) inelastic scattering of the neutron and the germanium nucleus was used to evaluate the maximum energy of the neutron beam. It was shown that the full width measurements of the curve do not provide an accurate measurement of the neutron energy. The upslope and the first leg of the downslope of these curves provided a group of equations that provided a reasonable estimate of the maximum energy of the neutron beam. The following group of equations were derived:

Table 11 Final Equations for Neutron Energy Determination

596 KEV CURVE

Upslope Equations:

3 keV Fit $X = (\ln((S \times (10000/M))/369.10142))/-0.009220$

5 keV Fit $X = (\ln((S \times (10000/M))/367.80462))/-0.010744$

Downslope Equations:

3 keV Fit $X = ((-S \times (10000/M))/508.31277)^{-1.67256}$

11 keV Fit $X = ((-S \times (10000/M))/495.78060)^{-1.68253}$

690 KEV CURVE

Upslope Equations:

3 keV Fit $X = (\ln((S \times (10000/M))/788.05459))/-0.025537$

5 keV Fit $X = (\ln((S \times (10000/M))/695.88448))/-0.024935$

Table 11 continued

690 KEV CURVE

Downslope Equations:

3 keV Fit $X = ((-S \times (10000/M))/1417.5361)^{-1.21022}$

11 keV Fit $X = ((-S \times (10000/M))/1345.4889)^{-1.22762}$

835 KEV CURVE

Upslope Equation:

3 keV Fit $X = (\ln((S \times (10000/M))/359.44913))/-0.018135$

5 keV Fit $X = (\ln((S \times (10000/M))/343.28974))/-0.019077$

It should be noted that these equations are only valid under low neutron flux conditions. Care should be taken to ensure that the dead time of the detector is low.

For quasi-monoenergetic neutron beams the high-purity coaxial and planar germanium detectors were found to be useful instruments in determining the maximum neutron energy. It is reasonable to conclude that these results will also apply to accelerator produced (structured) white-neutron sources; however, the application to spectra produced by continuous energy neutron(non-structured) sources would not be valid. The germanium detector can be used to not only measure gamma ray spectra by the Health Physicist but also as a useful tool in estimating the dose rate from a neutron source. To continue this evaluation, these equations should be verified with other neutron sources and their validity evaluated at higher neutron energies.

REFERENCES

Attix, F. H. (1986). Introduction to Radiological Physics and Radiation Dosimetry. New York:John Wiley and Sons.

Bockisch, A., Braum, G., Neuwirth, W. (1982). Stopping power for Ge ions produced by inelastic scattering of (d,t) fusion neutrons. Zeitschrift für Physik A: Atoms and Nuclei, 304, 369-370.

Brüchner, J., Wänke, H., Reedy, R. C., Neutron-induced gamma ray spectroscopy: Simulations for chemical mapping of planetary surfaces. Proceedings of the Seventeenth Lunar and Planetary Science Conference, Part 2 Journal of Geophysical Research, 92, E603-E616.

Bunting, R. L., Kraushaar, J. J. (1974) Short-lived radioactivity in Ge(Li) gamma-ray detectors by neutrons. Nuclear Instruments and Methods, 118, 565-572.

Cember, H., (1985) Introduction to Health Pysics (2nd ed.). New York:Pergamon.

Chasman, C., Jones, K. W., Ristinen, R. A. (1965a). Fast neutron bombardment of a lithium-drifted germanium gamma-ray detector. Nuclear Instruments and Methods, 37, 1-8.

Chasman, C., Jones, K. W., Ristinen, R. A. (1965b) Measurement of the energy loss of germanium atoms to electrons in germanium at energies below 100 keV. Physical Review Letters, 15, 245-248.

Chasman, C., Jones, K. W., Ristinen, R. A., Sample, J. T. (1967). Measurements of the energy loss of germanium atoms to electrons in germanium at energies below 100 keV. II. Physics Review, 154, 239-244.

Chilton, B. C., Shultis, J. K., Faw, R. E. (1984). Principles of Radiation Shielding.Englewood Cliffs NJ:Prentice-Hall.

Chung, C., Chen, R. C., (1991), Application of a germanium detector as a low flux neutron monitor. Nuclear Instruments and Methods in Physics Research, A301, 328-336.

Chung, K. C., Mittler, A., Brandenberger, J. D., McEllistrem, M. (1970). Ge(n, n'γ) reactions and low-lying state of Ge Isotopes. Physics Review C, 2, 139-148.

Kruse, H., Spectra processing with computer-graphics, In Carpenter, B. S., D'Agostino, M. D., and Yule, H. P. (Eds) Computers in Activation Analysis and Gamma-Ray Spectroscopy, Department of Energy: Proceedings of American Nuclear Society Topical Conference. Mayaguez, Puerto Rico.

Lieb, K. P., Kent, J. J., Moore, C. F. (1968). Isobaric-analog study of ^{90}Zr. Physical Review, 175, 1482-1490.

Lindhard, J., Nielsen, V., Scharff, M., Thomsen, P. V., (1963). Fys. Medd. Dan. Vid. Selsk, 33.

Lederer, C. M., Shirley, V. S. eds. (1978). Table of Isotopes. New York:John Wiley and Sons.

Protection Against Neutron Radiation (1971) Report #38. Washington D.C.:National Council on Radiation Protection and Measurements.

Smith, D. L. (1972). Fast-neutron flux measurement with a Lithium-drifted germanium detector. Nuclear Instruments and Methods, 102, 193-199.

Stelson, P. H., Dickens, J. K., Raman, S., Trammell, R. C. (1972). Deterioration of large Ge(Li) diodes caused by fast neutrons. Nuclear Instruments and Methods, 98, 481-484.

Youngblood, D. H., Bearse, R. C., Williams, N., Blaugrund, A. E. (1966). Speed of the $\Delta J = 1$, $\Delta T = 1$, M1 Transition in ^{26}Al. Physics Review, 164, 1370-1382.

APPENDIX A: Ganymed Printouts of Raw Data, Recoil Background Data and Gamma Ray/Conversion Electron Fitted Data.

596 keV Peak From 18.8 MeV Neutrons

L= 6edrun
C/f= 1.685 E1= 594.30 E2= 690.17 P= 6 R= 4.0 %= 30.

Chan.	keV	Counts	Back.	Fit	Res.
470	594.30	962	913.9	915.1	1.5
471	595.22	995	956.1	959.8	1.1
472	596.14	953	996.8	1006.8	-1.7
473	597.07	1035	1036.1	1060.0	-.8
474	597.99	1076	1073.7	1124.6	-1.5
475	598.91	1180	1109.6	1205.9	-.7
476	599.83	1338	1143.6	1305.9	.9
477	600.75	1437	1175.9	1419.3	.5
478	601.68	1542	1206.2	1531.2	.3
479	602.60	1652	1234.5	1621.3	.8
480	603.52	1639	1260.9	1671.4	-.8
481	604.44	1668	1285.3	1675.5	-.2
482	605.36	1587	1307.6	1643.6	-1.4
483	606.28	1652	1328.0	1598.3	1.3
484	607.21	1566	1346.5	1564.2	.0
485	608.13	1595	1362.9	1558.4	.9
486	609.05	1602	1377.5	1584.1	.4
487	609.97	1536	1390.2	1630.6	-2.4
488	610.89	1686	1401.0	1678.3	.2
489	611.82	1735	1410.1	1707.3	.7
490	612.74	1754	1417.5	1705.4	1.2
491	613.66	1695	1423.1	1672.8	.5
492	614.58	1546	1427.2	1620.3	-1.9
493	615.50	1526	1429.8	1562.8	-.9
494	616.42	1533	1430.9	1512.4	.5
495	617.35	1483	1430.6	1475.1	.2
496	618.27	1486	1429.0	1450.7	.9
497	619.19	1558	1426.2	1435.6	3.2
498	620.11	1422	1422.2	1425.9	-.1
499	621.03	1541	1417.2	1418.5	3.2
500	621.95	1427	1411.2	1411.6	.4
501	622.88	1462	1404.3	1404.4	1.5
502	623.80	1319	1396.6	1396.7	-2.1
503	624.72	1298	1388.2	1388.2	-2.5
504	625.64	1316	1379.1	1379.1	-1.7
505	626.56	1351	1369.4	1369.4	-.5
506	627.49	1329	1359.2	1359.2	-.8
507	628.41	1345	1348.6	1348.6	-.1
508	629.33	1353	1337.6	1337.6	.4
509	630.25	1296	1326.4	1326.4	-.8
510	631.17	1266	1314.9	1314.9	-1.4
511	632.09	1341	1303.3	1303.3	1.0
512	633.02	1263	1291.6	1291.6	-.8
513	633.94	1311	1279.9	1279.9	.9
514	634.86	1288	1268.2	1268.2	.6

515	635.78	1238	1256.6	1256.6	-.5
516	636.70	1236	1245.2	1245.2	-.3
517	637.63	1135	1233.9	1233.9	-2.9
518	638.55	1233	1222.8	1222.8	.3
519	639.47	1224	1211.9	1211.9	.3
520	640.39	1181	1201.4	1201.4	-.6
521	641.31	1205	1191.2	1191.2	.4
522	642.23	1216	1181.3	1181.3	1.0
523	643.16	1254	1171.8	1171.8	2.4
524	644.08	1184	1162.6	1162.6	.6
525	645.00	1112	1153.9	1153.9	-1.2
526	645.92	1158	1145.5	1145.5	.4
527	646.84	1098	1137.6	1137.6	-1.2
528	647.77	1151	1130.1	1130.1	.6
529	648.69	1167	1123.0	1123.0	1.3
530	649.61	1123	1116.2	1116.2	.2
531	650.53	1088	1109.9	1109.9	-.7
532	651.45	1095	1104.0	1104.0	-.3
533	652.37	1192	1098.4	1098.4	2.8
534	653.30	1168	1093.2	1093.2	2.2
535	654.22	1072	1088.3	1088.3	-.5
536	655.14	1093	1083.7	1083.7	.3
537	656.06	1095	1079.3	1079.3	.5
538	656.98	1000	1075.3	1075.3	-2.3
539	657.90	981	1071.4	1071.4	-2.8
540	658.83	1058	1067.7	1067.7	-.3
541	659.75	1106	1064.2	1064.2	1.3
542	660.67	1074	1060.8	1060.8	.4
543	661.59	1010	1057.5	1057.5	-1.5
544	662.51	1121	1054.3	1054.3	2.1
545	663.44	968	1051.0	1051.0	-2.6
546	664.36	1046	1047.8	1047.8	-.1
547	665.28	1055	1044.5	1044.5	.3
548	666.20	1097	1041.2	1041.2	1.7
549	667.12	1071	1037.8	1037.8	1.0
550	668.04	1001	1034.2	1034.2	-1.0
551	668.97	1036	1030.5	1030.5	.2
552	669.89	1002	1026.6	1026.6	-.8
553	670.81	1035	1022.6	1022.6	.4
554	671.73	984	1018.3	1018.3	-1.1
555	672.65	1005	1013.9	1013.9	-.3
556	673.58	962	1009.2	1009.2	-1.5
557	674.50	998	1004.4	1004.4	-.2
558	675.42	1053	999.4	999.4	1.7
559	676.34	1013	994.2	994.2	.6
560	677.26	971	988.9	988.9	-.6
561	678.18	1007	983.5	983.5	.7
562	679.11	972	978.1	978.1	-.2
563	680.03	988	972.7	972.7	.5

564	680.95	962	967.3	967.3	-.2
565	681.87	982	962.1	962.1	.6
566	682.79	952	957.2	957.2	-.2
567	683.72	925	952.6	952.6	-.9
568	684.64	927	948.5	948.5	-.7
569	685.56	962	945.0	945.0	.6
570	686.48	962	942.3	942.3	.6
571	687.40	990	940.4	940.4	1.6
572	688.32	928	939.7	939.7	-.4
573	689.25	902	940.2	940.2	-1.3
574	690.17	943	942.3	942.3	.0

690 keV Peak From 18.8 MeV Neutrons
L= 6edrun
C/f= 1.600 E1= 692.93 E2= 826.59 P= 6 R= 6.0 %= 30.

Chan.	keV	Counts	Back.	Fit	Res.
577	692.93	961	956.8	957.2	.1
578	693.86	976	1019.5	1021.6	-1.4
579	694.78	1006	1075.3	1085.3	-2.4
580	695.70	1154	1124.6	1160.4	-.2
581	696.62	1319	1167.9	1262.9	1.6
582	697.54	1462	1205.6	1393.4	1.8
583	698.46	1475	1238.1	1514.6	-1.0
584	699.39	1523	1265.8	1569.2	-1.2
585	700.31	1520	1288.9	1537.1	-.4
586	701.23	1485	1307.9	1459.1	.7
587	702.15	1479	1323.0	1391.7	2.3
588	703.07	1385	1334.5	1357.8	.7
589	703.99	1444	1342.9	1348.7	2.5
590	704.92	1448	1348.2	1349.3	2.6
591	705.84	1430	1350.8	1350.9	2.1
592	706.76	1348	1350.9	1350.9	-.1
593	707.68	1301	1348.8	1348.8	-1.3
594	708.60	1298	1344.7	1344.7	-1.3
595	709.53	1344	1338.8	1338.8	.1
596	710.45	1374	1331.2	1331.2	1.2
597	711.37	1317	1322.3	1322.3	-.1
598	712.29	1348	1312.1	1312.1	1.0
599	713.21	1291	1300.8	1300.8	-.3
600	714.13	1310	1288.5	1288.5	.6
601	715.06	1259	1275.5	1275.5	-.5
602	715.98	1242	1261.8	1261.9	-.6
603	716.90	1243	1247.6	1248.0	-.1
604	717.82	1140	1233.0	1235.0	-2.8
605	718.74	1118	1218.1	1227.0	-3.2
606	719.67	1181	1203.0	1232.3	-1.5
607	720.59	1220	1187.7	1259.6	-1.1
608	721.51	1274	1172.4	1303.9	-.8
609	722.43	1415	1157.2	1336.3	2.2
610	723.35	1358	1142.1	1323.8	.9
611	724.27	1217	1127.1	1264.6	-1.3
612	725.20	1159	1112.4	1189.9	-.9
613	726.12	1127	1098.0	1130.5	-.1
614	727.04	1041	1083.8	1094.2	-1.6
615	727.96	1039	1070.1	1073.5	-1.1
616	728.88	1068	1056.7	1062.3	.2
617	729.81	1084	1043.8	1062.3	.7
618	730.73	1025	1031.3	1080.7	-1.7
619	731.65	1135	1019.3	1117.9	.5
620	732.57	1163	1007.8	1154.5	.3
621	733.49	1159	996.8	1159.4	.0

622	734.41	1136	986.2	1120.6	.5
623	735.34	1032	976.2	1059.0	-.8
624	736.26	980	966.7	1004.7	-.8
625	737.18	1023	957.8	970.7	1.7
626	738.10	967	949.3	952.6	.5
627	739.02	972	941.3	941.9	1.0
628	739.95	969	933.8	933.9	1.1
629	740.87	984	926.8	926.8	1.8
630	741.79	930	920.3	920.3	.3
631	742.71	946	914.2	914.2	1.0
632	743.63	899	908.6	908.6	-.3
633	744.55	944	903.4	903.4	1.3
634	745.48	916	898.6	898.6	.6
635	746.40	898	894.2	894.2	.1
636	747.32	876	890.1	890.1	-.5
637	748.24	875	886.4	886.4	-.4
638	749.16	846	883.0	883.0	-1.3
639	750.09	880	879.9	879.9	.0
640	751.01	936	877.1	877.1	2.0
641	751.93	856	874.6	874.6	-.6
642	752.85	932	872.3	872.3	2.0
643	753.77	929	870.2	870.2	2.0
644	754.69	874	868.3	868.3	.2
645	755.62	877	866.6	866.6	.4
646	756.54	870	865.0	865.0	.2
647	757.46	841	863.5	863.5	-.8
648	758.38	871	862.2	862.2	.3
649	759.30	918	861.0	861.0	1.9
650	760.22	880	859.8	859.8	.7
651	761.15	828	858.7	858.7	-1.1
652	762.07	835	857.6	857.6	-.8
653	762.99	816	856.5	856.5	-1.4
654	763.91	825	855.5	855.5	-1.1
655	764.83	838	854.4	854.4	-.6
656	765.76	839	853.4	853.4	-.5
657	766.68	836	852.3	852.3	-.6
658	767.60	892	851.1	851.1	1.4
659	768.52	846	850.0	850.0	-.1
660	769.44	828	848.7	848.7	-.7
661	770.36	783	847.5	847.5	-2.3
662	771.29	828	846.1	846.1	-.6
663	772.21	845	844.7	844.7	.0
664	773.13	893	843.2	843.2	1.7
665	774.05	829	841.6	841.6	-.4
666	774.97	839	840.0	840.0	.0
667	775.90	834	838.3	838.3	-.1
668	776.82	845	836.5	836.5	.3
669	777.74	816	834.6	834.6	-.7
670	778.66	775	832.7	832.7	-2.0
671	779.58	822	830.7	830.7	-.3
672	780.50	853	828.7	828.7	.9

673	781.43	778	826.6	826.6	-1.7
674	782.35	769	824.5	824.5	-2.0
675	783.27	763	822.4	822.4	-2.1
676	784.19	786	820.2	820.2	-1.2
677	785.11	865	818.1	818.1	1.6
678	786.04	829	815.9	815.9	.5
679	786.96	829	813.7	813.7	.5
680	787.88	795	811.6	811.6	-.6
681	788.80	816	809.4	809.4	.2
682	789.72	810	807.4	807.4	.1
683	790.64	831	805.3	805.3	.9
684	791.57	829	803.4	803.4	.9
685	792.49	827	801.5	801.5	.9
686	793.41	797	799.7	799.7	-.1
687	794.33	819	798.0	798.0	.7
688	795.25	805	796.3	796.3	.3
689	796.17	847	794.8	794.8	1.8
690	797.10	813	793.4	793.4	.7
691	798.02	834	792.1	792.1	1.5
692	798.94	767	791.0	791.0	-.9
693	799.86	784	789.9	789.9	-.2
694	800.78	805	789.0	789.0	.6
695	801.71	810	788.2	788.2	.8
696	802.63	794	787.5	787.5	.2
697	803.55	835	786.9	786.9	1.7
698	804.47	781	786.4	786.4	-.2
699	805.39	826	786.0	786.0	1.4
700	806.31	809	785.7	785.7	.8
701	807.24	781	785.4	785.4	-.2
702	808.16	776	785.1	785.1	-.3
703	809.08	779	784.9	784.9	-.2
704	810.00	756	784.6	784.6	-1.0
705	810.92	759	784.2	784.2	-.9
706	811.85	692	783.8	783.8	-3.3
707	812.77	810	783.2	783.2	1.0
708	813.69	794	782.3	782.3	.4
709	814.61	805	781.3	781.3	.8
710	815.53	764	779.9	779.9	-.6
711	816.45	805	778.2	778.2	1.0
712	817.38	766	776.0	776.0	-.4
713	818.30	746	773.2	773.2	-1.0
714	819.22	703	769.9	769.9	-2.4
715	820.14	790	765.8	765.8	.9
716	821.06	787	761.0	761.0	.9
717	821.99	693	755.2	755.2	-2.3
718	822.91	760	748.3	748.3	.4
719	823.83	708	740.3	740.3	-1.2
720	824.75	716	731.0	731.0	-.6
721	825.67	757	720.3	720.3	1.3
722	826.59	769	708.0	708.0	2.2

835 keV Peak From 18.8 MeV Neutrons
L= 6edrun
C/f= 1.372 E1= 833.05 E2= 965.79 P= 6 R= 6.0 %= 30.

Chan.	keV	Counts	Back.	Fit	Res.
729	833.05	748	682.3	682.7	2.4
730	833.97	695	704.8	706.2	-.4
731	834.89	740	725.9	729.7	.4
732	835.81	714	745.5	755.0	-1.5
733	836.73	768	763.8	784.7	-.6
734	837.66	784	780.8	821.6	-1.3
735	838.58	848	796.5	867.3	-.7
736	839.50	869	811.0	920.1	-1.7
737	840.42	1048	824.4	973.8	2.4
738	841.34	1051	836.8	1018.6	1.0
739	842.27	1060	848.0	1045.1	.5
740	843.19	1039	858.3	1049.6	-.3
741	844.11	968	867.7	1036.6	-2.2
742	845.03	1034	876.2	1018.1	.5
743	845.95	1032	883.8	1008.6	.7
744	846.87	1035	890.7	1019.6	.5
745	847.80	1004	896.7	1054.9	-1.6
746	848.72	1126	902.1	1107.9	.5
747	849.64	1179	906.8	1163.4	.5
748	850.56	1244	910.9	1203.0	1.2
749	851.48	1195	914.3	1212.4	-.5
750	852.40	1136	917.2	1188.2	-1.5
751	853.33	1166	919.5	1138.6	.8
752	854.25	1032	921.4	1078.7	-1.4
753	855.17	1044	922.8	1023.1	.6
754	856.09	994	923.7	980.6	.4
755	857.01	1045	924.3	952.9	2.9
756	857.94	985	924.5	937.2	1.5
757	858.86	919	924.3	929.4	-.3
758	859.78	978	923.8	925.6	1.7
759	860.70	940	923.0	923.5	.5
760	861.62	899	921.9	922.1	-.8
761	862.54	922	920.6	920.6	.0
762	863.47	909	919.0	919.0	-.3
763	864.39	896	917.3	917.3	-.7
764	865.31	939	915.3	915.3	.8
765	866.23	860	913.2	913.2	-1.8
766	867.15	906	910.9	910.9	-.2
767	868.08	886	908.5	908.5	-.8
768	869.00	889	906.0	906.0	-.6
769	869.92	904	903.4	903.4	.0
770	870.84	874	900.7	900.7	-.9
771	871.76	899	897.9	897.9	.0
772	872.68	884	895.0	895.0	-.4
773	873.61	902	892.1	892.1	.3

774	874.53	840	889.2	889.2	-1.7
775	875.45	916	886.2	886.2	1.0
776	876.37	860	883.2	883.2	-.8
777	877.29	883	880.3	880.3	.1
778	878.22	851	877.3	877.3	-.9
779	879.14	926	874.3	874.3	1.7
780	880.06	893	871.3	871.3	.7
781	880.98	855	868.4	868.4	-.5
782	881.90	862	865.5	865.5	-.1
783	882.82	809	862.6	862.6	-1.8
784	883.75	902	859.8	859.8	1.4
785	884.67	837	857.0	857.0	-.7
786	885.59	851	854.2	854.2	-.1
787	886.51	874	851.5	851.5	.8
788	887.43	803	848.8	848.8	-1.6
789	888.35	912	846.2	846.2	2.2
790	889.28	885	843.7	843.7	1.4
791	890.20	870	841.2	841.2	1.0
792	891.12	831	838.8	838.8	-.3
793	892.04	839	836.4	836.4	.1
794	892.96	860	834.1	834.1	.9
795	893.89	770	831.8	831.8	-2.2
796	894.81	841	829.6	829.6	.4
797	895.73	830	827.5	827.5	.1
798	896.65	822	825.4	825.4	-.1
799	897.57	869	823.4	823.4	1.6
800	898.49	808	821.4	821.4	-.5
801	899.42	813	819.5	819.5	-.2
802	900.34	777	817.6	817.6	-1.4
803	901.26	760	815.7	815.7	-2.0
804	902.18	815	813.9	813.9	.0
805	903.10	829	812.2	812.2	.6
806	904.03	766	810.4	810.4	-1.6
807	904.95	821	808.8	808.8	.4
808	905.87	882	807.1	807.1	2.6
809	906.79	808	805.5	805.5	.1
810	907.71	780	803.8	803.8	-.8
811	908.63	813	802.3	802.3	.4
812	909.56	802	800.7	800.7	.0
813	910.48	749	799.1	799.1	-1.8
814	911.40	768	797.6	797.6	-1.1
815	912.32	831	796.0	796.0	1.2
816	913.24	854	794.5	794.5	2.1
817	914.17	771	792.9	792.9	-.8
818	915.09	794	791.3	791.3	.1
819	916.01	812	789.8	789.8	.8
820	916.93	839	788.2	788.2	1.8
821	917.85	777	786.6	786.6	-.3
822	918.77	795	785.0	785.0	.4
823	919.70	864	783.3	783.3	2.8
824	920.62	740	781.7	781.7	-1.5

825	921.54	797	780.0	780.0	.6
826	922.46	764	778.3	778.3	-.5
827	923.38	806	776.5	776.5	1.1
828	924.31	756	774.7	774.7	-.7
829	925.23	695	772.9	772.9	-2.9
830	926.15	777	771.1	771.1	.2
831	927.07	764	769.2	769.2	-.2
832	927.99	767	767.2	767.2	.0
833	928.91	751	765.3	765.3	-.5
834	929.84	698	763.3	763.3	-2.4
835	930.76	758	761.2	761.2	-.1
836	931.68	763	759.1	759.1	.1
837	932.60	764	757.0	757.0	.3
838	933.52	754	754.8	754.8	.0
839	934.45	724	752.6	752.6	-1.1
840	935.37	757	750.4	750.4	.2
841	936.29	702	748.1	748.1	-1.7
842	937.21	757	745.8	745.8	.4
843	938.13	737	743.5	743.5	-.2
844	939.05	766	741.2	741.2	.9
845	939.98	804	738.8	738.8	2.3
846	940.90	801	736.5	736.5	2.3
847	941.82	729	734.1	734.1	-.2
848	942.74	747	731.7	731.7	.6
849	943.66	728	729.4	729.4	-.1
850	944.58	762	727.0	727.0	1.3
851	945.51	716	724.7	724.7	-.3
852	946.43	731	722.4	722.4	.3
853	947.35	701	720.2	720.2	-.7
854	948.27	692	718.0	718.0	-1.0
855	949.19	692	715.8	715.8	-.9
856	950.12	735	713.8	713.8	.8
857	951.04	712	711.8	711.8	.0
858	951.96	647	709.9	709.9	-2.4
859	952.88	689	708.1	708.1	-.7
860	953.80	739	706.4	706.4	1.2
861	954.72	708	704.9	704.9	.1
862	955.65	698	703.5	703.5	-.2
863	956.57	710	702.3	702.3	.3
864	957.49	706	701.3	701.3	.2
865	958.41	713	700.5	700.5	.5
866	959.33	697	699.9	699.9	-.1
867	960.26	710	699.6	699.6	.4
868	961.18	705	699.5	699.5	.2
869	962.10	686	699.7	699.7	-.5
870	963.02	689	700.2	700.2	-.4
871	963.94	736	701.0	701.0	1.3
872	964.86	703	702.2	702.2	.0
873	965.79	682	703.7	703.7	-.8

596 keV Peak From 38.4 MeV Neutrons
L= 9edrun
C/f= 1.477 E1= 596.14 E2= 691.09 P= 6 R= 4.0 %= 30.

Chan.	keV	Counts	Back.	Fit	Res.
472	596.14	9193	8661.5	8974.3	2.3
473	597.07	9452	8947.9	9403.8	.5
474	597.99	9577	9216.8	9853.9	-2.8
475	598.91	10004	9468.7	10322.3	-3.2
476	599.83	10866	9704.3	10800.7	.6
477	600.75	11333	9924.1	11274.6	.5
478	601.68	11755	10128.6	11724.6	.3
479	602.60	12354	10318.3	12128.9	2.0
480	603.52	12635	10493.8	12467.6	1.5
481	604.44	12673	10655.7	12726.3	-.5
482	605.36	12801	10804.3	12899.5	-.9
483	606.28	12955	10940.3	12992.6	-.3
484	607.21	12957	11064.0	13020.0	-.6
485	608.13	12776	11176.1	13002.9	-2.0
486	609.05	13115	11276.9	12964.0	1.3
487	609.97	12865	11366.9	12923.1	-.5
488	610.89	12961	11446.6	12893.2	.6
489	611.82	12991	11516.5	12878.5	1.0
490	612.74	12985	11576.9	12875.1	1.0
491	613.66	12873	11628.3	12873.5	.0
492	614.58	12789	11671.1	12861.7	-.6
493	615.50	12766	11705.8	12829.3	-.6
494	616.42	12749	11732.7	12770.2	-.2
495	617.35	12631	11752.3	12683.4	-.5
496	618.27	12598	11764.8	12573.1	.2
497	619.19	12386	11770.8	12447.2	-.6
498	620.11	12178	11770.6	12315.2	-1.2
499	621.03	12208	11764.5	12185.7	.2
500	621.95	12281	11752.9	12065.6	2.0
501	622.88	12136	11736.2	11958.8	1.6
502	623.80	11841	11714.6	11866.7	-.8
503	624.72	11776	11688.5	11788.1	-.1
504	625.64	11754	11658.3	11720.8	.3
505	626.56	11837	11624.2	11661.8	1.6
506	627.49	11749	11586.5	11608.2	1.3
507	628.41	11538	11545.5	11557.5	-.2
508	629.33	11366	11501.6	11508.0	-1.3
509	630.25	11668	11355.0	11458.2	2.0
510	631.17	11241	11405.9	11407.5	-1.6
511	632.09	11282	11354.6	11355.4	-.7
512	633.02	11241	11301.4	11301.8	-.6
513	633.94	11328	11246.6	11246.7	.8
514	634.86	11130	11190.2	11190.3	-.6
515	635.78	10997	11132.7	11132.7	-1.3
516	636.70	11235	11074.1	11074.1	1.5
517	637.63	10990	11014.7	11014.7	-.2
518	638.55	10960	10954.7	10954.7	.1

519	639.47	10813	10894.3	10894.3	-.8
520	640.39	10544	10833.6	10833.6	-2.8
521	641.31	10800	10772.9	10772.9	.3
522	642.23	10516	10712.3	10712.3	-1.9
523	643.16	10544	10651.9	10651.9	-1.1
524	644.08	10516	10592.0	10592.0	-.7
525	645.00	10536	10532.6	10532.6	.0
526	645.92	10498	10473.8	10473.8	.2
527	646.84	10575	10415.9	10415.9	1.6
528	647.77	10347	10358.8	10358.8	-.1
529	648.69	10356	10302.8	10302.8	.5
530	649.61	10260	10247.9	10247.9	.1
531	650.53	10279	10194.2	10194.2	.8
532	651.45	10129	10141.7	10141.7	-.1
533	652.37	10242	10090.6	10090.6	1.5
534	653.30	9929	10040.9	10040.9	-1.1
535	654.22	10154	9992.6	9992.6	1.6
536	655.14	9914	9945.9	9945.9	-.3
537	656.06	9869	9900.7	9900.7	-.3
538	656.98	9823	9857.0	9857.0	-.3
539	657.90	9859	9814.9	9814.9	.4
540	658.83	9601	9774.4	9774.4	-1.8
541	659.75	9796	9735.5	9735.5	.6
542	660.67	9642	9698.2	9698.2	-.6
543	661.59	9790	9662.5	9662.5	1.3
544	662.51	9668	9628.3	9628.3	.4
545	663.44	9629	9595.6	9595.6	.3
546	664.36	9636	9564.4	9564.4	.7
547	665.28	9680	9534.6	9534.6	1.5
548	666.20	9612	9506.1	9506.1	1.1
549	667.12	9376	9478.9	9478.9	-1.1
550	668.04	9248	9453.0	9453.0	-2.1
551	668.97	9481	9428.2	9428.2	.5
552	669.89	9293	9404.4	9404.4	-1.2
553	670.81	9467	9381.5	9381.5	.9
554	671.73	9277	9359.5	9359.5	-.9
555	672.65	9425	9338.1	9338.1	.9
556	673.58	9338	9317.4	9317.4	.2
557	674.50	9403	9297.1	9297.1	1.1
558	675.42	9524	9277.0	9277.0	2.5
559	676.34	9325	9257.1	9257.1	.7
560	677.26	9080	9237.2	9237.2	-1.6
561	678.18	9182	9217.1	9217.1	-.4
562	679.11	9141	9196.6	9196.6	-.6
563	680.03	9219	9175.5	9175.5	.5
564	680.95	9079	9153.7	9153.7	-.8
565	681.87	8997	9130.9	9130.9	-1.4
566	682.79	9126	9106.9	9106.9	.2
567	683.72	8902	9081.6	9081.6	-1.9
568	684.64	8963	9054.6	9054.6	-1.0
569	685.56	9052	0235.7	9025.7	.3

570	686.48	8904	8994.7	8994.7	-1.0
571	687.40	9046	8961.3	8961.3	.9
572	688.32	9021	8925.3	8925.3	1.0
573	689.25	8748	8886.3	8886.3	-1.5
574	690.17	8871	8844.2	8844.2	.3
575	691.09	8993	8798.5	8798.5	2.1

690 keV Peak From 38.4 MeV Neutrons
L= 9edrun
C/f= 1.358 E1= 692.93 E2= 826.59 P= 6 R= 6.0 %= 30.

Chan.	keV	Counts	Back.	Fit	Res.
577	692.93	8765	8605.1	8642.3	1.3
578	693.86	8931	8935.0	9009.9	-.8
579	694.78	9261	9232.5	9372.1	-1.2
580	695.70	9529	9499.6	9740.0	-2.1
581	696.62	10131	9738.0	10120.6	.1
582	697.54	10673	9949.6	10512.1	1.6
583	698.46	11038	10136.0	10900.1	1.3
584	699.39	11249	10298.8	11257.9	-.1
585	700.31	11717	10439.5	11551.8	1.5
586	701.23	11570	10559.7	11751.5	-1.7
587	702.15	11782	10660.6	11840.7	-.5
588	703.07	11724	10743.8	11823.3	-.9
589	703.99	11706	10810.4	11722.8	-.2
590	704.92	11471	10861.7	11574.3	-1.0
591	705.84	11500	10898.9	11413.1	.8
592	706.76	11470	10923.1	11265.9	1.9
593	707.68	11357	10935.3	11146.5	2.0
594	708.60	11208	10936.6	11056.8	1.4
595	709.53	10820	10927.9	10991.1	-1.6
596	710.45	11172	10910.1	10940.8	2.2
597	711.37	10914	10884.1	10898.0	.2
598	712.29	10767	10850.7	10856.7	-.9
599	713.21	10745	10810.7	10813.8	-.7
600	714.13	10931	10764.8	10767.8	1.6
601	715.06	10673	10713.6	10719.2	-.4
602	715.98	10823	10658.0	10669.6	1.5
603	716.90	10466	10598.3	10621.7	-1.5
604	717.82	10425	10535.3	10578.7	-1.5
605	718.74	10585	10469.4	10544.2	.4
606	719.67	10262	10401.2	10520.0	-2.5
607	720.59	10315	10331.0	10505.6	-1.9
608	721.51	10278	10259.4	10496.4	-2.1
609	722.43	10610	10186.7	10484.0	1.2
610	723.35	10499	10113.4	10457.9	.4
611	724.27	10673	10039.7	10408.5	2.6
612	725.20	10426	9965.9	10330.8	.9
613	726.12	10313	9892.4	10225.9	.9
614	727.04	10049	9819.4	10101.1	-.5
615	727.96	9923	9747.1	9966.9	-.4
616	728.88	9636	9675.8	9834.3	-2.0
617	729.81	9440	9605.6	9711.2	-2.8
618	730.73	9529	9536.7	9601.7	-.7
619	731.65	9511	9469.3	9506.3	.0
620	732.57	9358	9403.5	9422.9	-.7
621	733.49	9467	9339.4	9348.8	1.2

622	734.41	9327	9277.1	9281.3	.5
623	735.34	9392	9216.6	9218.4	1.8
624	736.26	9083	9158.2	9158.8	-.8
625	737.18	9249	9101.7	9101.9	1.5
626	738.10	9008	9047.2	9047.3	-.4
627	739.02	8980	8994.8	8994.8	-.2
628	739.95	8908	8944.5	8944.5	-.4
629	740.87	8857	8896.2	8896.2	-.4
630	741.79	8899	8850.0	8850.0	.5
631	742.71	8862	8805.8	8805.8	.6
632	743.63	8780	8763.6	8763.6	.2
633	744.55	8761	8723.4	8723.4	.4
634	745.48	8697	8685.2	8685.2	.1
635	746.40	8690	8648.8	8648.8	.4
636	747.32	8603	8614.3	8614.3	-.1
637	748.24	8444	8581.5	8581.5	-1.5
638	749.16	8632	8550.4	8550.4	.9
639	750.09	8548	8521.0	8521.0	.3
640	751.01	8402	8493.1	8493.1	-1.0
641	751.93	8621	8466.7	8466.7	1.7
642	752.85	8474	8441.8	8441.8	.3
643	753.77	8430	8418.2	8418.2	.1
644	754.69	8551	8395.8	8395.8	1.7
645	755.62	8515	8374.6	8374.6	1.5
646	756.54	8384	8354.5	8354.5	.3
647	757.46	8396	8335.4	8335.4	.7
648	758.38	8225	8317.2	8317.2	-1.0
649	759.30	8317	8299.9	8299.9	.2
650	760.22	8291	8283.4	8283.4	.1
651	761.15	8411	8267.6	8267.6	1.6
652	762.07	8110	8252.4	8252.4	-1.6
653	762.99	8064	8237.7	8237.7	-1.9
654	763.91	8177	8223.5	8223.5	-.5
655	764.83	8200	8209.8	8209.8	-.1
656	765.76	8219	8196.4	8196.4	.2
657	766.68	8173	8183.3	8183.3	-.1
658	767.60	8175	8170.4	8170.4	.1
659	768.52	8196	8157.7	8157.7	.4
660	769.44	8117	8145.1	8145.1	-.3
661	770.36	8082	8132.6	8132.6	-.6
662	771.29	8026	8120.1	8120.1	-1.0
663	772.21	8115	8107.7	8107.7	.1
664	773.13	8211	8095.2	8095.2	1.3
665	774.05	7925	8082.6	8082.6	-1.8
666	774.97	8087	8070.0	8070.0	.2
667	775.90	8056	8057.2	8057.2	.0
668	776.82	8135	8044.3	8044.3	1.0
669	777.74	7852	8031.3	8031.3	-2.0
670	778.66	7923	8018.1	8018.1	-1.1
671	779.58	8124	8004.8	8004.8	1.3
672	780.50	7943	7991.3	7991.3	-.5

673	781.43	7976	7977.7	7977.7	.0
674	782.35	7835	7963.9	7963.9	-1.5
675	783.27	7798	7950.0	7950.0	-1.7
676	784.19	8129	7936.0	7936.0	2.2
677	785.11	8102	7921.8	7921.8	2.0
678	786.04	7862	7907.6	7907.6	-.5
679	786.96	7810	7893.3	7893.3	-.9
680	787.88	7836	7878.9	7878.9	-.5
681	788.80	7820	7864.5	7864.5	-.5
682	789.72	7929	7850.2	7850.2	.9
683	790.64	7833	7835.9	7835.9	.0
684	791.57	7715	7821.6	7821.6	-1.2
685	792.49	7859	7807.4	7807.4	.6
686	793.41	7682	7793.4	7793.4	-1.3
687	794.33	7747	7779.5	7779.5	-.4
688	795.25	7814	7765.8	7765.8	.5
689	796.17	7852	7752.4	7752.4	1.1
690	797.10	7713	7739.1	7739.1	-.3
691	798.02	7788	7726.2	7726.2	.7
692	798.94	7720	7713.5	7713.5	.1
693	799.86	7825	7701.1	7701.1	1.4
694	800.78	7831	7689.1	7689.1	1.6
695	801.71	7789	7677.4	7677.4	1.3
696	802.63	7716	7666.0	7666.0	.6
697	803.55	7595	7654.9	7654.9	-.7
698	804.47	7729	7644.2	7644.2	1.0
699	805.39	7652	7633.8	7633.8	.2
700	806.31	7509	7623.7	7623.7	-1.3
701	807.24	7654	7613.9	7613.9	.5
702	808.16	7718	7604.2	7604.2	1.3
703	809.08	7642	7594.8	7594.8	.5
704	810.00	7361	7585.4	7585.4	-2.6
705	810.92	7546	7576.1	7576.1	-.3
706	811.85	7573	7566.8	7566.8	.1
707	812.77	7558	7557.3	7557.3	.0
708	813.69	7532	7547.6	7547.6	-.2
709	814.61	7572	7537.4	7537.4	.4
710	815.53	7572	7526.8	7526.8	.5
711	816.45	7436	7515.5	7515.5	-.9
712	817.38	7429	7503.3	7503.3	-.9
713	818.30	7418	7490.0	7490.0	-.8
714	819.22	7357	7475.5	7475.5	-1.4
715	820.14	7434	7459.5	7459.5	-.3
716	821.06	7452	7441.7	7441.7	.1
717	821.99	7450	7421.8	7421.8	.3
718	822.91	7386	7399.6	7399.6	-.2
719	823.83	7484	7374.7	7374.7	1.3
720	824.75	7292	7346.7	7346.7	-.6
721	825.67	7422	7315.3	7315.3	1.2
722	826.59	7277	7280.1	7280.1	.0

835 keV Peak From 38.4 MeV Neutrons
L= 9edrun
C/f= 1.869 E1= 833.05 E2= 965.79 P= 6 R= 6.0 %= 30.

Chan.	keV	Counts	Back.	Fit	Res.
729	833.05	7396	7168.1	7168.3	2.6
730	833.97	7404	7314.3	7314.7	1.0
731	834.89	7427	7449.8	7450.8	-.3
732	835.81	7402	7575.2	7577.3	-2.0
733	836.73	7592	7690.8	7695.2	-1.2
734	837.66	7515	7797.3	7805.9	-3.3
735	838.58	7600	7895.0	7911.2	-3.5
736	839.50	7851	7984.4	8013.6	-1.8
737	840.42	8319	8065.8	8116.2	2.2
738	841.34	8345	8139.8	8223.1	1.3
739	842.27	8697	8206.7	8338.7	3.9
740	843.19	8833	8266.8	8467.3	3.9
741	844.11	8870	8320.5	8612.3	2.7
742	845.03	8901	8368.3	8775.1	1.3
743	845.95	8783	8410.3	8953.9	-1.8
744	846.87	8875	8447.0	9142.9	-2.8
745	847.80	9133	8478.7	9332.4	-2.1
746	848.72	9360	8505.7	9509.1	-1.5
747	849.64	9579	8528.2	9658.5	-.8
748	850.56	9719	8546.5	9766.5	-.5
749	851.48	10019	8561.0	9822.8	2.0
750	852.40	9988	8571.9	9822.3	1.7
751	853.33	9849	8579.3	9766.9	.8
752	854.25	9810	8583.7	9664.3	1.5
753	855.17	9673	8585.1	9527.4	1.5
754	856.09	9035	8583.8	9371.1	-3.5
755	857.01	9175	8580.0	9210.4	-.4
756	857.94	8932	8574.0	9057.6	-1.3
757	858.86	8916	8565.8	8921.4	-.1
758	859.78	8825	8555.8	8806.2	.2
759	860.70	8811	8544.0	8713.0	1.0
760	861.62	8563	8530.6	8639.9	-.8
761	862.54	8534	8515.7	8583.5	-.5
762	863.47	8546	8499.6	8539.9	.1
763	864.39	8506	8482.4	8505.3	.0
764	865.31	8604	8464.1	8476.6	1.4
765	866.23	8477	8445.0	8451.5	.3
766	867.15	8343	8425.1	8428.4	-.9
767	868.08	8440	8404.6	8406.1	.4
768	869.00	8199	8383.5	8384.2	-2.0
769	869.92	8174	8361.9	8362.2	-2.1
770	870.84	8337	8340.0	8340.1	.0
771	871.76	8473	8317.8	8317.8	1.7
772	872.68	8285	8295.4	8295.4	-.1
773	873.61	8273	8272.9	8272.9	.0

774	874.53	8351	8250.3	8250.3	1.1
775	875.45	8395	8227.7	8227.7	1.8
776	876.37	8194	8205.2	8205.2	-.1
777	877.29	8184	8182.8	8182.8	.0
778	878.22	8255	8160.6	8160.6	1.0
779	879.14	8159	8138.6	8138.6	.2
780	880.06	8231	8116.8	8116.8	1.3
781	880.98	8115	8095.3	8095.3	.2
782	881.90	7971	8074.1	8074.1	-1.2
783	882.82	7941	8053.2	8053.2	-1.3
784	883.75	7822	8032.7	8032.7	-2.4
785	884.67	7959	8012.6	8012.6	-.6
786	885.59	8044	7992.9	7992.9	.6
787	886.51	7950	7973.6	7973.6	-.3
788	887.43	7956	7954.7	7954.7	.0
789	888.35	7959	7936.2	7936.2	.3
790	889.28	7987	7918.1	7918.1	.8
791	890.20	7821	7900.5	7900.5	-.9
792	891.12	7975	7883.2	7883.2	1.0
793	892.04	7819	7866.4	7866.4	-.5
794	892.96	7861	7850.1	7850.1	.1
795	893.89	7851	7834.1	7834.1	.2
796	894.81	7753	7818.5	7818.5	-.7
797	895.73	7685	7803.3	7803.3	-1.3
798	896.65	7836	7788.5	7788.5	.5
799	897.57	7817	7774.1	7774.1	.5
800	898.49	7845	7760.0	7760.0	1.0
801	899.42	7754	7746.2	7746.2	.1
802	900.34	7812	7732.7	7732.7	.9
803	901.26	7773	7719.6	7719.6	.6
804	902.18	7751	7706.7	7706.7	.5
805	903.10	7717	7694.0	7694.0	.3
806	904.03	7617	7681.6	7681.6	-.7
807	904.95	7781	7669.4	7669.4	1.3
808	905.87	7706	7657.3	7657.3	.6
809	906.79	7798	7645.5	7645.5	1.7
810	907.71	7637	7633.8	7633.8	.0
811	908.63	7618	7622.2	7622.2	.0
812	909.56	7451	7610.7	7610.7	-1.8
813	910.48	7496	7599.3	7599.3	-1.2
814	911.40	7457	7587.9	7587.9	-1.5
815	912.32	7592	7576.6	7576.6	.2
816	913.24	7502	7565.3	7565.3	-.7
817	914.17	7691	7554.0	7554.0	1.6
818	915.09	7466	7542.7	7542.7	-.9
819	916.01	7478	7531.3	7531.3	-.6
820	916.93	7386	7519.9	7519.9	-1.5
821	917.85	7578	7508.4	7508.4	.8
822	918.77	7495	7496.8	7496.8	.0
823	919.70	7462	7485.2	7485.2	-.3
824	920.62	7570	7473.4	7473.4	1.1

825	921.54	7458	7461.4	7461.4	.0
826	922.46	7531	7449.3	7449.3	.9
827	923.38	7539	7437.1	7437.1	1.2
828	924.31	7190	7424.7	7424.7	-2.7
829	925.23	7421	7412.2	7412.2	.1
830	926.15	7287	7399.5	7399.5	-1.3
831	927.07	7552	7386.6	7386.6	1.9
832	927.99	7370	7373.5	7373.5	.0
833	928.91	7397	7360.3	7360.3	.4
834	929.84	7429	7346.9	7346.9	1.0
835	930.76	7422	7333.3	7333.3	1.0
836	931.68	7252	7319.6	7319.6	-.8
837	932.60	7178	7305.7	7305.7	-1.5
838	933.52	7280	7291.7	7291.7	-.1
839	934.45	7279	7277.5	7277.5	.0
840	935.37	7237	7263.2	7263.2	-.3
841	936.29	7126	7248.8	7248.8	-1.4
842	937.21	7306	7234.4	7234.4	.8
843	938.13	7201	7219.8	7219.8	-.2
844	939.05	7286	7205.3	7205.3	.9
845	939.98	7357	7190.7	7190.7	2.0
846	940.90	7013	7176.1	7176.1	-1.9
847	941.82	7175	7161.6	7161.6	.2
848	942.74	7207	7147.1	7147.1	.7
849	943.66	7083	7132.7	7132.7	-.6
850	944.58	7152	7118.5	7118.5	.4
851	945.51	7245	7104.5	7104.5	1.7
852	946.43	7005	7090.7	7090.7	-1.0
853	947.35	7115	7077.1	7077.1	.5
854	948.27	7107	7063.9	7063.9	.5
855	949.19	7026	7051.0	7051.0	-.3
856	950.12	7018	7038.5	7038.5	-.2
857	951.04	6967	7026.5	7026.5	-.7
858	951.96	7202	7015.0	7015.0	2.2
859	952.88	6946	7004.0	7004.0	-.7
860	953.80	6974	6993.7	6993.7	-.2
861	954.72	6845	6984.1	6984.1	-1.7
862	955.65	6897	6975.3	6975.3	-.9
863	956.57	6914	6967.3	6967.3	-.6
864	957.49	7055	6960.1	6960.1	1.1
865	958.41	6973	6954.0	6954.0	.2
866	959.33	6810	6948.9	6948.9	-1.7
867	960.26	7105	6944.9	6944.9	1.9
868	961.18	6903	6942.0	6942.0	-.5
869	962.10	6893	6940.5	6940.5	-.6
870	963.02	7067	6940.3	6940.3	1.5
871	963.94	6951	6941.6	6941.6	.1
872	964.86	6951	6944.4	6944.4	.1
873	965.79	6900	6948.7	6948.7	-.6

596 keV Peak From 65.5 MeV Neutrons
L= 65n

C/f = .846 E1= 596.95 E2= 695.33 P= 6 R= 6.0 %= 30.

Chan.	keV	Counts	Back.	Fit	Res.
582	596.95	1109	1104.8	1113.0	-.1
583	597.89	1138	1130.8	1142.5	-.1
584	598.84	1172	1154.2	1171.0	.0
585	599.78	1196	1175.2	1199.1	-.1
586	600.73	1235	1193.9	1228.0	.2
587	601.67	1271	1210.4	1259.2	.3
588	602.62	1267	1224.9	1294.7	-.8
589	603.57	1364	1237.6	1332.2	.9
590	604.51	1326	1248.5	1350.9	-.7
591	605.46	1355	1257.8	1345.0	.3
592	606.41	1314	1265.5	1324.0	-.3
593	607.35	1333	1271.9	1302.8	.8
594	608.30	1262	1277.1	1289.9	-.8
595	609.24	1265	1281.0	1285.2	-.6
596	610.19	1322	1283.9	1284.9	1.0
597	611.14	1279	1285.7	1286.0	-.2
598	612.08	1376	1286.7	1286.7	2.5
599	613.03	1273	1286.9	1286.9	-.4
600	613.97	1293	1286.3	1286.3	.2
601	614.92	1258	1285.0	1285.0	-.8
602	615.86	1305	1283.1	1283.1	.6
603	616.81	1273	1280.7	1280.7	-.2
604	617.76	1238	1277.8	1277.8	-1.1
605	618.70	1275	1274.5	1274.5	.0
606	619.65	1220	1270.8	1270.8	-1.4
607	620.59	1257	1266.8	1266.8	-.3
608	621.54	1236	1262.6	1262.6	-.8
609	622.49	1282	1258.1	1258.1	.7
610	623.43	1190	1253.4	1253.4	-1.8
611	624.38	1254	1248.6	1248.6	.2
612	625.33	1282	1243.6	1243.6	1.1
613	626.27	1228	1238.6	1238.6	-.3
614	627.22	1216	1233.5	1233.5	-.5
615	628.16	1277	1228.3	1228.3	1.4
616	629.11	1245	1223.2	1223.2	.6
617	630.05	1258	1218.0	1218.0	1.1
618	631.00	1195	1212.9	1212.9	-.5
619	631.95	1206	1207.9	1207.9	-.1
620	632.89	1182	1202.9	1202.9	-.6
621	633.84	1194	1197.9	1197.9	-.1
622	634.78	1158	1193.1	1193.1	-1.0
623	635.73	1213	1188.3	1188.3	.7
624	636.68	1185	1183.6	1183.6	.0
625	637.62	1187	1179.0	1179.0	.2

626	638.57	1203	1174.5	1174.5	.8
627	639.52	1215	1170.2	1170.2	1.3
628	640.46	1161	1165.9	1165.9	-.1
629	641.41	1162	1161.8	1161.8	.0
630	642.35	1212	1157.7	1157.7	1.6
631	643.30	1160	1153.8	1153.8	.2
632	644.24	1171	1150.0	1150.0	.6
633	645.19	1120	1146.3	1146.3	-.8
634	646.14	1089	1142.6	1142.6	-1.6
635	647.08	1137	1139.1	1139.1	-.1
636	648.03	1125	1135.7	1135.7	-.3
637	648.97	1121	1132.3	1132.3	-.3
638	649.92	1123	1129.0	1129.0	-.2
639	650.87	1127	1125.8	1125.8	.0
640	651.81	1116	1122.7	1122.7	-.2
641	652.76	1104	1119.6	1119.6	-.5
642	653.71	1149	1116.5	1116.5	1.0
643	654.65	1073	1113.6	1113.6	-1.2
644	655.60	1111	1110.6	1110.6	.0
645	656.54	1088	1107.7	1107.7	-.6
646	657.49	1037	1104.8	1104.8	-2.1
647	658.43	1127	1101.9	1101.9	.8
648	659.38	1066	1099.1	1099.1	-1.0
649	660.33	1144	1096.2	1096.2	1.4
650	661.27	1117	1093.4	1093.4	.7
651	662.22	1088	1090.6	1090.6	-.1
652	663.16	1086	1087.7	1087.7	-.1
653	664.11	1141	1084.9	1084.9	1.7
654	665.06	1122	1082.1	1082.1	1.2
655	666.00	1116	1079.2	1079.2	1.1
656	666.95	1042	1076.4	1076.4	-1.0
657	667.90	1083	1073.5	1073.5	.3
658	668.84	1040	1070.6	1070.6	-.9
659	669.79	1073	1067.8	1067.8	.2
660	670.73	1005	1064.9	1064.9	-1.9
661	671.68	1067	1062.0	1062.0	.2
662	672.63	1016	1059.1	1059.1	-1.3
663	673.57	1057	1056.3	1056.3	.0
664	674.52	1109	1053.5	1053.5	1.7
665	675.46	1061	1050.7	1050.7	.3
666	676.41	1096	1047.9	1047.9	1.5
667	677.35	1044	1045.2	1045.2	.0
668	678.30	1000	1042.6	1042.6	-1.3
669	679.25	1076	1040.0	1040.0	1.1
670	680.19	1027	1037.5	1037.5	-.3
671	681.14	997	1035.1	1035.1	-1.2
672	682.09	1036	1032.9	1032.9	.1
673	683.03	1044	1030.8	1030.8	.4
674	683.98	1029	1028.8	1028.8	.0
675	684.92	1044	1027.1	1027.1	.5
676	685.87	1009	1025.5	1025.5	-.5

677	686.82	1014	1024.2	1024.2	-.3
678	687.76	1079	1023.1	1023.1	1.7
679	688.71	984	1022.4	1022.4	-1.2
680	689.65	981	1021.9	1021.9	-1.3
681	690.60	1055	1021.8	1021.8	1.0
682	691.54	1035	1022.0	1022.0	.4
683	692.49	990	1022.7	1022.7	-1.0
684	693.44	1015	1023.8	1023.8	-.3
685	694.38	1045	1025.3	1025.3	.6
686	695.33	1034	1027.4	1027.4	.2

690 KeV Peak From 65.5 MeV Neutrons
L= 65m
C/f= .910 E1= 692.49 E2= 830.61 P= 5 R= 4.0 %= 30.

Chan.	keV	Counts	Back.	Fit	Res.
683	692.49	990	993.4	995.6	-.2
684	693.44	1015	1009.5	1012.7	.1
685	694.38	1045	1024.3	1029.1	.5
686	695.33	1034	1037.9	1044.8	-.3
687	696.28	1055	1050.3	1060.5	-.2
688	697.22	1073	1061.6	1076.5	-.1
689	698.17	1133	1071.8	1093.6	1.2
690	699.11	1129	1081.0	1112.8	.5
691	700.06	1122	1089.2	1135.8	-.4
692	701.01	1144	1096.5	1164.6	-.6
693	701.95	1167	1102.9	1176.5	.0
694	702.90	1150	1108.5	1209.8	-.3
695	703.84	1245	1113.3	1240.5	.5
696	704.79	1234	1117.3	1241.8	.0
697	705.73	1199	1120.6	1225.4	-.6
698	706.68	1221	1123.3	1201.5	.6
699	707.63	1163	1125.3	1154.3	.3
700	708.57	1094	1126.6	1134.3	-1.2
701	709.52	1176	1127.5	1128.9	1.4
702	710.47	1154	1127.8	1128.0	.8
703	711.41	1096	1127.6	1127.6	-.9
704	712.36	1080	1126.9	1126.9	-1.4
705	713.30	1069	1125.8	1125.8	-1.7
706	714.25	1126	1124.3	1124.3	.1
707	715.20	1085	1122.5	1122.5	-1.1
708	716.14	1185	1120.3	1120.3	1.9
709	717.09	1092	1117.7	1117.7	-.8
710	718.03	1087	1114.9	1114.9	-.8
711	718.98	1108	1111.8	1111.8	-.1
712	719.92	1145	1108.5	1108.5	1.1
713	720.87	1076	1104.9	1104.9	-.9
714	721.82	1123	1101.2	1101.2	.7
715	722.76	1073	1097.3	1097.3	-.7
716	723.71	1109	1093.2	1093.2	.5
717	724.66	1135	1089.0	1089.0	1.4
718	725.60	1084	1084.6	1084.6	.0
719	726.55	1138	1080.2	1080.2	1.7
720	727.49	1027	1075.7	1075.7	-1.5
721	728.44	1090	1071.1	1071.1	.6
722	729.39	1150	1066.5	1066.5	2.5
723	730.33	1097	1061.9	1061.9	1.1
724	731.28	989	1057.2	1057.2	-2.1
725	732.22	1066	1052.5	1052.5	.4
726	733.17	1050	1047.8	1047.8	.1
727	734.11	1027	1043.2	1043.2	-.5

728	735.06	1076	1038.5	1038.5	1.2
729	736.01	1036	1033.9	1033.9	.1
730	736.95	1043	1029.4	1029.4	.4
731	737.90	975	1024.9	1024.9	-1.6
732	738.84	986	1020.5	1020.5	-1.1
733	739.79	998	1016.1	1016.1	-.6
734	740.74	1055	1011.9	1011.9	1.3
735	741.68	1061	1007.7	1007.7	1.7
736	742.63	943	1003.6	1003.6	-1.9
737	743.58	1045	999.6	999.6	1.4
738	744.52	1008	995.7	995.7	.4
739	745.47	999	991.9	991.9	.2
740	746.41	998	988.2	988.2	.3
741	747.36	965	984.7	984.7	-.6
742	748.30	976	981.2	981.2	-.2
743	749.25	922	977.9	977.9	-1.8
744	750.20	998	974.7	974.7	.7
745	751.14	953	971.6	971.6	-.6
746	752.09	1001	968.6	968.6	1.0
747	753.03	947	965.8	965.8	-.6
748	753.98	984	963.0	963.0	.7
749	754.93	952	960.4	960.4	-.3
750	755.87	926	957.9	957.9	-1.0
751	756.82	897	955.6	955.6	-1.9
752	757.77	976	953.3	953.3	.7
753	758.71	966	951.2	951.2	.5
754	759.66	945	949.1	949.1	-.1
755	760.60	954	947.2	947.2	.2
756	761.55	919	945.4	945.4	-.9
757	762.49	927	943.7	943.7	-.5
758	763.44	938	942.1	942.1	-.1
759	764.39	935	940.6	940.6	-.2
760	765.33	940	939.2	939.2	.0
761	766.28	962	937.9	937.9	.8
762	767.22	920	936.6	936.6	-.5
763	768.17	979	935.5	935.5	1.4
764	769.12	884	934.4	934.4	-1.7
765	770.06	931	933.4	933.4	-.1
766	771.01	949	932.5	932.5	.5
767	771.96	951	931.6	931.6	.6
768	772.90	924	930.8	930.8	-.2
769	773.85	940	930.0	930.0	.3
770	774.79	963	929.3	929.3	1.1
771	775.74	960	928.6	928.6	1.0
772	776.68	896	928.0	928.0	-1.1
773	777.63	932	927.4	927.4	.2
774	778.58	904	926.8	926.8	-.8
775	779.52	907	926.2	926.2	-.6
776	780.47	926	925.7	925.7	.0
777	781.41	941	925.2	925.2	.5
778	782.36	873	924.6	924.6	-1.7

779	783.31	934	924.1	924.1	.3
780	784.25	923	923.6	923.6	.0
781	785.20	928	923.0	923.0	.2
782	786.15	958	922.5	922.5	1.2
783	787.09	921	921.9	921.9	.0
784	788.04	925	921.3	921.3	.1
785	788.98	940	920.7	920.7	.6
786	789.93	902	920.0	920.0	-.6
787	790.88	959	919.3	919.3	1.3
788	791.82	953	918.6	918.6	1.1
789	792.77	922	917.8	917.8	.1
790	793.71	924	917.0	917.0	.2
791	794.66	944	916.1	916.1	.9
792	795.60	928	915.2	915.2	.4
793	796.55	882	914.2	914.2	-1.1
794	797.50	876	913.2	913.2	-1.2
795	798.44	915	912.1	912.1	.1
796	799.39	913	911.0	911.0	.1
797	800.34	954	909.8	909.8	1.5
798	801.28	898	908.5	908.5	-.3
799	802.23	932	907.1	907.1	.8
800	803.17	856	905.7	905.7	-1.7
801	804.12	871	904.3	904.3	-1.1
802	805.07	890	902.8	902.8	-.4
803	806.01	905	901.2	901.2	.1
804	806.96	879	899.5	899.5	-.7
805	807.90	903	897.8	897.8	.2
806	808.85	851	896.1	896.1	-1.5
807	809.79	895	894.3	894.3	.0
808	810.74	926	892.4	892.4	1.1
809	811.69	880	890.5	890.5	-.4
810	812.63	887	888.6	888.6	-.1
811	813.58	912	886.7	886.7	.9
812	814.53	859	884.7	884.7	-.9
813	815.47	862	882.7	882.7	-.7
814	816.42	866	880.6	880.6	-.5
815	817.36	941	878.6	878.6	2.1
816	818.31	857	876.6	876.6	-.7
817	819.26	912	874.6	874.6	1.3
818	820.20	871	872.6	872.6	-.1
819	821.15	888	870.6	870.6	.6
820	822.09	848	868.7	868.7	-.7
821	823.04	870	866.9	866.9	.1
822	823.98	867	865.1	865.1	.1
823	824.93	900	863.4	863.4	1.2
824	825.88	890	861.7	861.7	1.0
825	826.82	811	860.2	860.2	-1.7
826	827.77	823	858.8	858.8	-1.2
827	828.72	840	857.6	857.6	-.6
828	829.66	854	856.5	856.5	-.1
829	830.61	892	855.6	855.6	1.2

835 keV Peak From 65.5 MeV Neutrons

L= 65n
C/f= .728 E1= 832.50 E2= 964.94 P= 6 R= 2.0 %= 50.

Chan.	keV	Counts	Back.	Fit	Res.
831	832.50	845	863.0	863.5	-.6
832	833.45	876	873.2	874.7	.0
833	834.39	907	882.3	886.1	.7
834	835.34	896	890.4	899.1	-.1
835	836.28	922	897.6	915.0	.2
836	837.23	909	903.8	934.9	-.8
837	838.17	1002	909.3	958.3	1.4
838	839.12	964	914.0	982.5	-.6
839	840.07	978	918.0	1002.8	-.8
840	841.01	1043	921.3	1014.5	.9
841	841.96	1026	924.1	1015.3	.3
842	842.91	958	926.2	1006.7	-1.5
843	843.85	1021	927.8	993.8	.9
844	844.80	998	929.0	983.3	.5
845	845.74	976	929.7	980.2	-.1
846	846.69	989	930.0	986.3	.1
847	847.64	988	929.9	999.5	-.4
848	848.58	987	929.5	1014.1	-.9
849	849.53	1061	928.8	1023.6	1.2
850	850.47	1017	927.8	1023.2	-.2
851	851.42	1016	926.5	1012.1	.1
852	852.36	998	925.1	993.1	.2
853	853.31	962	923.4	971.4	-.3
854	854.26	935	921.6	951.6	-.5
855	855.20	933	919.6	936.2	-.1
856	856.15	939	917.5	925.7	.4
857	857.09	926	915.3	918.9	.2
858	858.04	927	913.1	914.4	.4
859	858.99	935	910.7	911.2	.8
860	859.93	904	908.3	908.4	-.1
861	860.88	875	905.8	905.9	-1.0
862	861.83	930	903.3	903.4	.9
863	862.77	868	900.8	900.8	-1.1
864	863.72	930	898.3	898.3	1.1
865	864.66	915	895.8	895.8	.6
866	865.61	856	893.4	893.4	-1.3
867	866.55	862	890.9	890.9	-1.0
868	867.50	866	888.5	888.5	-.8
869	868.45	913	886.1	886.1	.9
870	869.39	900	883.7	883.7	.5
871	870.34	878	881.4	881.4	-.1
872	871.28	858	879.2	879.2	-.7
873	872.23	883	877.0	877.0	.2
874	873.18	850	874.9	874.9	-.8

875	874.12	899	872.8	872.8	.9
876	875.07	870	870.8	870.8	.0
877	876.02	846	868.9	868.9	-.8
878	876.96	861	867.0	867.0	-.2
879	877.91	875	865.2	865.2	.3
880	878.85	911	863.4	863.4	1.6
881	879.80	850	861.7	861.7	-.4
882	880.74	855	860.1	860.1	-.2
883	881.69	868	858.5	858.5	.3
884	882.64	860	857.0	857.0	.1
885	883.58	896	855.5	855.5	1.4
886	884.53	841	854.1	854.1	-.5
887	885.47	801	852.8	852.8	-1.8
888	886.42	863	851.5	851.5	.4
889	887.37	868	850.2	850.2	.6
890	888.31	809	849.0	849.0	-1.4
891	889.26	855	847.8	847.8	.2
892	890.21	831	846.6	846.6	-.5
893	891.15	835	845.5	845.5	-.4
894	892.10	869	844.4	844.4	.8
895	893.04	834	843.3	843.3	-.3
896	893.99	851	842.3	842.3	.3
897	894.93	853	841.2	841.2	.4
898	895.88	804	840.2	840.2	-1.3
899	896.83	844	839.1	839.1	.2
900	897.77	834	838.1	838.1	-.1
901	898.72	900	837.0	837.0	2.1
902	899.66	836	836.0	836.0	.0
903	900.61	855	834.9	834.9	.7
904	901.56	873	833.9	833.9	1.4
905	902.50	766	832.8	832.8	-2.3
906	903.45	843	831.7	831.7	.4
907	904.40	853	830.5	830.5	.8
908	905.34	843	829.4	829.4	.5
909	906.29	833	828.2	828.2	.2
910	907.23	811	827.0	827.0	-.6
911	908.18	827	825.7	825.7	.0
912	909.13	805	824.4	824.4	-.7
913	910.07	830	823.1	823.1	.2
914	911.02	824	821.7	821.7	.1
915	911.96	825	820.3	820.3	.2
916	912.91	803	818.9	818.9	-.6
917	913.85	811	817.4	817.4	-.2
918	914.80	823	815.8	815.8	.3
919	915.75	824	814.2	814.2	.3
920	916.69	818	812.6	812.6	.2
921	917.64	809	810.9	810.9	-.1
922	918.59	806	809.2	809.2	-.1
923	919.53	808	807.4	807.4	.0
924	920.48	844	805.6	805.6	1.4
925	921.42	767	803.8	803.8	-1.3

926	922.37	774	801.9	801.9	-1.0
927	923.32	813	799.9	799.9	.5
928	924.26	795	798.0	798.0	-.1
929	925.21	788	796.0	796.0	-.3
930	926.15	782	793.9	793.9	-.4
931	927.10	764	791.9	791.9	-1.0
932	928.04	799	789.8	789.8	.3
933	928.99	744	787.7	787.7	-1.6
934	929.94	807	785.6	785.6	.8
935	930.88	759	783.5	783.5	-.9
936	931.83	784	781.4	781.4	.1
937	932.78	783	779.2	779.2	.1
938	933.72	760	777.1	777.1	-.6
939	934.67	787	775.0	775.0	.4
940	935.61	735	772.9	772.9	-1.4
941	936.56	777	770.8	770.8	.2
942	937.51	773	768.7	768.7	.2
943	938.45	804	766.7	766.7	1.3
944	939.40	781	764.7	764.7	.6
945	940.34	801	762.8	762.8	1.4
946	941.29	787	760.9	760.9	.9
947	942.23	760	759.0	759.0	.0
948	943.18	715	757.3	757.3	-1.5
949	944.13	777	755.6	755.6	.8
950	945.07	806	754.0	754.0	1.9
951	946.02	780	752.5	752.5	1.0
952	946.97	790	751.0	751.0	1.4
953	947.91	716	749.7	749.7	-1.2
954	948.86	771	748.5	748.5	.8
955	949.80	699	747.4	747.4	-1.8
956	950.75	763	746.5	746.5	.6
957	951.70	743	745.6	745.6	-.1
958	952.64	739	745.0	745.0	-.2
959	953.59	731	744.4	744.4	-.5
960	954.53	707	744.1	744.1	-1.4
961	955.48	752	743.9	743.9	.3
962	956.42	687	743.8	743.8	-2.1
963	957.37	754	744.0	744.0	.4
964	958.32	746	744.3	744.3	.1
965	959.26	756	744.9	744.9	.4
966	960.21	745	745.6	745.6	.0
967	961.16	728	746.5	746.5	-.7
968	962.10	773	747.7	747.7	.9
969	963.05	746	749.1	749.1	-.1
970	963.99	753	750.7	750.7	.1
971	964.94	768	752.6	752.6	.6

APPENDIX B: Lotus 123 Macro for Evaluation of Width Measurements.

	A	B	C	D	E	F	G	H	I	J	K	L	M	N	O	P	Q
1							*** GRAPHING INFORMATION *			GRAPHING INFORMATION			LOC	LOC	ENERGY		RISE
2	ENERGY									LOG(DATA)	LOG(HALFMAX)		MIN	MAX	AT MAX		LEG
3	LEVEL	DATA															
4																	
5	594.3	8483.9								3.929	4.027		0	4331	0		8484
6	595.22	9083.4								3.958	4.027		0	3732	0		9083
7	596.14	9622.6		MAX:	*********					3.983	4.027		0	3193	0		9623
8	597.07	10105.6		MIN:	8483.900					4.005	4.027		0	2710	0		10106
9	597.99	10536.1		HALF-MAX:	10649.55					4.023	4.027		0	2279	0		10536
10	598.91	10918								4.038	4.027		0	1897	0		10918
11	599.83	11254.6		E1:	598.26					4.051	4.027		0	1561	0		11255
12	600.75	11549.3		E2:	641.75					4.063	4.027		0	1266	0		11549
13	601.68	11805.3								4.072	4.027		0	1010	0		11805
14	602.6	12025.5		PEAK:	610.89					4.080	4.027		0	790	0		12026
15	603.52	12212.7								4.087	4.027		0	603	0		12213
16	604.44	12369.7					4.03			4.092	4.027		0	446	0		12370
17	605.36	12499					4.01			4.097	4.027		0	316	0		12499
18	606.28	12602.8					4.00			4.100	4.027		0	212	0		12603
19	607.21	12683.5					3.99			4.103	4.027		0	132	0		12684
20	608.13	12743.2					3.97			4.105	4.027		0	72	0		12743
21	609.05	12783.8					3.96			4.107	4.027		0	31	0		12784
22	609.97	12807.2					3.94			4.107	4.027		0	8	0		12807
23	610.89	12815.2					3.93			4.108	4.027		0	0	611		0
24	611.82	12809.3								4.108	4.027		0	0	0		0
25	612.74	12791.1								4.107	4.027		0	0	0		0
26	613.66	12762								4.106	4.027		0	0	0		0
27	614.58	12723.3								4.105	4.027		0	0	0		0
28	615.5	12676.2								4.103	4.027		0	0	0		0
29	616.42	12621.9								4.101	4.027		0	0	0		0
30	617.35	12561.3								4.099	4.027		0	0	0		0
31	618.27	12495.5								4.097	4.027		0	0	0		0
32	619.19	12425.2								4.094	4.027		0	0	0		0
33	620.11	12351.4								4.092	4.027		0	0	0		0
34	621.03	12274.7								4.089	4.027		0	0	0		0
35	621.95	12195.9								4.086	4.027		0	0	0		0
36	622.88	12115.4								4.083	4.027		0	0	0		0
97	679.11	9158.7								3.962	4.027		0	0	0		0
98	680.03	9134.7								3.961	4.027		0	0	0		0
99	680.95	9111.1								3.960	4.027		0	0	0		0
100	681.87	9087.8								3.958	4.027		0	0	0		0
101	682.79	9064.5								3.957	4.027		0	0	0		0
102	683.72	9041.2								3.956	4.027		0	0	0		0
103	684.64	9017.6								3.955	4.027		0	0	0		0
104	685.56	8993.6								3.954	4.027		0	0	0		0
105	686.48	8968.9								3.953	4.027		0	0	0		0
106	687.4	8943.1								3.951	4.027		0	0	0		0
107	688.32	8916								3.950	4.027		0	0	0		0
108	689.25	8887.1								3.949	4.027		0	0	0		0
109	690.17	8856.1								3.947	4.027		0	0	0		0
110															611		
111																	
112																	

	R	S	T	U	V	W	X	Y	Z	AA	AB	AC	AD	AE
1														
2	POS CNG PNT	E-VAL	C-VAL	NEG CNG PNT	E-VAL	C-VAL		FALL LEG	POS CNG PNT	E-VAL	C-VAL	NEG CNG PNT	E-VAL	C-VAL
3														
4	========	========	========	========	========	========		========	========	========	========	========	========	========
5	2166	0	0	-99999	0	0		0	99999	0	0	-99999	0	0
6	1566	0	0	-99999	0	0		0	99999	0	0	-99999	0	0
7	1027	0	0	-99999	0	0		0	99999	0	0	-99999	0	0
8	544	0	0	-99999	0	0		0	99999	0	0	-99999	0	0
9	113	598	10536	-99999	0	0		0	99999	0	0	-99999	0	0
10	99999	0	0	-268	599	10918		0	99999	0	0	-99999	0	0
11	99999	0	0	-605	0	0		0	99999	0	0	-99999	0	0
12	99999	0	0	-900	0	0		0	99999	0	0	-99999	0	0
13	99999	0	0	-1156	0	0		0	99999	0	0	-99999	0	0
14	99999	0	0	-1376	0	0		0	99999	0	0	-99999	0	0
15	99999	0	0	-1563	0	0		0	99999	0	0	-99999	0	0
16	99999	0	0	-1720	0	0		0	99999	0	0	-99999	0	0
17	99999	0	0	-1849	0	0		0	99999	0	0	-99999	0	0
18	99999	0	0	-1953	0	0		0	99999	0	0	-99999	0	0
19	99999	0	0	-2034	0	0		0	99999	0	0	-99999	0	0
20	99999	0	0	-2094	0	0		0	99999	0	0	-99999	0	0
21	99999	0	0	-2134	0	0		0	99999	0	0	-99999	0	0
22	99999	0	0	-2158	0	0		0	99999	0	0	-99999	0	0
23	99999	0	0	-99999	0	0		12815	99999	0	0	-2166	0	0
24	99999	0	0	-99999	0	0		12809	99999	0	0	-2160	0	0
25	99999	0	0	-99999	0	0		12791	99999	0	0	-2142	0	0
26	99999	0	0	-99999	0	0		12762	99999	0	0	-2112	0	0
27	99999	0	0	-99999	0	0		12723	99999	0	0	-2074	0	0
28	99999	0	0	-99999	0	0		12676	99999	0	0	-2027	0	0
29	99999	0	0	-99999	0	0		12622	99999	0	0	-1972	0	0
30	99999	0	0	-99999	0	0		12561	99999	0	0	-1912	0	0
31	99999	0	0	-99999	0	0		12496	99999	0	0	-1846	618	12496
32	99999	0	0	-99999	0	0		12425	99999	0	0	-1776	0	0
33	99999	0	0	-99999	0	0		12351	99999	0	0	-1702	0	0
34	99999	0	0	-99999	0	0		12275	99999	0	0	-1625	0	0
35	99999	0	0	-99999	0	0		12196	99999	0	0	-1546	0	0
36	99999	0	0	-99999	0	0		12115	99999	0	0	-1466	0	0
97	99999	0	0	-99999	0	0		9159	1491	0	0	-99999	0	0
98	99999	0	0	-99999	0	0		9135	1515	0	0	-99999	0	0
99	99999	0	0	-99999	0	0		9111	1538	0	0	-99999	0	0
100	99999	0	0	-99999	0	0		9088	1562	0	0	-99999	0	0
101	99999	0	0	-99999	0	0		9065	1585	0	0	-99999	0	0
102	99999	0	0	-99999	0	0		9041	1608	0	0	-99999	0	0
103	99999	0	0	-99999	0	0		9018	1632	0	0	-99999	0	0
104	99999	0	0	-99999	0	0		8994	1656	0	0	-99999	0	0
105	99999	0	0	-99999	0	0		8969	1681	0	0	-99999	0	0
106	99999	0	0	-99999	0	0		8943	1706	0	0	-99999	0	0
107	99999	0	0	-99999	0	0		8916	1734	0	0	-99999	0	0
108	99999	0	0	-99999	0	0		8887	1762	0	0	-99999	0	0
109	99999	0	0	-99999	0	0		8856	1793	0	0	-99999	0	0
110 =	========	========	========	========	========	========		========	========	========	========	========	========	========
111		598	10536		599	10918				642	10612		618	12496
112 =	========	========	========	========	========	========		========	========	========	========	========	========	========

CELL EQUATIONS USED FOR THE LOTUS 123 MACRO TO CALCULATE WIDTH MEASUREMENTS. • = Cell row number # = Width value

Cell(s)	Equation
E7	@MAX(B5..B109)
E8	@MIN(B5..B109)
E9	(($E$7-$E$8)/#)+$E$8
E11	+V111-((V111-S111)*((W111-E9)/W111-T111)))
E12	+AD111+((AA111-AD111)*(AE111-E9)/AE111-AB111)))
E14	+$O$111
J5--J109	@LOG(B5)
K5--K109	@LOG((($E$7-$E$8)/#)+$E$8)
M5	+$E$8-B5
M6--M109	@IF(M(•-1)=0,0,+$E$8-B•
N5	+E7-B5
N6--N109	@IF(N•=0,0,+$MAX-B•)
O5--O109	@IF(B•=$E$7,A5,0)
Q5--Q109	@IF(M•=0#AND#N•>0,B•,0)
R5--R109	@IF(Q•>0,(IF($E$9-Q•>0,$E$9-Q•,99999)),99999)
S5--S109	@IF(R•=@MIN($R$5..$R$109),A•,0)
T5--T109	@IF(S•>0,Q•,0)
U5--U109	@IF(Q•>0,(IF($E$9-Q•<=0,$E$9-Q•,-99999)),-99999)
V5--V109	@IF(U•=@MAX($U$5..$U$109),A•,0)
W5--W109	@IF(V•>0,Q•,0)
Y5--Y109	@IF(N•=0,0,B•,0)
Z5--Z109	@IF(Y•>0,(@IF($E$9-Y•>0,$E$9-Y•,99999)),99999)

AA5--AA109	@IF(Z•=@MIN($Z$5..$Z$109),A•,0)
AB5--AB109	@IF(AA•>0,Y•,0)
AC5--AC109	@IF(Y•>0,@IF($E$9-Y•<=0,$E$9-Y•,-99999))),-99999)
AD5--AD109	@IF(AC•=MAX($AC$5..$AC$109),A•,0)
AE5--AE109	@IF(AD•>0,Y•,0)
O111	@SUM(O5..O109)
S111	@SUM(S5..S109)
T111	@SUM(T5..T109)
U111	@SUM(U5..U109)
W111	@SUM(W5..W109)
AA111	@SUM(AA5..AA109)
AB111	@SUM(AB5..AB109)
AD111	@SUM(AD5..AD109)
AE111	@SUM(AE5..AE109)

APPENDIX C: Computer Program (ESCATTR) to Evaluate Scattered Neutron Energy from Laboratory System.

```
/*****************************************************************************
 escattrc.c

            Calculate scatter energies.
            Developed for G. Beck by S. Shimose

 02/04/91  STS  Color support added.
 01/30/91  STS  create
*****************************************************************************/
#include <fcntl.h>
#include <sys\types.h>
#include <sys\stat.h>
#include <io.h>
#include <stdio.h>
#include <stdlib.h>
#include <malloc.h>
#include <math.h>
#include <string.h>
#include <dos.h>
#include <ansimacr.h>

#define   MK_FARPTR(seg,offs)   (void far *)( ( (long)(seg)<<16 ) | offs )

#define   MGA_ADDR        0xb0000000
#define   MGA_CTRL_REG    0x3b8
#define   MGA_SEG         0xb000
#define   CGA_ADDR        0xb8000000
#define   CGA_CTRL_REG    0x3d8
#define   CGA_SEG         0xb800

#define   TRUE            1
#define   FALSE           0

#define   NORMAL          0x17
#define   HIGH_INTEN      0x0f
#define   REVERSE         0x70
#define   BLINK           0x80

#define   BLACK           0
#define   BLUE            1
#define   GREEN           2
#define   CYAN            3
#define   RED             4
#define   MAGENTA         5
#define   BROWN           6
#define   WHITE           7
#define   DARK_GRAY       8
#define   LITE_BLUE       9
#define   LITE_GREEN      10
```

```
#define   LITE_CYAN      11
#define   LITE_RED       12
#define   LITE_MAGENTA   13
#define   YELLOW         14
#define   BRIGHT_WHITE   15

#define   OPEN_ERR       -10
#define   SEEK_ERR       -11
#define   READ_ERR       -14
#define   WRITE_ERR      -15
#define   CLOSE_ERR      -16

#define   F1             59
#define   F2             60
#define   F3             61
#define   F4             62
#define   F5             63
#define   F6             64
#define   F7             65
#define   F8             66
#define   F9             67
#define   F10            68
#define   UPARROW        72
#define   DNARROW        80
#define   RTARROW        77
#define   LFARROW        75

#define   FF             0xc
#define   CR             0xd
#define   SP             0x20
#define   ESC            0x1b

#define   LPT1           0
#define   LPT2           1
#define   LPT3           2

#define   SCRNBUFSIZE    2001
#define   MAXINFIELDS    3
#define   MAXOUTFIELDS   42

typedef struct  fieldspec
          {
            int  row;
            int  col;
            int  len;
          } FIELDSPEC;

typedef struct eneries
          {
```

```
            double  hival;
            double  loval;
            int     complex;
           } ENERGIES;

typedef struct string16
           {
            char  bufr[16];
           } STRING16;

/*-----------------------------------------------------------------*/

int             calculate_energy(ENERGIES *Eprime,double E,double Q,double A);
unsigned char   check_lpt_status(int,unsigned char *);
int             edit_fields(STRING16 *fldbufr,FIELDSPEC *fldptr,int maxflds,
                            double *E,double *Q,double *A,int new);
void            init_Eprime(ENERGIES *Eprime,int count);

/*-----------------------------------------------------------------*/

char        escreen[20] = {"escreen.txt"};
char        txtbufr[SCRNBUFSIZE];

STRING16    instring[MAXINFIELDS];

FIELDSPEC   inputfld[MAXINFIELDS] =   { {4,6,15},{4,34,15},{4,62,15} };
FIELDSPEC   outputfld[MAXOUTFIELDS] = { {10, 6,15},{10,23,15},
                                        {11, 6,15},{11,23,15},
                                        {12, 6,15},{12,23,15},
                                        {13, 6,15},{13,23,15},
                                        {14, 6,15},{14,23,15},
                                        {15, 6,15},{15,23,15},
                                        {16, 6,15},{16,23,15},
                                        {17, 6,15},{17,23,15},
                                        {18, 6,15},{18,23,15},
                                        {19, 6,15},{19,23,15},
                                        {10,46,15},{10,63,15},
                                        {11,46,15},{11,63,15},
                                        {12,46,15},{12,63,15},
                                        {13,46,15},{13,63,15},
                                        {14,46,15},{14,63,15},
                                        {15,46,15},{15,63,15},
                                        {16,46,15},{16,63,15},
                                        {17,46,15},{17,63,15},
                                        {18,46,15},{18,63,15},
                                        {19,46,15},{19,63,15},
                                        {20,46,15},{20,63,15} };

unsigned        mode_control_reg,display_seg;
```

```
unsigned long    dsply_buf_addr;

main(argc,argv)
   int    argc;
   char   *argv[];
   {
    int             i,clear,fsize,quit,exit_key;
    ENERGIES        Eprime[MAXOUTFIELDS/2];
    double          E,A,Q,ws;
    FILE            *pstream;
    char            device[40],outtext[80];
    char            key;
    unsigned char   perr,pstatbyte;

/*
    if ( !get_dsply_info (&dsply_buf_addr, &mode_control_reg, &display_seg) )
      {
       cls();
       printf ("EGA probably present.  Change to MCGA or CGA.\n");
       exit(-1);
      }
*/
    dsply_buf_addr = CGA_ADDR;
    mode_control_reg = CGA_CTRL_REG;
    display_seg = CGA_SEG;

    cls();
    (void)clrw(0,0,24,79,NORMAL);

    (void)strcpy(device,"LPT1");
    if (argc == 2)
      {
       (void)strcpy(device,argv[1]);
       pstream = fopen(device,"r+");
       if (pstream != NULL)
         {
          fclose(pstream);
          sprintf(outtext,"Output File \"%s\" already exists.  OK to append? <y/n> ",
                device);
          writev(outtext,12,5,(int)strlen(outtext),NORMAL);
          key = 0;
          while (!(key=='Y' || key=='y' || key=='N' || key=='n') )
             key = getch();
          if (key=='N' || key=='n')
            {
             cls();
             exit(0);
            }
         }
```

```
     }
  else
     {
      perr = 1;
      while (perr)
         {
          perr = check_lpt_status(LPT1,&pstatbyte);
          if (perr)   /* bits 0, 3, and 5 are error bits */
             {
              if (read_bit(3,&pstatbyte))
                 {
                  pstatbyte = 1;
                  sprintf(outtext,"Printer is OFF.  Press 'C' when ready.");
                  writev(outtext,24,20,(int)strlen(outtext),NORMAL);
                  key = 0;
                  while ( !((key == 'C') || (key == 'c')) )
                     key = getch();
                  putcur(24,20,0);
                  writec(' ',40,0);
                  continue;
                 }
              if (read_bit(5,&pstatbyte))
                 {
                  putcur(24,20,0);
                  sprintf(outtext,"Add paper.  Press any key when ready.");
                  writev(outtext,24,20,(int)strlen(outtext),NORMAL);
                  (void)getch();
                  putcur(24,20,0);
                  writec(' ',40,0);
                  continue;
                 }
              if (read_bit(0,&pstatbyte))
                 {
                  putcur(24,20,0);
                  sprintf(outtext,"Timed Out.  Press a key to resume.");
                  writev(outtext,24,20,(int)strlen(outtext),NORMAL);
                  (void)getch();
                  putcur(24,20,0);
                  writec(' ',40,0);
                  continue;
                 }
             }
         }
     }
   pstream = fopen(device,"a+");
   if (pstream == NULL)
      {
       cls();
       printf("Error OPENing Device/File \"%s\".\n\n",device);
```

```
        exit(0);
       }
    fclose(pstream);

    fsize = read_textfile(escreen,txtbufr,SCRNBUFSIZE);
    txtbufr[fsize] = 0;
    if (fsize <= 0 || fsize > SCRNBUFSIZE)
       {
        cls();
        if (fsize > SCRNBUFSIZE)
           printf("Size of \"%s\" [%d] exceeds input buffer size [%d].\n\n",
                  escreen,fsize,SCRNBUFSIZE);
        exit(0);
       }

    E = A = Q = 0;
    (void)init_Eprime(&Eprime[0],21);

    clear = TRUE;
    quit = FALSE;
    while (!quit)
       {
        if (clear)
           fill_text_screen(txtbufr,dsply_buf_addr,NORMAL);
        exit_key = edit_fields(&instring[0],&inputfld[0],MAXINFIELDS,&E,&Q,&A,
                               clear);
        if (exit_key > 1)
           clear = FALSE;
        switch( exit_key )
           {
            case  F1:
               putcur(22,7,0);
               writea(REVERSE,2,0);
               if (!calculate_energy(&Eprime[0],E,Q,A))
                  {
                   writev("A = -1 is not allowed.",24,28,20,REVERSE);
                   (void)clrw(10,6,20,21,NORMAL);
                   (void)clrw(10,23,20,39,NORMAL);
                   (void)clrw(10,46,20,61,NORMAL);
                   (void)clrw(10,63,20,78,NORMAL);
                   delay(30L);
                   putcur(24,28,0);
                   writeca(' ',NORMAL,22,0);
                  }
               else
                  {
                   for (i=0; i<MAXOUTFIELDS; i+=2)
                      {
                       if (!Eprime[i/2].complex)
```

```
                {
                 sprintf(outtext,"% E  ",Eprime[i/2].hival);
                 writev(outtext,outputfld[i].row,outputfld[i].col,
                        (int)strlen(outtext),NORMAL);
                 sprintf(outtext,"% E  ",Eprime[i/2].loval);
                 writev(outtext,outputfld[i+1].row,outputfld[i+1].col,
                        (int)strlen(outtext),NORMAL);
                }
             else
                {
                 putcur(0);
                 writev(" Complex Number ",outputfld[i].row,
                         outputfld[i].col,20,NORMAL);
                 writev(" Complex Number ",outputfld[i+1].row,
                         outputfld[i+1].col,20,NORMAL);
                }
             }
          }
        putcur(22,7,0);
        writea(NORMAL,2,0);
        break;
      case  F3:
        putcur(22,27,0);
        writea(REVERSE,2,0);
        pstream = fopen(device,"a+");
        fprintf(pstream,"\n\n");
        fprintf(pstream,"          Calculation of Scatter Energy\n");
        fprintf(pstream,"          ----------------------------\n");
        fprintf(pstream,"              E = % E\n",E);
        fprintf(pstream,"              Q = % E\n",Q);
        fprintf(pstream,"              A = % E\n\n\n",A);
        fprintf(pstream,"      ws       E'\(ws,E\)+        E'\(ws,E\)-\n\n");
        ws = -1.0;
        for (i=0; i<MAXOUTFIELDS; i+=2)
           {
            fprintf(pstream,"      % .1f    % E    % E\n",
                    ws,Eprime[i/2].hival,Eprime[i/2].hival);
            ws += 0.1;
           }
        fputc(FF,pstream);
        fclose(pstream);
        putcur(22,27,0);
        writea(NORMAL,2,0);
        break;
      case  F5:
        putcur(22,48,0);
        writea(REVERSE,2,0);
        clear = TRUE;
        putcur(22,48,0);
```

```
                writea(NORMAL,2,0);
                break;
             case  F10:
                quit = TRUE;
                cls();
                break;
             default:
                break;
           }
        }
    }

/*******************************************************
 check_lpt_status

   Issue a BIOS printer port status request

 01/27/90  STS  pass in LPT#; actual status byte returned as formal argument
 01/23/90  STS  remove argument; status returned as return value
 07/26/88  STS  status passed back as arguement
*******************************************************/
unsigned char
check_lpt_status(lptnum,stat)
   int             lptnum;        /* 0:  LPT1, 1: LPT2 , 2:  LPT3 */
   unsigned char  *stat;
   {
    union REGS     regs;

    regs.h.ah = 2;
    regs.x.dx = lptnum;
    int86(0x17,&regs, &regs);
    *stat = regs.h.ah;
    return(*stat &= 0x29);  /* Bits 0, 3, and 5 are the error bits */
   }

/**************************************************************************
 calculate_energy

 01/31/91  STS  create
**************************************************************************/
int
calculate_energy(Eprime,E,Q,A)
   ENERGIES     *Eprime;
   double       E;
   double       Q;
   double       A;
   {
    int         i,valid;
    double      factor,root,rootarg[21],ws;
```

```

   valid = TRUE;
   factor = (A+1) * (A+1);
   if (factor == 0)
      valid = FALSE;
   else
      {
       ws = -1.0;
       for (i=0; i<21; i++)
          {
           rootarg[i] = E * (ws * ws + A * A - 1) + A * (A + 1) * Q;
           if (rootarg[i] < 0)
              {
               (Eprime+i)->hival = 0;
               (Eprime+i)->loval = 0;
               (Eprime+i)->complex = TRUE;
              }
           else
              {
               root = exp(0.5 * log(rootarg[i]));
               (Eprime+i)->hival = ws * exp(0.5 * log(E));
               (Eprime+i)->loval = (Eprime+i)->hival;
               (Eprime+i)->hival += root;
               (Eprime+i)->loval -= root;
               (Eprime+i)->hival *= (Eprime+i)->hival;
               (Eprime+i)->loval *= (Eprime+i)->loval;
               (Eprime+i)->hival /= factor;
               (Eprime+i)->loval /= factor;
              }
           ws += 0.1;
          }
      }
    return(valid);
   }

/******************************************************************************
 init_Eprime

 01/31/91  STS  create
******************************************************************************/
void
init_Eprime(Eprime,count)
   ENERGIES  *Eprime;
   int        count;
   {
    int   i;

    for (i=0; i<count; i++)
       {
```

```
        (Eprime+i)->hival = 0;
        (Eprime+i)->loval = 0;
        (Eprime+i)->complex = FALSE;
       }
   }

/***************************************************************************
 edit_fields

 01/31/91  STS  create
***************************************************************************/
int
edit_fields(fldbufr,fldptr,maxflds,E,Q,A,new)
   STRING16      *fldbufr;
   FIELDSPEC     *fldptr;
   int           maxflds;
   double        *E;
   double        *Q;
   double        *A;
   int           new;
   {
    int  i,key,fldnum,done,valid;

    if (new)
       {
        for (i=0; i<maxflds; i++)
           {
            (fldbufr+i)->bufr[0] = 0;
            putcur((fldptr+i)->row,(fldptr+i)->col,0);
            writec(' ',(fldptr+i)->len,0);
           }
        *A = *Q = *E = 0;
       }
    for (i=0; i<maxflds; i++)
       writeva((fldptr+i)->row,(fldptr+i)->col,(fldptr+i)->len,
              NORMAL);

    fldnum = 0;
    done = FALSE;
    key = 0;
    while (!done)
       {
        putcur((fldptr+fldnum)->row,(fldptr+fldnum)->col,0);
/*
        writeva((fldptr+fldnum)->row,(fldptr+fldnum)->col,
               (fldptr+fldnum)->len,REVERSE);
*/

        key = getch();
```

```
        if (key != CR && key != 0 && key != SP)
           continue;
        if (key == 0)
           key = getch();
        switch( key )
           {
            case CR:  ;
            case SP:
               stredit((fldptr+fldnum)->row,(fldptr+fldnum)->col,REVERSE,
                     NORMAL,(fldptr+fldnum)->len,(fldbufr+fldnum)->bufr,
                     FALSE,TRUE,24,70,&done);
            case RTARROW:
               writeva((fldptr+fldnum)->row,(fldptr+fldnum)->col,
                     (fldptr+fldnum)->len,NORMAL);
               fldnum++;
               if (fldnum >= maxflds)
                  fldnum = 0;
               break;
            case LFARROW:
               writeva((fldptr+fldnum)->row,(fldptr+fldnum)->col,
                     (fldptr+fldnum)->len,NORMAL);
               fldnum--;
               if (fldnum < 0)
                  fldnum = maxflds - 1;
               break;
            case F1:  ;
            case F3:  ;
            case F5:
               valid = TRUE;
               for (i=0; i<maxflds; i++)
                  if (strlen((fldbufr+i)->bufr)<=0)
                     valid = FALSE;
               if (valid)
                  {
                   *E = atof((fldbufr+0)->bufr);
                   *Q = atof((fldbufr+1)->bufr);
                   *A = atof((fldbufr+2)->bufr);
                   valid = (int)key;
                  }
               done = TRUE;
               break;
            case F10:
               valid = (int)key;
               done = TRUE;
               break;
            default:
               break;
           }
        }
```

```
    writeva((fldptr+fldnum)->row,(fldptr+fldnum)->col,(fldptr+fldnum)->len,
            NORMAL);
    return(valid);
   }
```

Calculation of Scatter Energy
áááááááááááááááááááááááááááááá

E = 1.880000E+001
Q = -5.960000E-001
A = 7.328616E+001

ws	E'(ws,E)+	E'(ws,E)-
-1.0	1.722144E+001	1.722144E+001
-0.9	1.726928E+001	1.726928E+001
-0.8	1.731725E+001	1.731725E+001
-0.7	1.736535E+001	1.736535E+001
-0.6	1.741359E+001	1.741359E+001
-0.5	1.746197E+001	1.746197E+001
-0.4	1.751048E+001	1.751048E+001
-0.3	1.755912E+001	1.755912E+001
-0.2	1.760790E+001	1.760790E+001
-0.1	1.765682E+001	1.765682E+001
-0.0	1.770587E+001	1.770587E+001
0.1	1.775506E+001	1.775506E+001
0.2	1.780439E+001	1.780439E+001
0.3	1.785385E+001	1.785385E+001
0.4	1.790345E+001	1.790345E+001
0.5	1.795318E+001	1.795318E+001
0.6	1.800306E+001	1.800306E+001
0.7	1.805307E+001	1.805307E+001
0.8	1.810322E+001	1.810322E+001
0.9	1.815351E+001	1.815351E+001
1.0	1.820393E+001	1.820393E+001

Calculation of Scatter Energy
ááááááááááááááááááááááááááááá

E = 1.880000E+001
Q = -6.900000E-001
A = 7.130423E+001

ws	E'(ws,E)+	E'(ws,E)-
-1.0	1.710351E+001	1.710351E+001
-0.9	1.715247E+001	1.715247E+001
-0.8	1.720158E+001	1.720158E+001
-0.7	1.725082E+001	1.725082E+001
-0.6	1.730021E+001	1.730021E+001
-0.5	1.734974E+001	1.734974E+001
-0.4	1.739941E+001	1.739941E+001
-0.3	1.744922E+001	1.744922E+001
-0.2	1.749918E+001	1.749918E+001
-0.1	1.754928E+001	1.754928E+001
-0.0	1.759952E+001	1.759952E+001
0.1	1.764990E+001	1.764990E+001
0.2	1.770044E+001	1.770044E+001
0.3	1.775111E+001	1.775111E+001
0.4	1.780193E+001	1.780193E+001
0.5	1.785290E+001	1.785290E+001
0.6	1.790401E+001	1.790401E+001
0.7	1.795526E+001	1.795526E+001
0.8	1.800667E+001	1.800667E+001
0.9	1.805821E+001	1.805821E+001
1.0	1.810991E+001	1.810991E+001

Calculation of Scatter Energy
ááááááááááááááááááááááááááááá

E = 1.880000E+001
Q = -8.350000E-001
A = 7.130423E+001

ws	E'(ws,E)+	E'(ws,E)-
-1.0	1.696256E+001	1.696256E+001
-0.9	1.701132E+001	1.701132E+001
-0.8	1.706022E+001	1.706022E+001
-0.7	1.710926E+001	1.710926E+001
-0.6	1.715844E+001	1.715844E+001
-0.5	1.720777E+001	1.720777E+001
-0.4	1.725723E+001	1.725723E+001
-0.3	1.730684E+001	1.730684E+001
-0.2	1.735659E+001	1.735659E+001
-0.1	1.740649E+001	1.740649E+001
-0.0	1.745652E+001	1.745652E+001
0.1	1.750671E+001	1.750671E+001
0.2	1.755703E+001	1.755703E+001
0.3	1.760750E+001	1.760750E+001
0.4	1.765812E+001	1.765812E+001
0.5	1.770888E+001	1.770888E+001
0.6	1.775978E+001	1.775978E+001
0.7	1.781084E+001	1.781084E+001
0.8	1.786203E+001	1.786203E+001
0.9	1.791338E+001	1.791338E+001
1.0	1.796487E+001	1.796487E+001

Calculation of Scatter Energy
áááááááááááááááááááááááááááááá

E = 3.840000E+001
Q = -5.960000E-001
A = 7.328616E+001

ws	E'(ws,E)+	E'(ws,E)-
-1.0	3.578023E+001	3.578023E+001
-0.9	3.587879E+001	3.587879E+001
-0.8	3.597762E+001	3.597762E+001
-0.7	3.607673E+001	3.607673E+001
-0.6	3.617611E+001	3.617611E+001
-0.5	3.627576E+001	3.627576E+001
-0.4	3.637569E+001	3.637569E+001
-0.3	3.647590E+001	3.647590E+001
-0.2	3.657638E+001	3.657638E+001
-0.1	3.667714E+001	3.667714E+001
-0.0	3.677818E+001	3.677818E+001
0.1	3.687950E+001	3.687950E+001
0.2	3.698110E+001	3.698110E+001
0.3	3.708297E+001	3.708297E+001
0.4	3.718512E+001	3.718512E+001
0.5	3.728756E+001	3.728756E+001
0.6	3.739028E+001	3.739028E+001
0.7	3.749328E+001	3.749328E+001
0.8	3.759656E+001	3.759656E+001
0.9	3.770012E+001	3.770012E+001
1.0	3.780397E+001	3.780397E+001

Calculation of Scatter Energy
áááááááááááááááááááááááááááááá

E = 3.840000E+001
Q = -6.900000E-001
A = 7.130423E+001

ws	E'(ws,E)+	E'(ws,E)-
-1.0	3.563415E+001	3.563415E+001
-0.9	3.573517E+001	3.573517E+001
-0.8	3.583648E+001	3.583648E+001
-0.7	3.593807E+001	3.593807E+001
-0.6	3.603995E+001	3.603995E+001
-0.5	3.614213E+001	3.614213E+001
-0.4	3.624459E+001	3.624459E+001
-0.3	3.634734E+001	3.634734E+001
-0.2	3.645039E+001	3.645039E+001
-0.1	3.655373E+001	3.655373E+001
-0.0	3.665736E+001	3.665736E+001
0.1	3.676129E+001	3.676129E+001
0.2	3.686551E+001	3.686551E+001
0.3	3.697003E+001	3.697003E+001
0.4	3.707484E+001	3.707484E+001
0.5	3.717995E+001	3.717995E+001
0.6	3.728535E+001	3.728535E+001
0.7	3.739106E+001	3.739106E+001
0.8	3.749706E+001	3.749706E+001
0.9	3.760336E+001	3.760336E+001
1.0	3.770996E+001	3.770996E+001

Calculation of Scatter Energy
áááááááááááááááááááááááááááááá

E = 3.840000E+001
Q = -8.350000E-001
A = 7.130423E+001

ws	E'(ws,E)+	E'(ws,E)-
-1.0	3.549318E+001	3.549318E+001
-0.9	3.559400E+001	3.559400E+001
-0.8	3.569510E+001	3.569510E+001
-0.7	3.579649E+001	3.579649E+001
-0.6	3.589817E+001	3.589817E+001
-0.5	3.600014E+001	3.600014E+001
-0.4	3.610241E+001	3.610241E+001
-0.3	3.620496E+001	3.620496E+001
-0.2	3.630780E+001	3.630780E+001
-0.1	3.641094E+001	3.641094E+001
-0.0	3.651437E+001	3.651437E+001
0.1	3.661809E+001	3.661809E+001
0.2	3.672211E+001	3.672211E+001
0.3	3.682643E+001	3.682643E+001
0.4	3.693104E+001	3.693104E+001
0.5	3.703594E+001	3.703594E+001
0.6	3.714114E+001	3.714114E+001
0.7	3.724664E+001	3.724664E+001
0.8	3.735244E+001	3.735244E+001
0.9	3.745854E+001	3.745854E+001
1.0	3.756494E+001	3.756494E+001

Calculation of Scatter Energy
áááááááááááááááááááááááááááá

E = 6.550000E+001
Q = -5.960000E-001
A = 7.328616E+001

ws	E'(ws,E)+	E'(ws,E)-
-1.0	6.144064E+001	6.144064E+001
-0.9	6.160932E+001	6.160932E+001
-0.8	6.177848E+001	6.177848E+001
-0.7	6.194809E+001	6.194809E+001
-0.6	6.211818E+001	6.211818E+001
-0.5	6.228873E+001	6.228873E+001
-0.4	6.245976E+001	6.245976E+001
-0.3	6.263125E+001	6.263125E+001
-0.2	6.280322E+001	6.280322E+001
-0.1	6.297566E+001	6.297566E+001
-0.0	6.314857E+001	6.314857E+001
0.1	6.332196E+001	6.332196E+001
0.2	6.349582E+001	6.349582E+001
0.3	6.367017E+001	6.367017E+001
0.4	6.384498E+001	6.384498E+001
0.5	6.402028E+001	6.402028E+001
0.6	6.419606E+001	6.419606E+001
0.7	6.437232E+001	6.437232E+001
0.8	6.454905E+001	6.454905E+001
0.9	6.472628E+001	6.472628E+001
1.0	6.490398E+001	6.490398E+001

Calculation of Scatter Energy
áááááááááááááááááááááááááááá

E = 6.550000E+001
Q = -6.900000E-001
A = 7.130423E+001

ws	E'(ws,E)+	E'(ws,E)-
-1.0	6.125565E+001	6.125565E+001
-0.9	6.142864E+001	6.142864E+001
-0.8	6.160211E+001	6.160211E+001
-0.7	6.177608E+001	6.177608E+001
-0.6	6.195055E+001	6.195055E+001
-0.5	6.212550E+001	6.212550E+001
-0.4	6.230096E+001	6.230096E+001
-0.3	6.247691E+001	6.247691E+001
-0.2	6.265336E+001	6.265336E+001
-0.1	6.283031E+001	6.283031E+001
-0.0	6.300775E+001	6.300775E+001
0.1	6.318570E+001	6.318570E+001
0.2	6.336416E+001	6.336416E+001
0.3	6.354311E+001	6.354311E+001
0.4	6.372257E+001	6.372257E+001
0.5	6.390253E+001	6.390253E+001
0.6	6.408300E+001	6.408300E+001
0.7	6.426398E+001	6.426398E+001
0.8	6.444547E+001	6.444547E+001
0.9	6.462747E+001	6.462747E+001
1.0	6.480997E+001	6.480997E+001

Calculation of Scatter Energy
áááááááááááááááááááááááááááááá

E = 6.550000E+001
Q = -8.350000E-001
A = 7.130423E+001

ws	E'(ws,E)+	E'(ws,E)-
-1.0	6.111467E+001	6.111467E+001
-0.9	6.128746E+001	6.128746E+001
-0.8	6.146073E+001	6.146073E+001
-0.7	6.163450E+001	6.163450E+001
-0.6	6.180876E+001	6.180876E+001
-0.5	6.198352E+001	6.198352E+001
-0.4	6.215877E+001	6.215877E+001
-0.3	6.233452E+001	6.233452E+001
-0.2	6.251077E+001	6.251077E+001
-0.1	6.268751E+001	6.268751E+001
-0.0	6.286476E+001	6.286476E+001
0.1	6.304251E+001	6.304251E+001
0.2	6.322076E+001	6.322076E+001
0.3	6.339951E+001	6.339951E+001
0.4	6.357877E+001	6.357877E+001
0.5	6.375853E+001	6.375853E+001
0.6	6.393880E+001	6.393880E+001
0.7	6.411958E+001	6.411958E+001
0.8	6.430086E+001	6.430086E+001
0.9	6.448266E+001	6.448266E+001
1.0	6.466496E+001	6.466496E+001